博士論文

Studies on sardine (*Sardinops* spp.) stocks using oxygen stable isotope ratios in otoliths

(耳石の酸素安定同位体比を用いたマイワシ属資源の研究)

坂本達也

Acknowledgement

The author would like to express my sincere thanks to Associate Professor Kosei Komatsu, Graduate School of Frontier Sciences, University of Tokyo for his implicit and sometimes explicit supports throughout this thesis.

I wish to express appreciation to my thesis committee members, Associate Professor Kosei Komatsu, Professor Shinichi Ito, Professor Shingo Kimura, Professor Katsufumi Sato and Associate Professor Sachihiko Itoh, Atmosphere and Ocean Research institute, University of Tokyo for their critical readings and helpful comments for this dissertation.

I am very grateful to Associate Professor Kotaro Shirai, Dr. Tomihiko Higuchi and Ms. Noriko Izumoto, Atmosphere and Ocean Research institute, University of Tokyo and Associate Professor Toyoho Ishimura, National Institute of Technology, Ibaraki College for kindly supporting and performing the isotope analyses.

I wish to express appreciation to Dr. Michio Yoneda, National Research Institute of Fisheries and Environment of Inland Sea for performing excellent rearing experiments of sardine juveniles.

I greatly appreciate Dr. Chikako Watanabe and Dr. Yasuhiro Kamimura, National Research Institute of Fisheries Science, Dr. Motomitsu Takahashi, Seikai National Fisheries Research Institute, Dr. Carl David van der Lingen, Department of Agriculture, Forestry and Fisheries, South Africa and Dr. David Checkley, Dr. Jennifer Rodgers-Wolgast, Dr. Ralf Goericke and Dr, David Wolgast, Scripps Institution of Oceanography, University of California San Diego for kindly providing massive numbers of sardine otolith and seawater samples.

I am very grateful to Professor Shinichi Ito, Associate Professor Sachihiko Itoh and Professor Ichiro Yasuda, Atmosphere and Ocean Research institute, University of Tokyo, for providing insightful comments and technical advices, and also their continued encouragements from the beginning of the studies.

I greatly appreciate Mr. Zhang who kindly taught me the basics of otolith microstructure analysis and micromilling, and provided the seawater $\delta^{18}O$ data in 2012 and 2013. Thanks are extended to Dr. Yoshiro Watanabe, Assistant Professor Toshiro Saruwatari, Atmosphere and Ocean Research institute, University of Tokyo for providing excellent environment for otolith microstructure analysis.

I am also very grateful to Dr. Takashi Setou, who kindly provided FRA-ROMS model data and performed accuracy analysis on the model data.

Abstract

Sardines, *Sardinops* spp., are short-lived, small pelagic fish that occur widely in temperate areas of global oceans, especially abundant in highly productive areas such as the Kuroshio-Oyashio system or coastal upwelling regions. They efficiently feed on planktons and play crucial roles in energy transfer from low to high trophic levels in marine food webs. Sardines are also economically important because they are a major target of coastal pelagic fisheries. Caught sardines are mainly processed to fishmeal, of which demand is increasing year by year due to the expansion of aquaculture and stock breeding industries or canned for human consumption. However, their abundances are known to fluctuate intensely in multi-decadal scale. The fluctuations are presumably driven by environmental variabilities, although the actual mechanisms have not been revealed. In addition, sardines are highly mobile, and their habitat areas shrink and expand following the variabilities of abundance, which often makes population structures unclear. These cause large difficulties in fisheries managements aiming for sustainable and efficient use of sardine stocks.

Introduction of high-resolution analysis of oxygen stable isotope (δ^{18}O) in otoliths can cut off new aspects of sardine ecology, and thus contribute to solve the problems. Otoliths are calcium carbonate crystals formed in the inner ear of fish. Oxygen stable isotope ratios (δ^{18}O) in otoliths are known to reflect ambient water temperature. Although the application of the isotope analysis has been limited to large otolith species due to the analytical limitation of conventional mass spectrometry, recent remarkable developments in microscale sampling techniques and microvolume analysing systems have opened the door for applications to small otolith species such as sardines. Otolith

$\delta^{18}O$ analysis would allow direct and quantitative estimations of ambient water temperature that the fish experienced, which has never been possible in other methods used in researches of sardine stocks.

Here in this thesis, high-resolution otolith $\delta^{18}O$ analysis was introduced to sardines for the first time in the world, to describe movements and the effect of temperature on growth rates during early life history stages of sardines. By extending the target of the analysis to the sardines off South Africa, Japan and California coasts, I also tried to clarify general differences in ecology of sardines in western and eastern boundary current systems.

At first, the temperature dependence of $\delta^{18}O$ in sardine otolith was calibrated through rearing experiment. Japanese sardine juveniles were reared in three different water temperatures over the course of a month. Otolith $\delta^{18}O$ ($\delta_{otolith}$) was then analysed by extracting the portions formed during the rearing period using a micromill. $\delta^{18}O$ of the rearing water (δ_{water}) was also analysed. A linear relationship between otolith $\delta^{18}O$ and ambient water temperature was identified as follows: $\delta_{otolith} - \delta_{water} = -0.18*T + 2.69$ ($r^2 = 0.91$, $p < 0.01$). This equation is slightly different from that proposed for inorganic aragonite, with resulting application to wild Japanese sardine captured in the Pacific Ocean showing that it estimates a more realistic *in situ* temperature than equations previously used. Therefore, it was concluded that the sardine-specific isotopic fractionation equation should be used when interpreting otolith $\delta^{18}O$ of sardines.

As a first application, geographical differences in nursery environments of the South African sardine were examined to test the multiple stock hypothesis. The sardine is found off entire coast of South Africa, which includes the western cool region dominated by coastal upwelling and the south-eastern warm region dominated by the western

boundary current Agulhas Current, and has recently been hypothesised to be comprised of two or three discrete subpopulations. Sardine otoliths were collected from sardines captured in west, central, south and east coast in summer and winter during 2015–2017, both adults and juveniles, and δ^{18}O and growth rates during the first 2 months from hatch were examined. From west to south coast, adults and summer captured juveniles showed clear longitudinal gradients in both ambient water temperature and growth rates, while the gradient was not evident in winter captured juveniles. The difference between seasons was attributed to the seasonality of upwelling, which are often intensified even in the south coast during summer. It was concluded that sardines in the west and south coast have significant differences in their nursery environments and resulting larval growths, although the extent may vary seasonally, and provided a new evidence that supports the existence of multiple subpopulations in the region.

Next, I tried to figure out how temperature variations contributed to the recent increase of stock abundances of two sardines in the North Pacific, the Japanese and the Pacific sardine. Although many studies concluded that sardine abundance in the western North Pacific increases in cooler period while in the eastern North Pacific the abundance increases in warmer period, the mechanism connecting the environmental change and sardine production has not been revealed. On otoliths of age-0 Japanese sardines collected during 2006–2010 and 2014–15 and age-1 Pacific sardines collected during 1987, 1991–1998 and 2005–2007, δ^{18}O analysis in 15–30 days resolution and microstructure analysis were performed to estimate temperature and growth histories during early life history stages. The mean temperature histories showed the difference in basic thermal environment between the two regions, warmer in the western North Pacific especially in larval stage. The comparison between temperature histories and growth trajectories

showed that in both sides of North Pacific, larval growths are enhanced in relatively warmer waters while juvenile growths showed no or weak negative correlation with temperature, suggesting the general feature of *Sardinops* species. The positive correlations were stronger in the Japanese sardine in larval stages and were stronger in the Pacific sardine in the early juvenile stage, suggesting that the response in the early juvenile stages can be responsible for the response of biomass to the temperature variations. Because the inter-annual variations of temperature were not necessarily associated by cool or warm temperature events, however, other potential drivers, such as predations, need to be considered to fully understand the mechanism of the population fluctuations.

Finally, a method to estimate migration history from otolith δ^{18}O profile by combining numerical simulation was developed, which will be valuable in future studies. Tracking the movement of migratory fish is of great importance in marine biology. Although otolith δ^{18}O has been a potential alternative to tagging and electronic loggers that could not be attached to small fish, the poor resolution of conventional δ^{18}O analysis and the longitudinal homogeneity of open ocean environments have prevented from estimation of migration history. First, using micro-volume carbonate analysing system, otolith δ^{18}O profiles with 10–30 days resolution through entire lives of 6 unmatured Japanese sardines captured in the offshore Oyashio region, were obtained. An individual-based model with random swimming behaviour in a realistic environment generated by a data assimilation model FRA-ROMS was run to search the routes that are consistent with the otolith δ^{18}O profiles. Although otolith δ^{18}O profiles themselves did not show apparent signs of migration, the analysis combined with simulations successfully showed clear northward migration routes heading for the capture point in the Oyashio region. This

method will be a valuable for revealing migration routes in early life stages, thereby providing crucial information to understand population structures and the environmental cause of recruitment variabilities, and to validate and improve fish movement models.

The comparison of sardines in South Africa and North Pacific revealed the general features of *Sardinops* spp. that sardines living in upwelling regions experience lower temperature in the early life stage than those in western boundary current regions, and larval growth are enhanced in warmer waters. Therefore, the basic environment for sardine is different between upwelling and warm current regions, which may be the key to understand why response of the abundance to the temperature variation are opposite between those regions. Overall, I demonstrated that the high-resolution otolith $\delta^{18}O$ is capable of answering scientific questions regarding sardine stocks that need to be solved for effective fisheries managements and also that it may be more powerful when combined with numerical simulations. As the temperature dependence of $\delta^{18}O$ is a general feature of fish otoliths, the technique and the methods described here will be valuable for studying ecology of numerous fishes, thereby leading to better relationships between human and marine living resources in the future world.

Contents

Chapter 1

General Introduction

Sardines, *Sardinops* spp., are short-lived, small pelagic fish that are distributed widely in global temperate oceans, especially abundant in highly productive areas such as the Kuroshio-Oyashio system or coastal upwelling regions off the west coast of continents (Fig. 1). The shallow genetic divergences between and within regional populations suggested a common ancestry about 200-500 kya (Okazaki et al., 1996; Bowen and Grant, 1997) and thus genus *Sardinops* is considered to be comprised of three subspecies, rather than species, which are *Sardinops sagax ocellatus* in southern Africa, Australia and New Zealand, *Sardinops sagax sagax* in South and North America, and *Sardinops sagax melanostictus* in western North Pacific (Grant and Bowen, 1998). They efficiently feed

on phytoplankton and zooplankton (van der Lingen et al., 2006), and often dominate the ecological niche of plankton feeders together with anchovies, playing crucial roles in energy transfer from low to high trophic levels in marine food webs (Cury et al, 2000). Sardines have also been major targets of pelagic fisheries in many coastal regions, supporting economies of coastal country with their large abundance. The captured sardines are mainly processed into fishmeal (Merino et al., 2014), of which demand is increasing year by year due to the expansion of stock breeding aquaculture (Naylor et al., 2000; Merino et al., 2012), or canned for human consumption. Therefore, sardines are key species in coastal marine system both ecologically and economically, and humans need to manage fisheries on sardines in efficient and sustainable ways.

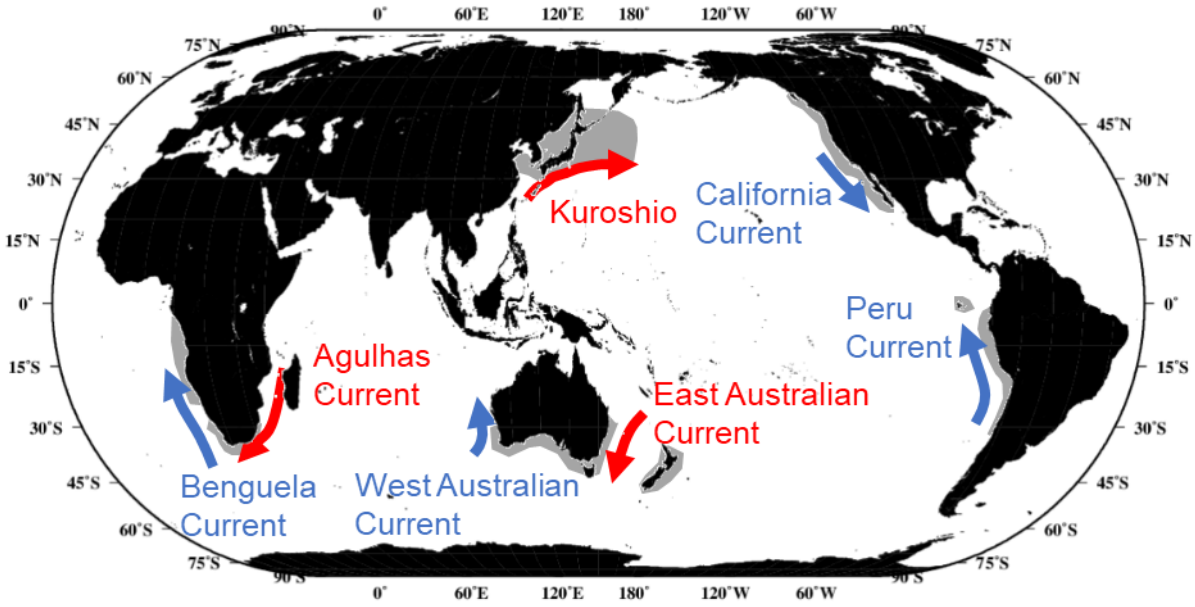

Figure 1. Schematics of Distribution of *Sardinops* spp. (gray shaded) and western (red) or eastern (blue) boundary currents nearby. Sardine distribution was drawn based on Parrish et al. (1989) and Checkley et al. (2009).

However, successful managements on sardine fisheries are not easy. In the 20th century, sardine stocks have exhibited intense fluctuation, even in two orders of

magnitudes in some regions, in multi-decadal scales (Schwartzlose et al., 1999). Many studies have concluded that basin-scale environmental variabilities have drove the fluctuations of abundance of sardine stocks, rather than fishing pressures (e.g. Chavez et al., 2003). However, there has been no theory that can fully explain the fluctuations, which makes future predictions difficult. In addition, sardines are highly mobile, and their habitat areas shrink and expand following the variabilities of abundance (Barange et al., 2009), which often makes population structures unclear. Without the accurate knowledges of population structures, fisheries can exert an unexpectedly high pressure on certain regional populations, leading to overfishing of some stock components (Coetzee et al., 2008).

One large obstacle in solving these problems is the difficulty of tracking the locations and the ambient environments of fish in open ocean. With this information, it would be possible to more closely examine how environmental variabilities affect fish survivals or understand how regional populations move and mix each other, although obtaining the information has not been easy because sardines, especially during larval and juvenile stages, are too fragile to put artificial tags on them. Recently, numerical models that simulate realistic ocean environments and fish movements have been developed (e.g. Rose et al., 2015). However, observation data that can complement and validate model simulations is still missing, due to the lack of appropriate technique.

The oxygen stable isotope ratio ($\delta^{18}O$) in otolith might change the situation. Otoliths are calcium carbonate crystals formed in the inner ear of fish, and their chemical composition is known to record ambient water chemistry (Campana, 1999). In particular, the oxygen stable isotope ratio reflects both temperature and $\delta^{18}O$ of surrounding water (Kim et al., 2007), and thus has often been used as a temperature proxy (e.g. Carpenter,

2003; Shiao et al., 2009). Because conventional isotope ratio mass spectrometry required large sample amounts, the application of otolith $\delta^{18}O$ has been limited to fish species with large otoliths. However, recent developments in techniques to analyse $\delta^{18}O$ in calcium carbonates are remarkable. For example, high-precision micromilling system Geomill 326 that can move the drill pit in 1/1000 mm scale was developed (Sakai, 2009). Moreover, the analysing system MICAL3c has been developed, which requires only 0.2 μg, approximately 1/100 of the sample quantity required for conventional mass spectrometry (Ishimura et al., 2004; 2008; Nishida and Ishimura, 2017). These technical improvements will allow an accurate analysis of narrow growth increments in small otoliths and provide direct estimates of the ambient temperature that sardines experienced in their early life history, which has never been possible in other methods used in researches studying sardines.

In this study, the high-resolution otolith $\delta^{18}O$ analysis to sardines is performed for the first time in the world to cut off new aspects of sardine movements and growth during early life history stages, which may contribute to solve the issues regarding sardine stocks. By extending the target of the analysis to the sardines off South Africa coast which includes both western boundary current and coastal upwelling systems (Fig. 1), and off Japan and California coasts which are typical western boundary current and coastal upwelling region, respectively, I also aimed to clarify general differences in ecology of sardines in western and eastern boundary current systems. Furthermore, I try to develop a new method to estimate migration history of sardine based on otolith $\delta^{18}O$ profiles and numerical simulations, which allows more detailed description of fish migrations in future studies.

This thesis is comprised of 6 chapters including this general introduction. Before

challenging the actual problems, the temperature dependence of otolith $\delta^{18}O$ in sardine through rearing experiment was confirmed and calibrated, which is described in Chapter 2. In Chapter 3, otolith $\delta^{18}O$ analysis was introduced to the South African sardine that is widely distributed off South African coast, to understand its population structure. In Chapter 4, $\delta^{18}O$ analysis was performed to archived otoliths of the Japanese sardine and the Pacific sardine that live in either side of the North Pacific, to give insights into the effect of temperature on the fluctuations of their biomass. In Chapter 5, a newly developed method to estimate migration history of sardines using otolith $\delta^{18}O$ analysis and numerical simulation is described. Finally, in Chapter 6, directions for future studies are discussed based on comparisons between the regions.

Chapter 2

Temperature dependence of $\delta^{18}O$ in otolith of juvenile Japanese sardine: laboratory rearing experiment with micro-scale analysis

2.1 Introduction

The Japanese sardine larvae and juveniles travel a long distance from the temperate Kuroshio region to the subarctic Oyashio region during spring to autumn. Environmental factors such as temperature and food density along the migration route have been suggested to affect survival rate and ultimately control recruitment abundance (Takasuka et al., 2007, 2008, Takahashi et al., 2008, 2009, Nishikawa et al., 2013). These hypotheses have yet to be verified since it is difficult to accurately define the environment that the

sardine individuals experience during migration. For large bodied species such as the bluefin tuna, archival tagging has been a useful tool for tracking the migration routes of individuals (e.g. Block et al., 2005). Due to their small size and fragility, it is impossible to tag a larval or juvenile sardine. Due to this limitation, estimates have been made using numerical models (Okunishi et al., 2009, 2012). Modelling approaches are inherently based on many assumptions, often difficult to validate (Humston et al., 2000) and the accuracy of the results must be verified by comparison with *in situ* data. A new method to determine the environmental factors that sardines experience during early life stages is therefore necessary.

The stable oxygen isotope ratio ($\delta^{18}O$) in biogenic carbonates has often been used as a temperature proxy of ambient water. The otolith of fish is mainly composed of aragonite (Campana, 1999) and the temperature dependency of otolith $\delta^{18}O$ has been quantified in various species (Kalish et al., 1991; Thorrold et al., 1997; Høie et al., 2004; Storm-Suke et al., 2007; Godiksen et al., 2010; Geffen, 2012; Kitagawa et al., 2013). This temperature dependency is often expressed using the following simplified formula, referred to as the fractionation equation:

$$\delta_{otolith} - \delta_{water} = a*T + b \qquad (1)$$

where $\delta_{otolith}$ is the $\delta^{18}O$ of the otolith, δ_{water} is the $\delta^{18}O$ of ambient water, and T is the temperature of ambient water, while a and b are constants. Generally, the fractionation equation constants of otoliths are not significantly different from those reported for inorganic aragonite (Kim et al., 2007), indicating that the otolith is formed in or near isotopic equilibrium with ambient water (e.g. Høie et al., 2004). Several authors have noted that the intercepts in Eq. (1) differ significantly among species, although the slopes are similar (Høie et al., 2004; Storm-Suke et al., 2007; Godiksen et al., 2010). Hence, to

obtain an accurate estimation of the temperatures an individual has experienced, species- or genus-specific fractionation equations have been recommended instead of the equation for inorganic aragonite (Storm-Suke et al., 2007; Godiksen et al., 2010).

In the Japanese sardine, temperature dependency of otolith $\delta^{18}O$ has not been quantitated. Regarding species in the *Sardinops* genus, Dorval et al. (2011) determined the following formula for the Pacific sardine, *Sardinops sagax sagax*, from rearing experiments using three different temperatures:

$$\delta_{otolith} - \delta_{water} = -0.132*T + 2.455. \quad (2).$$

It should be noted that the slope of Eq. (2) is exceptionally gradual compared to those of inorganic aragonite and other species examined previously. One limitation of this equation is that Dorval et al. (2011) estimated the $\delta^{18}O$ of the otolith deposited during the rearing period indirectly by calculating a mass-balance relationship. This calculation is based on the trend across the whole otolith $\delta^{18}O$ composition with an increase of otolith weight expected with growth (Kalish, 1991; Høie et al., 2004). The use of this estimation was inevitable since the newly formed region of the otolith was too small to directly analyse the isotopic composition by conventionally used mass spectrometry. Due to indirect estimation being inherently uncertain, Eq. (2) must be tested for the ability to precisely estimate temperatures experienced by the Japanese sardine.

In the present study, we aimed to accurately determine the relationship between temperature and otolith $\delta^{18}O$ of the Japanese sardine. To accomplish this, juvenile Japanese sardines were reared at three different temperatures. Using a micro-volume analyser and micro-scale sampling techniques, the oxygen isotope composition of the otolith regions deposited during the rearing period were directly analysed, which minimized potential errors that could be caused by indirect estimation.

2.2 Materials and Methods

2.2.1 Laboratory experiments

Juvenile Japanese sardines were caught in Sukumo Bay, in the Kochi Prefecture of western Japan, in April 2015, and were transported to the Hakatajima station (Ehime Prefecture) of the National Research Institute of Fisheries and Environment of Inland Sea, Japan Fisheries Research and Education Agency. A total of approximately 200 specimens were maintained in a 2-ton circular tank under a photoperiod cycle of 14 h light and 10 h dark. A total of 59 specimens randomly selected were available for otolith analysis. Fish were fed daily with approximately 3% of their body weight (g) of commercial dry pellets (Marubeni Nisshin Feed Co., Ltd., Tokyo, Japan, New Arteck: protein 52%, oil 11%, ash 18%, fiber 3%).

Specimens were kept at three different temperatures maintained using a hot water circular pump system or cooler (IWAKI Co., Ltd, Tokyo, Japan, REI-SEA FZ-602AY). The water temperature in the tank was recorded every hour using a data logger (Onset, MA, USA, Tidbit V2). First, specimens were kept in the 2-ton rearing tank at temperatures ranging from 18°C to 19°C for 35 days and then were reared in water at 22°C for 35 days. Finally, a total of 20 randomly selected specimens were kept in the 1-ton rearing tank at temperatures ranging from 14°C to 15°C for 28 days, after two days for assimilation prior to the start of the experiment. The filtered seawater exchange rate was maintained at 360% (300 L h^{-1}) of tank volume/day in the 2-ton rearing tank, while it was maintained at 180% (75 L h^{-1}) of tank volume/day in the 1-ton rearing tank. The ranges of dissolved oxygen and pH over the experiments were 5.8–6.3 mg/L and 6.9–7.5, respectively. At the end of each period characterized by a constant temperature, 19–20 juveniles were randomly removed from the tank. Standard lengths of the individuals were measured before freezing.

Rearing water samples for isotopic analysis were taken from the tank at least twice during each fixed temperature period. Water samples were placed in 2 mL glass screw vials and preserved in a refrigerated storage area until isotopic analysis to prevent evaporation.

2.2.2 $\delta^{18}O$ analysis of otoliths and rearing water

Sagittal otoliths were dissected out and adherent bits of tissue were removed using a needle and a thin paintbrush under 10–20 magnification. Otoliths were rinsed with Milli-Q water and air-dried for 2–3 hours. After these cleaning procedures, otoliths were embedded in epoxy resin Petropoxy 154 (Burnham Petrographics LLC), ground with sandpaper (no. 2000), polished with a lapping film (no. 4000), and smoothed with alumina polishing suspension (BAIKOWSKI International Corporation).

Otolith microstructures were observed using an otolith measurement system (Ratoc System Engineering Co. Ltd., Tokyo, Japan). To distinguish the portion of the otolith recently deposited during the rearing period from that deposited when individuals were maintained in a tank at a constant temperature, 28 daily rings were counted from the edge of otoliths with clearly visible rings. Otoliths with indistinctive increments were excluded from further analysis. Photos were taken of each area distinguished for micro-scale sampling (Fig. 1a).

Newly deposited areas were extracted using a high-precision micromilling system (GEOMILL326, Izumo-web, Japan). This system consisted of a micromill, a CMOS camera, a video monitor, and an image analyser controlled by a computer, and allowed for accurate sampling at 1/1000 mm scales, which enabled us to avoid contamination of pre-experiment otolith material (Sakai, 2009). After milling, otolith powder was collected into an aluminum micro-Petri dish for isotope analysis. It was confirmed that the drill pass did not invade the inner area by checking each remaining

portion of the otolith using the otolith measurement system (Fig 1b).

Stable oxygen isotope ratios of the otolith powder were determined using a continuous-flow isotope ratio mass spectrometry system (MICAL3c with IsoPrime 100) at the National Institute of Technology, Ibaraki College. Using this system, the $\delta^{18}O$ of ultra-microvolume carbonate samples (as low as 0.2 μg) were analysed with high precision and accuracy (Ishimura et al., 2004, 2008, Kitagawa et al., 2013), which allowed to directly analyse the portion deposited during the rearing experiment. Collected powder was reacted with phosphoric acid at 25°C, and the resulting liberated CO_2 gas was introduced into the mass spectrometer via vacuum purification line. The $\delta^{18}O$ values were reported in δ-notation against the VPDB (Vienna Pee Dee Belemnite) reference standard, and given as a ‰ value. Reproducibility was better than ± 0.10 ‰ or lower throughout the entire analysis. In order to facilitate the comparison with isotopic values reported in previous studies, the acid fractionation factor of calcite was used.

Oxygen isotope composition of rearing water samples was determined using the Picarro L2120-i Analyser at the Atmosphere and Ocean Research Institute, University of Tokyo. Before introduction into the analyser, samples were filtered using membrane filter (pore size: 0.45 μm, Toyo Roshi Kaisha, Ltd.) to reduce suspended particles in order to avoid blocking the sampling line. Data were reported in δ-notation against the VSMOW (Vienna Standard Mean Ocean Water) reference standard and long-term instrument reproducibility was ± 0.08 ‰.

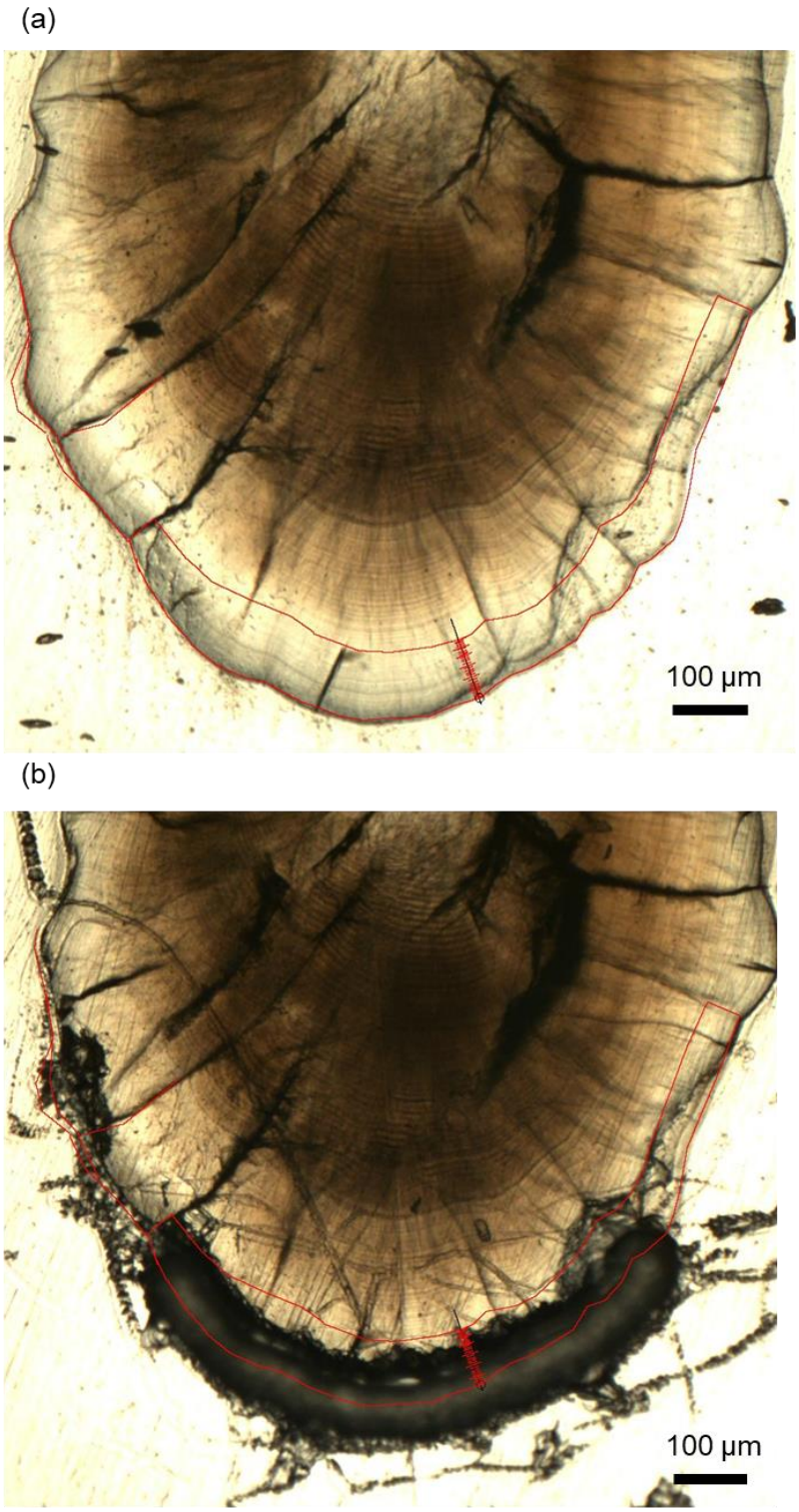

Figure 1. Otolith image (a) before milling and (b) after milling. The newly deposited area during the rearing period was identified by counting 28 daily increments (short red lines) from the edge, and was the portion extracted.

2.3. Results

The average temperatures during the 28 days before sampling were 14.6°C, 18.7°C, and 22.0°C for each experiment and the mean $\delta^{18}O$ values of the rearing water were -0.56‰, -0.38‰, and -0.39‰, respectively. During each experiment, fluctuations of water $\delta^{18}O$ and temperature were kept at a low level (standard deviation < 0.07‰ and < 0.10°C, respectively).

Standard lengths of captured juveniles ranged from 65.2 to 109.2 mm. Within the total of 59 individuals available, 28 otoliths had indistinct daily rings at the edge. Ultimately 10, 10 and 11 otolith $\delta^{18}O$ samples for lower, medium and higher rearing temperature, respectively, were analysed. The average and SD values of $\delta^{18}O$ for the otoliths from each rearing temperature were -0.35 ± 0.21‰ at 14.55°C, -1.23 ± 0.15‰ at 18.67°C and -1.61 ± 0.16‰ at 22.02°C, revealing a negative correlation between otolith $\delta^{18}O$ and temperature. The sample with an exceptionally high $\delta^{18}O$ value (+0.22‰) from the lowest rearing temperature was regarded as an outlier (Grubbs' test, $p < 0.01$) and was excluded from further analysis. Linear regression between the temperature and oxygen isotope fractionation using the least square method demonstrated a relationship described by Eq. (1) for the Japanese sardine as follows:

$$\delta_{otolith} - \delta_{water} = -0.18*T + 2.69 \qquad (r^2 = 0.91,\ p < 0.01), \qquad (3)$$

where the standard error was ± 0.18 ‰ including analytical error (± 0.10‰).

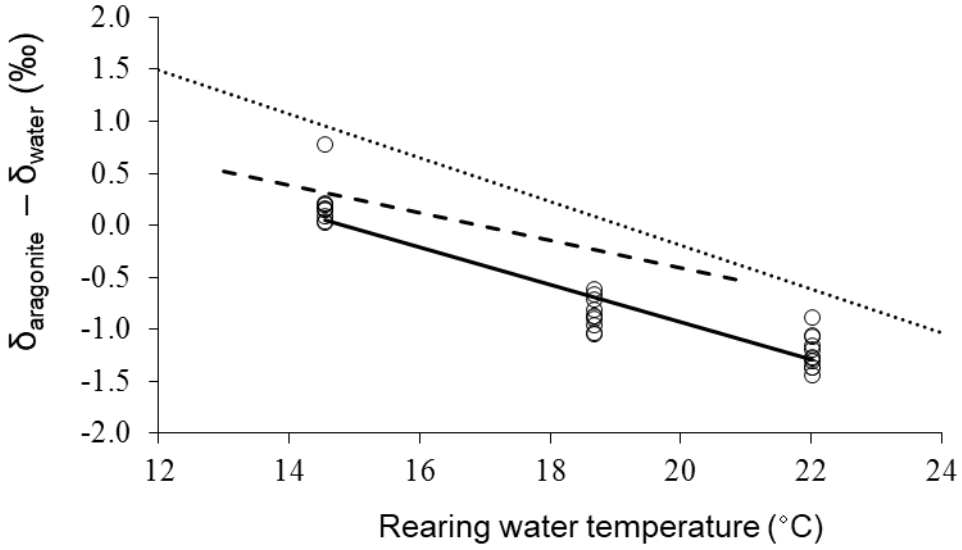

Figure 2. Comparison of fractionation relationship for Japanese sardine (open plots and solid line) and inorganic aragonite (dotted line), recalculated from Kim et al., (2007) using an acid fractionation factor of 1.01025 to facilitate comparison (Sharma & Clayton, 1965), and Pacific sardine (dashed line, Dorval et al., 2011). Y-axis stands for carbonate $\delta^{18}O$ in VPDB scale minus water $\delta^{18}O$ in the VSMOW scale.

2.4. Discussion

If the otolith were deposited in equilibrium with ambient seawater, the relationship between otolith $\delta^{18}O$ and temperature was expected to be consistent with the expression proposed for inorganic aragonite by Kim et al. (2007):

$$1000\ln\alpha_{aragonite\text{-}water} = 17.88*1000/(T+273.15) - 31.14, \quad (4)$$

where

$$\alpha_{aragonite\text{-}water} = (\delta^{18}O_{aragonite} + 1000)/ (\delta^{18}O_{water} + 1000).$$

Even though many authors have concluded that oxygen isotope fractionation in the otolith occurs at, or near, equilibrium with ambient water, some studies noted differences in the intercept of fractionation equations among species (Høie et al., 2004; Storm-Suke et al., 2007; Godiksen et al., 2010). Eq. (3) shows a similar slope but an approximately 0.8‰

lower intercept in comparison with Eq. (4) (Fig. 2). Even though Eq. (3) is similar to a range of other published fractionation equations for fish otolith (Fig. 3), the 0.8‰ difference in the intercept corresponds to 4°C difference in temperature estimation. Therefore, it was suggested that oxygen isotope fractionation in the otolith of Japanese sardine juveniles occurs near, but not exactly at equilibrium with ambient water.

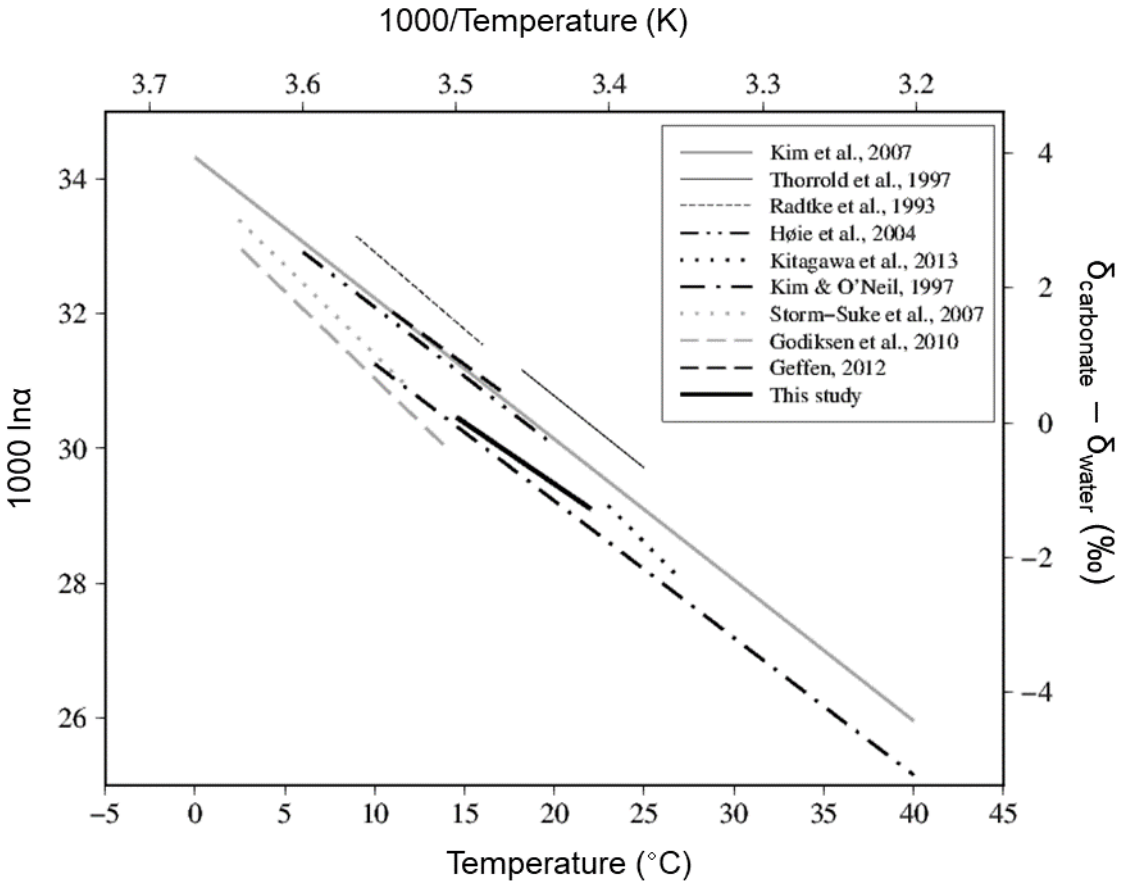

Figure 3. Comparison of the result of this study with previously reported fractionation equations for other fish species and inorganic aragonite−water. Left Y-axis represents one thousand-fold of $\alpha = (\delta^{18}O_{aragonite} + 1000)/ (\delta^{18}O_{water} + 1000)$. The calcite−water isotope fractionation curve of Kim & O'Neil (1997) was also included.

To precisely estimate ambient water temperature from the $\delta^{18}O$ of the otolith of the Japanese sardine, I recommend Eq. (3) for Japanese sardine juveniles, instead of Eq.

(4), which is used for inorganic aragonite. Oda et al. (2016) reported the δ^{18}O of the edge of otolith of wild Japanese sardine captured in the Pacific Ocean and estimated temperature using Eq. (4). The calculated temperatures were inconsistent with those *in situ*. For example, the averages were 17.2°C for the offshore group and 28.6°C for the coastal group, which were 7.2°C and 4.5°C higher than the *in situ* temperature at the sampling point, respectively. Temperature estimations calculated using Eq. (3) for Japanese sardine juveniles, lead to a more realistic value, with estimated temperatures of 12.8°C and 25.7°C on average, and discrepancies from the *in situ* temperature were significantly lowered to 2.8°C and 1.6°C, respectively.

Both fractionation equations for the Pacific sardine (Eq. (2)) and the Japanese sardine (Eq. (3)) consistently calculated lower temperature than those determined using the equation for the inorganic aragonite (Fig. 2). Both slope and intercept were different between Eq. (2) and (3). These differences may have been caused by the variation in methodology. Dorval et al. (2011) did not directly measure the δ^{18}O of otolith regions deposited in the rearing period but instead estimated them using the mass balance relationship equation:

$$\delta^{18}O_{total,\,x} = \delta^{18}O_0\,(M_0/M_x) + \delta^{18}O_{0\text{-}x}\,((M_x - M_0)/M_x),$$

where $\delta^{18}O_{total,\,x}$ is the mean δ^{18}O measured at the end of time x, $\delta^{18}O_0$ is the mean isotope ratio measured at time 0 from the baseline sample, and $\delta^{18}O_{0\text{-}x}$ is the mean isotope ratio of the otolith material deposited from time 0 to time x (Dorval et al., 2011). M_0 and M_x represent otolith weight of the baseline sample and the sample collected at time x (Dorval et al., 2011), respectively. Accuracy of the calculation is strongly affected by the accuracy of the otolith weight at the given time, and is inherently difficult to access. The slope obtained in the present study (-0.18), based on direct analysis of growth increments during

the rearing period, was similar to that for inorganic carbonate (Kim et al., 2007) and the otolith of other species (Thorrold et al., 1997; Høie et al., 2004; Storm-Suke et al., 2007; Geffen, 2012), suggesting that Eq. (3) is more appropriate for sardines. Still, it cannot completely be denied that some other effects, such as difference in body size and life stage, or habitat region, have made the difference in the equations. Therefore, although the Eq. (3) would be used for sardines from all regions throughout this thesis, validations using samples from each life stage and region are needed in future for further accurate calculations of temperature.

The methodologies used in this study could also be useful for understanding the temperature history of other fish species. For species that have otoliths with visible daily rings, the combination of daily ring reading and the accurate micro-milling technique will allow us to extract the otolith area deposited in any age range of interest. Specifically, with the help of ultra-microvolume isotope analysis, the temperature history during the larval and juvenile stages can be estimated, which could be a key factor determining recruitment variability. Utilizing the ultra-microvolume isotope analysis, it is possible to apply the otolith micro-milling technique to small fish species, among which analysis previously limited by the detection threshold of conventional isotopic ratio mass spectrometry.

Chapter 3

Testing the multiple-stock hypothesis of the South African sardine using oxygen stable isotope ratio in otolith

3.1 Introduction

South Africa is a special country where we can see both eastern boundary current upwelling system and western boundary current system within a continuous coastline (Fig. 1). The west coast is a typical coastal upwelling region, where atmospheric pressure system seasonally creates strong alongshore winds (Hutchings et al., 2009). The winds push surface waters offshore through Ekman drift, and upwelling of cool deep waters for compensation provide nutrients to the euphotic zone, which result in high plankton productions in coastal area especially during austral summer. In contrast, the east coast is

dominated by the fast and warm Agulhas Current throughout year. The western-boundary current runs south-westwards following the continental shelf, which produces warm, oligotrophic and advective environment in the east to south coast. Located between the west and east coasts, the south coast is characterised by the broad shelf called the Agulhas Bank, which is an irregular extension of the South African coastal plain. The hydrological condition on the Agulhas Bank is primarily related to strong forcing by the Agulhas Current in the outer shelf and wind driven upwelling in the inner shelf, but shows complex patterns both spatially and temporally due to the smaller structures such as meanders and frontal eddies, or midshelf and shelfbreak upwellings (Swart and Largier, 1987). Among this drastic geographical variation of environment, the South African sardine *Sardinops sagax ocellatus* is found off entire coast.

Sardine has been a major target in the small pelagic fishery off west and south coasts of South Africa. Since the establishment of sardine fishery in South Africa in the late 1940s, the annual catch ranged from 16000 to 410000 tons over the period 1950-2015 (de Moor et al., 2017), with two large peaks in mid-1960s and mid-2000s. Sardine had only been exploited from the west of Cape Agulhas before 1987 but in recent decades the catch from the east of Cape Agulhas has become to occupy a significant portion in the total catch, even more than half during some years in late 2000s. Sardine is also caught in the east coast by local fishery communities using beach-seines, although the amount has never exceeded 1% of the catch from the west and south coasts (van der Lingen, 2010). However, the economic value of sardine off the east coast is recently increasing due to the growth of tourism (van der Lingen, 2010). In every austral winter, some portion of sardine population is known to show long migration from the Agulhas Bank up the east coast to Durban, which is called the “Sardine run”. This migration is accompanied by

many marine predators such as whales, dolphins, sharks and seabirds, which provides opportunities to witness the dynamic interaction between prey and predator and thus attracted numerous tourists in recent years.

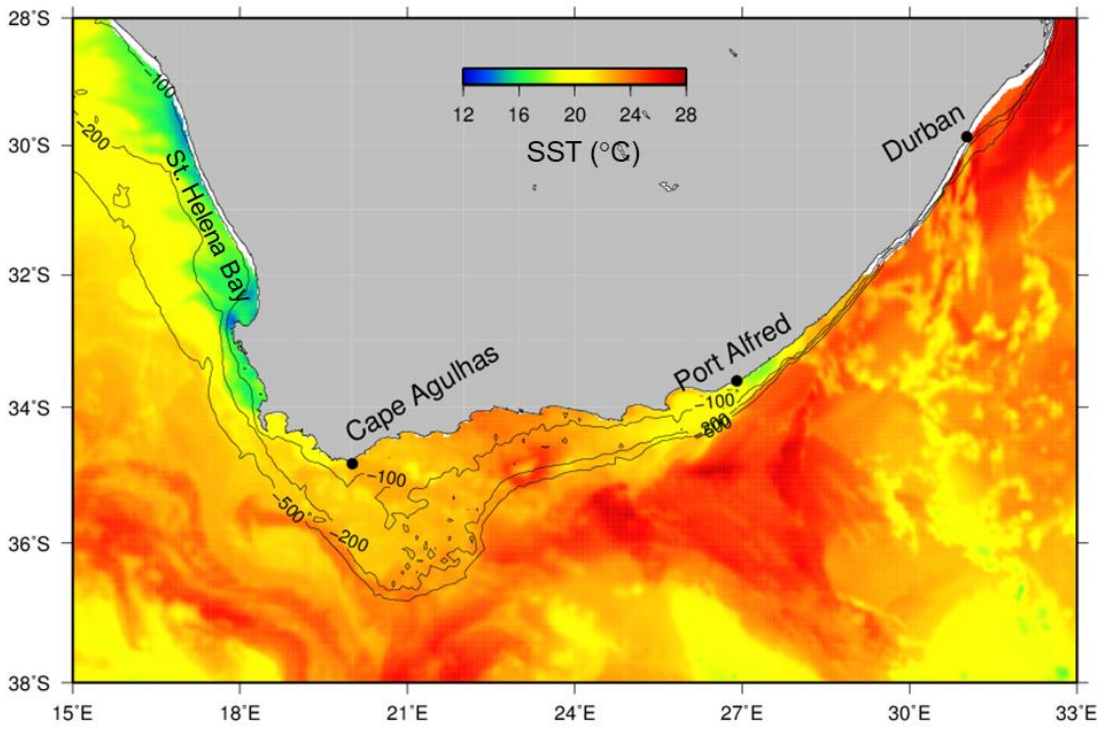

Figure 1.Typical distribution of sea surface temperature in summer.
Satellite based SST product for 1th January 2017 from GHRSST Level 4 OSTIA Global Foundation Sea Surface Temperature Analysis (JPL OurOcean Project, 2010) is shown together with bathymetry. The intense costal upwelling in the west of Cape Agulhas and the warm Agulhas current flowing south-eastward following the shelf edge are clearly evident. Smaller scale upwelling is also present around Port Alfred.

Understanding the population structure of such an exploited species is crucial for sustainable fishery. In the management of South African purse-seine fisheries, the sardine off the west and south coasts had been treated as a single stock. However, the possible existence of several discrete subpopulations on the west, south and potentially east coast that have different spawning grounds, has been suggested recently. This idea was initially based on the finding that distributions of sardine adults and eggs are separated into two at around central Agulhas Bank during low to medium biomass periods (Coetzee et al.

2008; van der Lingen, 2011). Since, the hypothesis, referred to as the “multiple-stock hypothesis”, has been tested through various methods. The individual based model coupled with 3-D hydrodynamic model showed that sardine recruitment pattern can be divided into two main systems at around Cape Agulhas (~20°E) (Miller et al., 2006). A “tetracotyle”-type metacercarian parasite of the genus *Cardiocephaloides* was also used to detect the separation of subpopulations, and showed that the prevalence, infection intensity and abundance of the parasite are strongly different between sardines from west and south coast (Weston et al., 2015; van der Lingen, 2015). More recently, a genetic study using evolutionary neutral, single nucleotide polymorphism markers showed that sardines in the west, south and east coast have a genetic structure called the “isolation by distance”, which indicates that the sardines are not panmictic (Teske et al., 2018). These studies suggest that the exchanges between individuals in the west and the east of Cape Agulhas are limited to some extent, supporting the existence of several discrete subpopulations. However, although spawning in each potential subpopulation occur at the shelf-edge and larvae and juveniles are assumed to recruit inshore (Fig. 2), the actual movements in the early life stages and differences of ecological characteristics between the potential subpopulations, such as nursey environment and the resulting growth rates, are yet to be addressed.

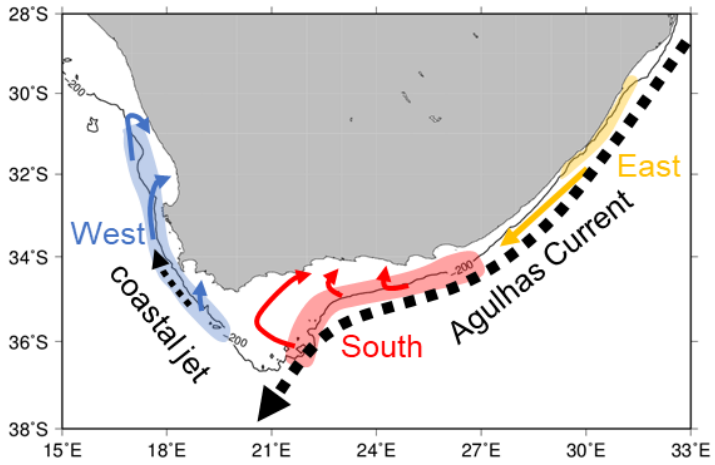

Figure 2. Schematics of presumed spawning grounds (shaded) and movement patterns in early life stage (arrows) for each sub-populations.
Spawning grounds are drawn based on van der Lingen (2011) for west and south coast and Connel (2010) for east coast.

Otolith, a calcium carbonate crystal formed in the inner ear, records various kinds of information of fish life. In the larval and juvenile stage, clear daily rings are formed in sardine otoliths (e.g. Hayashi, 1989). As otolith radius is strongly correlated to body length, the width between the rings can be used as a proxy of daily growth, thereby allowing to reveal the growth trajectory in early life stages (Campana, 1990). Moreover, the chemical composition of otolith reflects ambient water chemistry and as otoliths are metabolically inert, the composition is preserved even after the fish died (Campana, 1999). Because the oxygen stable isotope ratio (δ^{18}O) in otolith is known to sensitively reflect temperature and δ^{18}O of ambient water (e.g. Hoie et al., 2004), analysing otolith δ^{18}O for the first several months of life can specify nursey environment the fish had utilised.

In this study, nursery temperatures and early life growth rates of sardines along the South Africa coast were examined using otolith δ^{18}O and microstructure analyses, in order to test the multiple-stock hypothesis. The continental shelf in the South Africa coast was divided into four regions by longitude; West (< 20°E), Central (20-22°E), South (22-

27°E) and East (> 27°E), and obtained adult (> 14cm CL (Caudal Length)) and juvenile (< 14 cm CL) sardines from all regions to observe geographic differences in sardine ecology. The distribution of seawater $\delta^{18}O$ was also investigated along the entire coast to support the interpretation of otolith $\delta^{18}O$.

3.2 Materials and Methods

3.2.1 Seawater sampling and $\delta^{18}O$ analysis

Near-surface seawater samples for isotope analysis were collected from the entire coast of South Africa, during the two cruise surveys and nearshore samplings during 2017 winter (Fig 3a). In the 2017 pelagic recruitment survey conducted by the Department of Agriculture, Forestry and Fisheries (DAFF) in west to south coast during June to July 2017, seawater pumped up by the Continuous, Underway Fish Egg Sampler (CUFES) were collected at in-shore and off-shore points of each line transect. In another hydrographic survey conducted in the south to east coast during July to August 2017, seawater samples were collected at 5 m depth by CTD-attached Niskin bottles Samplers. All samples, taken as duplicates, were preserved in sealed 10 ml glass-vials to avoid evaporation and air-transported to Japan. Within each sample, 2 ml were membrane-filtered (pore size: 0.45 μm, Toyo Roshi Kaisha, Ltd.) for isotope analysis to reduce suspended particles and avoid blocking the sampling line. $\delta^{18}O$ of the samples were analysed at the National Institute of Technology, Ibaraki College using the Picarro L2120-i system with precision better than ± 0.05 ‰.

3.2.2 Otolith samples

Adult and juvenile sardines were collected from coastal to shelf waters off the west, the

south and the east coast of South Africa during 2015 to 2017 (Fig. 3b-d). Adults, typically 16-18 cm CL, were collected from 3 and 11 midwater trawl samples taken during the 2015 pelagic recruitment survey in June 2015, and the 2016 pelagic biomass survey in November to December 2016, respectively (Fig. 3b). Juveniles, 6-12 cm CL, were collected from 2, 8 and 10 midwater trawl samples taken during the 2016 and 2017 pelagic biomass survey in November to December (Fig. 3c) and the pelagic recruitment survey in June 2017 (Fig. 3d), respectively. Additional samples collected from the east coast using a beach-seine net were obtained in 2015 June and 2017 July, of which size range were 14-17 and 14-19 cm CL, respectively. The latter was divided into two groups with their body length larger or smaller than 15 cm CL, and referred to as adults and juveniles, respectively, considering the faster growth in the warm eastern region. Samples were frozen shortly after capture and defrosted at DAFF to extract the sagittal otoliths, which were air-transported to Atmosphere and Ocean Research Institute, the University of Tokyo, Japan (AORI) for microstructure and isotope analyses.

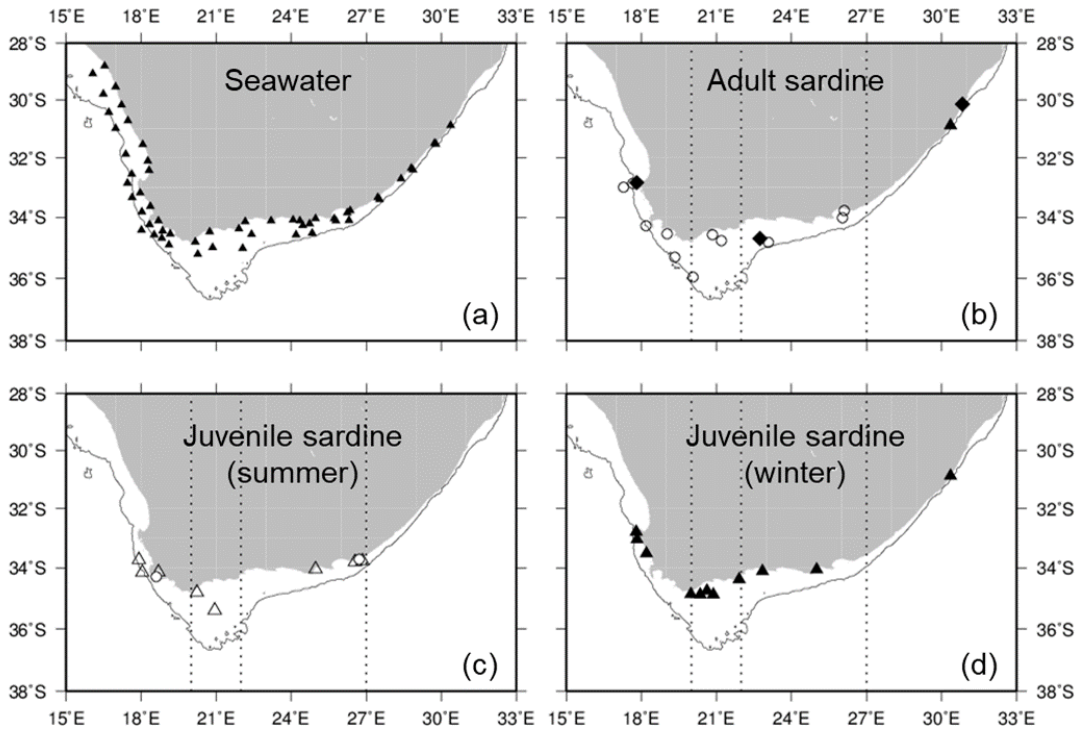

Figure 3. Sampling locations of (a) sub-surface seawater, (b) adult sardine, (c) juvenile sardine captured in summer and (d) juvenile sardine captured in winter.
The shape and filled/open represent the sampling year and season, respectively. (♦: 2015, ●: 2016 and ▲: 2017, and filled: winter (June to August) and open: summer (November to January)).

3.2.3 Otolith growth analysis

Otoliths were cleaned using wooden toothpicks and thin paintbrushs under 10–20× magnification, rinsed with Milli-Q water, and air-dried for a few hours. Otoliths were then embedded in Petropoxy 154 (Burnham Petrographics LLC) resin and kept at 80 °C for 12 h to cure the resin. Embedded otoliths were ground with sandpaper (no. 2000) and polished with an alumina suspension (BAIKOWSKI International Corporation) to reveal the daily rings. The position and number of daily rings in otoliths were examined from the core as far as possible along the axis of the postrostrum using an otolith measurement system (RATOC System Engineering Co. Ltd.). The daily rings became indistinct after 100-150 counts from the core before reaching the edge in most of the samples, except for the juveniles captured in June-July 2017 for which estimations of hatch date were possible.

The first daily ring was assumed to be formed after 3 days post hatch (dph) based on the observation that the mean difference between larval age and daily ring counts for 18 pilchard larvae reared in the laboratory from eggs collected at sea was 3.3 days (Thomas, 1986). The daily increment widths were averaged in 10 days intervals (3-10, 11-20, 21-30, …, 91-100 dph) for each individual, then the mean within each station was calculated for comparison between regions. From the otolith radius at 60 dph, corresponding body length was calculated by using the linear relationship between standard length and otolith radius of juvenile Japanese sardine (Takahashi et al., 2008) for comparison with isotope data.

3.2.4 Otolith isotope analysis

For up to 8 individuals per station, the otolith area formed during the first 60 days was milled out using the high-precision micro-milling system Geomill 326 for isotope analysis. The resulting powder was collected using a stainless micro-cup, and the $\delta^{18}O$ was measured at AORI using the DELTA V plus system with precision of ± 0.10-0.16 ‰. The $\delta^{18}O$ values were reported in δ-notation relative to the VPDB (Vienna Pee Dee Belemnite) scale, and given as a ‰ value.

To exclude the effect of seawater $\delta^{18}O$ variation on otolith $\delta^{18}O$ and convert the otolith $\delta^{18}O$ difference to temperature scale, water temperature was calculated from otolith $\delta^{18}O$ based on the relationship between otolith $\delta^{18}O$ and temperature established for the Japanese sardine (Sakamoto et al., 2017; $\delta_{otolith} - \delta_{seawater} = -0.18*T + 2.69$), to which seawater $\delta^{18}O$ estimated from longitude using the fitted quadratic function (see Results) was substituted.

3.3 Results

3.3.1 Distribution of seawater $\delta^{18}O$

The near-surface seawater δ^{18}O analysed at 50 locations along the entire coast of South Africa showed a strong longitudinal variation, together with an inshore-offshore difference. In the St. Helena Bay where strong upwelling cells exist, seawater δ^{18}O was relatively low around +0.2 ‰. Seawater δ^{18}O increased with longitude until about 23 °E where the shelf narrows, then became relatively stable at +0.5-+0.6 ‰ in the south and east coast (Fig. 4a). Off-shore stations generally showed higher value than nearby in-shore stations throughout the entire coast (Fig. 4b). A quadratic curve for δ^{18}O-longitude relationship was fitted to express the geographical variation of δ^{18}O by the least squares methods as follows; $\delta^{18}O = -0.003*(Longitude)^2 + 0.1578*(Longitude) - 1.5505$ ($r^2 = 0.57$, $p < 0.001$, root mean square error = 0.09).

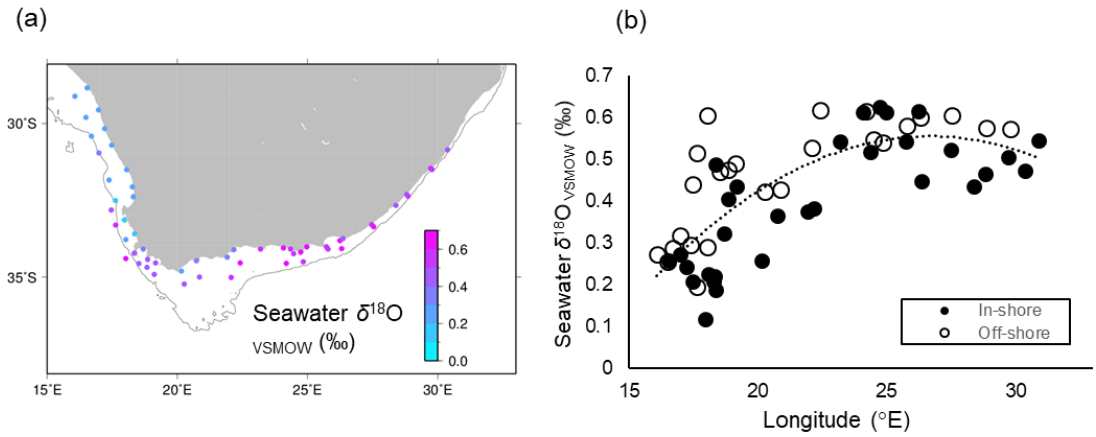

Figure 4. (a) Horizontal distribution and (b) longitudinal variation of near-surface seawater δ^{18}O.
The dotted line in (b) shows the fitted quadratic curve.

3.3.2 Otolith $\delta^{18}O$ and daily increment width

For adult samples, both otolith δ^{18}O in the first two months from hatch and daily

increment width until 100 dph showed a clear longitudinal trend. The otolith $\delta^{18}O$ showed higher value about +0.8 ‰ in the West region, lower values (+0.3-+0.4 ‰) in the South and East, and mediate values in the Central regions (Fig. 5a). A significant negative correlation between otolith $\delta^{18}O$ and longitude was found for the West to the South region by linear regression analysis ($p < 0.05$). The daily increment widths were significantly higher in the South and lower in the West and the Central region for 11-70dph (ANOVA + Tukey-Kramer test, $p < 0.05$). In the South, the daily increment width peaked at about 9 μm in 51-60 dph while in the West and the Central, it peaked at about 7 μm in 71-90 dph showing lower growth with later peak in early-life stages (Fig. 5b). The East followed a growth trajectory similar to those in the South. Although samples from different seasons and years were combined, remarkable difference in otolith $\delta^{18}O$ or increment width between them did not appear.

Juvenile samples captured in summer showed trends similar to those of the adults. Otolith $\delta^{18}O$ showed higher value about +0.9 ‰ in the West region, lower values about +0.4 ‰ in the South, and mediate values in the Central (Fig. 5c). Again, a significant negative correlation between otolith $\delta^{18}O$ and longitude for the West to the South region was detected ($p < 0.05$). The daily increment widths in the South were significantly higher than those in the West for 41-100 dph (ANOVA + Tukey-Kramer test, $p < 0.05$). In the South, it peaked at about 8 μm in 61-70 dph while in the West, stable increment widths about 5.5 μm continued through 31-100 dph with no remarkable peak (Fig. 5d). In the Central, it peaked at about 6 μm in 81-90 dph.

Juvenile samples captured in winter showed a different trend from the previous two sets. Otolith $\delta^{18}O$ were highest in the South at about +0.8 ‰, lower in the West at about +0.6 ‰ and lowest in the East at +0.5 ‰ (Fig. 5e). The linear regression analysis

showed a weak but significant positive correlation ($p < 0.05$) between otolith $\delta^{18}O$ and longitude for the West to the South region, revealing the strong seasonal variation of the environmental gradient in the sardine habitat. The daily increment widths were higher in the east which peaked at about 9 μm in 61-70 dph (Fig. 5f), while no significant difference was detected in any age range for the West to the South, peaking at about 7 μm in 81-90 dph. The estimated hatch date distribution was similar among the West to the South, as most of the individuals hatched during the period from November 2016 to January 2017, whereas individuals in the East hatched earlier in September to October 2016 (Fig. 6).

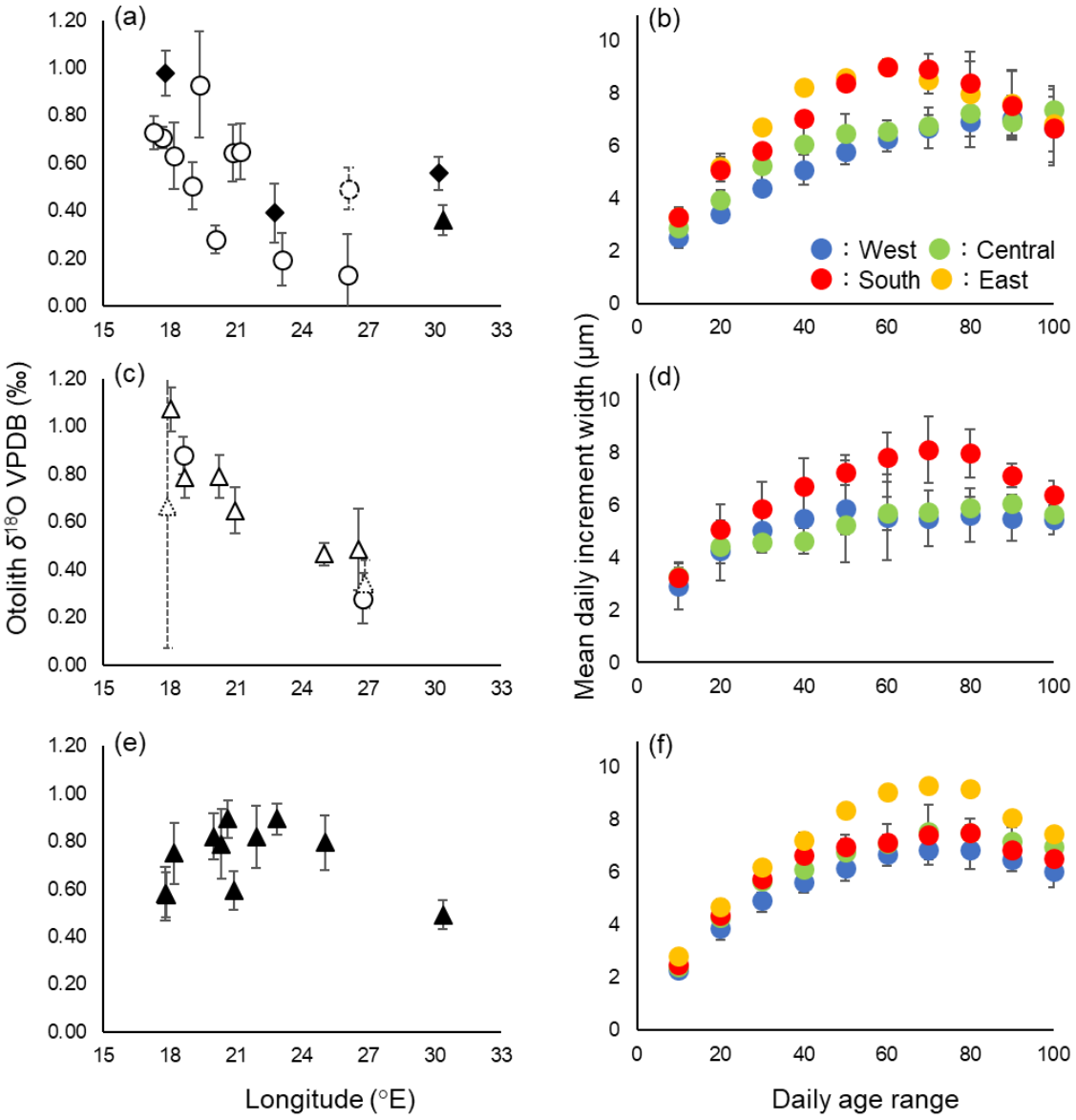

Figure 5. Geographical variations of otolith $\delta^{18}O$ and daily increment width for (a), (b) adults, (c), (d) juveniles captured in summer and (e), (f) juveniles captured in winter.
In (a), (c) and (e), station means and standard errors are shown, and the shape and filled/open represent the sampling year and season, respectively. (◆: 2015, ●: 2016 and ▲: 2017, and filled: winter (June to August) and open: summer (November to January)). Edge dotted plots are the stations that included only two individuals. In (b), (d) and (f), means and standard deviations of station means that belong two each region (West, Central, South and East) are shown.

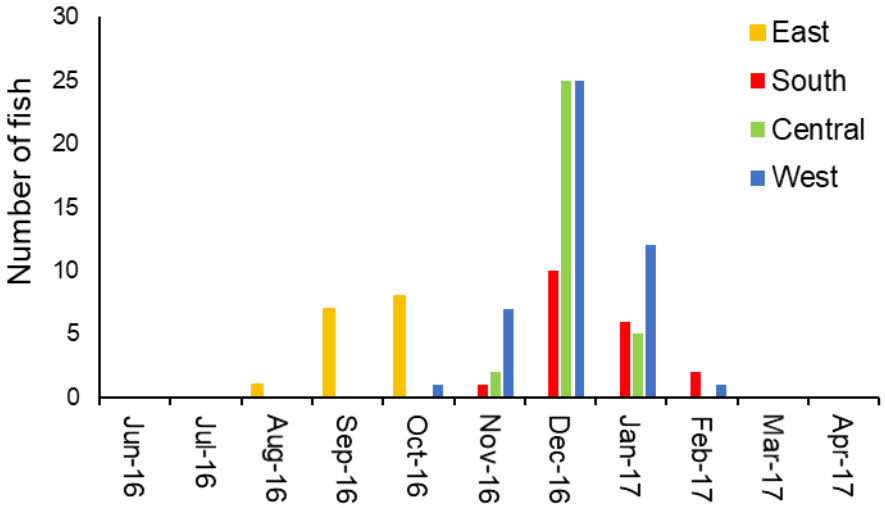

Figure 6. Estimated hatch date of juveniles captured in June-July 2017.

3.3.3 Ambient water temperature and growth

When the otolith $\delta^{18}O$ is converted into water temperature, taking into account the spatial variation of seawater $\delta^{18}O$, the overall trends for adults and juveniles captured in summer did not change remarkably. The estimated temperatures were highest in the South at about 16°C, high in the East at about 15°C and low in the West and the Central at 11-14°C (Fig. 7a). Meanwhile, the trend for the juveniles captured in winter was different. Although the otolith $\delta^{18}O$ showed an increase with longitude in the West to the South region, estimated temperature did not decrease but were stable at about 13°C, suggesting the increase of otolith $\delta^{18}O$ were due to the increase of seawater $\delta^{18}O$, with a consistent water temperature.

With all 3 samples sets combined, the standard length at 60 dph and the ambient water temperature estimated for the period from hatch to 60 dph showed a significant positive correlation (Fig. 7b), suggesting that higher water temperature result in faster growth during the early life stages of the South African sardine. The distribution of plots showed a separated pattern, divided at about 14.5°C. The higher temperature group included most of the plots from the South and the East, one from the Central and none

from the West, while the lower temperature group included most of the plots from the West and the Central, and the two from the winter-captured juveniles in the South (Fig. 7b). This separation indicated the existence of two types in sardine growth and nursery habitat; slower growth in cool upwelling waters and faster growth in warm waters from the Agulhas Current.

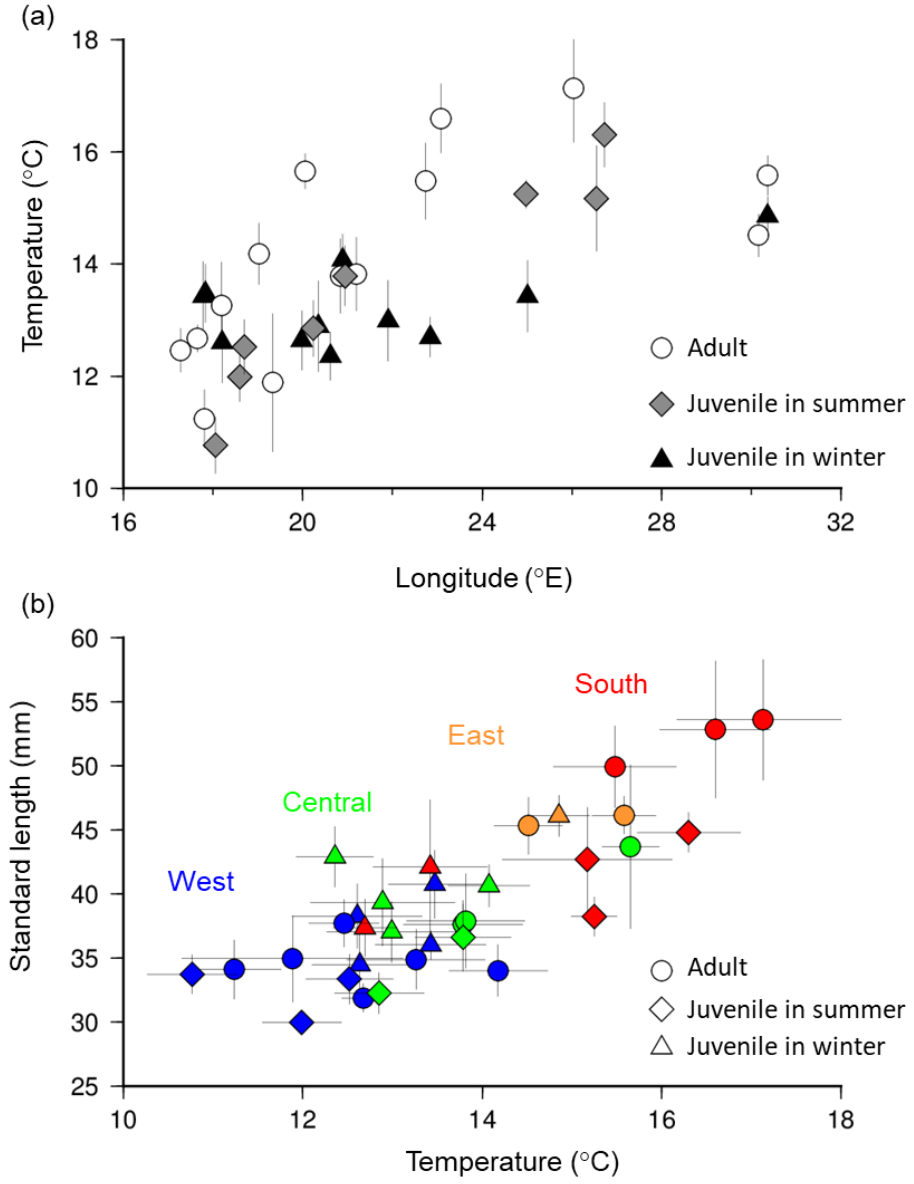

Figure 7. (a) Longitudinal variation of estimated temperature and (b) relationship between estimated temperature and standard length at 2 months from hatch.
Station means and standard errors are shown. Stations including less than 3 individuals were excluded. The colours in (b) represent the areas of capture.

3.4 Discussion

Sardine is a key fishery resource in South Africa. Recently, discussion such as the sardine population off South African coast is comprised of several subpopulations and thus should be treated as multiple stocks in management strategies, has been invoked. To test the hypothesis, this study investigated nursery environments and resulting early life growths of the South African sardine along the entire coast of South Africa, by introducing otolith $\delta^{18}O$ for the first time for the species. Geographic gradients of them were revealed, warmer and faster growth in the south to east coast, and cooler and slower growth in the west coast, thereby suggesting the existence of several discrete subpopulations in the region that use different type of nursey habitats.

The positive correlations between captured longitude and nursey temperature for juveniles captured during summer, and also for adults in ~18 cm CL, indicate that the geographical gradient of nursery temperature is conserved up to ~18 cm CL and thus the sardines remain stationary in the first several years. Weston et al. (2015) found that sardine off the west coast showed infection of the “tetracotyle”-type metacercarian, which is considered to occur only in cool water, at a size of 14 cm CL whereas only sardine from the south coast showed infection at a size larger than 17 cmCL, which also suggest that young sardines are unlikely to move region to region. Therefore, our results support the existence of multiple discrete recruitment systems in the west and the south coast, with potential mixing of older fish. However, although the boundary of the two systems has been considered as Cape Agulhas (~20°E), the fish in the Central area (20-22°E) showed similar nursery temperature and early life growth to those of fish in the west coast, rather than south coast, for all sample sets that were analysed. This is curious because coastal upwelling intensity is obviously different in the west and the east of Cape Agulhas,

stronger in the west. This can be attributed to the relatively weaker influence of the Agulhas Current to the coastal area of 20-22°E compared to the South region, as the current is still offshore due to the width of Agulhas Bank. Therefore, the biogeographical boundary may exist at the several degrees east of Cape Agulhas, which can be important information when setting the boundary of management units.

The extent of the difference of growth and temperature between the West and the South regions seems to change seasonally. In contrast to the juveniles captured during summer that showed a strong west to south increasing trend in their nursery temperature, juveniles captured in the south coast in 2017 winter showed similar temperatures to those captured in the west coast. In summer, when the winter-captured juveniles hatched, wind-driven coastal upwelling often occur along the south coast, in addition to the strong upwelling in the west coast (Lamont et al., 2018). In addition, a ridge of cool water extending along the 100m isobath quasi-permanently appears in the eastern Agulhas Bank due to the shelf edge upwelling during spring and summer (Swart and Largier, 1987). The disappearance of the temperature gradient in the summer-hatched cohort suggest that those in the south coast have utilised the upwelled waters and thus produced the high otolith δ^{18}O. Despite this large seasonal difference, such individuals with high otolith δ^{18}O and slow growth were rarely found in the adults captured in the south coast. This is probably because the summer-hatched cohorts are not the main part of recruitments in the south coast, as the spawning in the southern area is more abundant in winter to spring (van der Lingen and McGrath, 2017).

The possibility that winter-captured juveniles may not be the main cohort of recruitments in the south coast is implicative for stock-assessments because the abundance of juveniles in winter has been used as a proxy of the recruitment abundance.

It has been suggested that the recruitment is an order of magnitude smaller in the south coast than in the west coast (de Moor et al., 2017), despite the comparable abundance of adults. Although this has been attributed to higher predation pressure on the Agulhas Bank during early life history stages (Hutching et al., 2009), the results in this study suggest the possibility that the recruitment abundance in the south coast has been consistently underestimated. It is likely that cohorts hatched in winter to spring in the south coast that grow faster were too large to be discriminated as juveniles by the season of winter survey is conducted, as the criterion dividing juvenile and adults is based on the growth curve of sardines off the west coast that grow slower. Therefore, for the south coast, the abundance of juvenile during wintertime may not reflect recruitment abundance, and thus the use of abundance in different season may increase the accuracy of recruitment abundance. As this is an important issue for fishery managements, investigations using larger sample size are necessary to further confirm the conclusion.

Among the entire coast of South Africa, sardines grew faster in warmer temperature in the first two months from hatch (Fig. 7). This is consistent with the previous observation in the west coast that sardine larvae captured at higher temperature had faster growth rate during 5 days before capture (Thomas, 1986). Laboratory experiments for European sardine have shown that at good feeding conditions, sardine larvae growth increased with increasing temperature, but this was achieved at the expense of a significant increase of foraging events (Garrido et al., 2016), which indicate the fast growth in warm waters require sufficient food supply. In the south coast, the food availability is probably supported by spring plankton blooms because spawning in the south coast peaks during winter to spring (van der Lingen and McGrath, 2017), rather than coastal upwellings. Therefore, the potential subpopulations in the west and the south

coast seem to have different strategies to utilise different ocean enrichment process. This leads to the hypothesis that factors driving the biomass fluctuation can be different between regions, which will be the scope of future studies. In upwelling systems, the key for larval survival has been considered as the retention in stably productive coastal area (Agostini and Bakun, 2002). In the south coast, however, temporal and spatial match-mismatch between larvae and prey can be more important because the enrichment process do not last as long as coastal upwellings in the west coast. As the match-mismatch has been considered as a key process of sardine survivals in warm current systems in the western North Pacific (Nishikawa and Yasuda, 2008; Kodama et al., 2018), it can also be the case in the south coast.

To clarify whether the individuals forming the Sardine run in the east coast is a discrete population from the southern subpopulations, further investigations are needed. The estimated hatch dates of fish under 14 cm CL captured during the sardine run were between August and October, which is consistent with the season when eggs are found in the east coast (Connell, 2010) but this is also the season when sardine in the south coast mainly spawn. In addition, the otolith δ^{18}O values and growth rate in early life stages did not show remarkable difference between east and south coasts, which contradicted the hypothesis that lower δ^{18}O value (higher temperature) would appear in the east where the dominance of the Agulhas Current is more severe. Even if the individuals in the sardine run had originated from the east coast spawning ground, therefore, they seem to have been rapidly transported and grown in cooler areas in the south coast, such as coastal area around Port Alfred, where strong upwelling event is frequently observed (Lutjeharms et al., 2000). Future studies performing δ^{18}O analyses in higher resolution using MICAL3c (Ishimura et al., 2004; 2008) may allow us to have more accurate view on life history of

sardine run fish.

Despite the apparent west to south trend in station means of otolith $\delta^{18}O$, discrimination of stocks in the individual level using this marker may not be reliable because, in addition to the seasonality described above, there are large variations within each station even for the juveniles captured in the same location. The inshore-offshore environmental difference, as apparent in seawater $\delta^{18}O$ that consistently showed higher value in offshore stations for entire coast, may be responsible for the variation. Sardine mainly spawns at the shelf edge, and recruits to the coast. Because the coastal area is more subject to upwellings, it is generally cooler. Therefore, the difference in duration of offshore stay of larvae can easily create the variation of otolith $\delta^{18}O$ analysed for 2 months post hatch even within the same longitude. It is therefore important to find markers that are not affected by this in-offshore environmental gradient for stock discrimination to assess the extent of mixing.

Overall, the newly introduced high-resolution otolith $\delta^{18}O$ analysis and otolith microstructure analysis suggested the existence of several discrete subpopulations in the west and the south coast of South Africa that grow in different nursery environments and in different speeds. As this can be reflecting the general features of sardines in western boundary current regions and upwelling regions, the comparison with other systems would be of particular interest. Because stock structures of small pelagic fish have been issues for fisheries managements elsewhere in the world (e.g. Gaughan et al., 2002; Baldwin et al., 2012), the application of the method used here will provide valuable implications for successful managements.

Chapter 4

The relationship between temperature and early life growth rates of sardines: Comparison across the North Pacific

4.1 Introduction

Two sardine species or subspecies, Japanese sardine *Sardinops sagax melanostictus* and Pacific sardine, *Sardinops sagax sagax* live in the either sides of mid-latitudes of North Pacific, where the western boundary current Kuroshio and coastal upwelling, respectively, dominates regional environments (Fig. 1). The two sardines are closely related (Grant and Bowen, 1998), and have been major targets of pelagic fisheries due to their large abundance, thereby supporting the fishery economy in coastal countries. Each sardine

population is assumed to be comprised of several subpopulations and the most economically important ones in each region are the Pacific stock of Japanese sardine and the Northern subpopulation of Pacific sardine. The Pacific stock of Japanese sardine, hereafter simply the Japanese sardine, spawns during winter to spring in the southern coast of Japanese Island (Oozeki et al., 2007). Eggs and larvae are transported eastward by the Kuroshio, and after metamorphoses juveniles began to migrate northward heading for the Oyashio region (Kuroda, 1991). The Northern subpopulation of Pacific sardine, hereafter simply the Pacific sardine, spawns off southern California and Baja California during spring in waters of 12–16°C (Checkley et al., 2000; Lynn, 2003; Jacobson et al., 2005; Reiss et al., 2008). The movements of larvae and juveniles have not been well documented because surveys have concentrated on investigating distribution and abundance of eggs and adults, although they are assumed to approach the coast in unknown timing as the adults are often captured in fisheries in coastal waters (Weber et al., 2015), especially off Southern California Bight, which is the coastline between Point Conception and San Diego (Fig. 1).

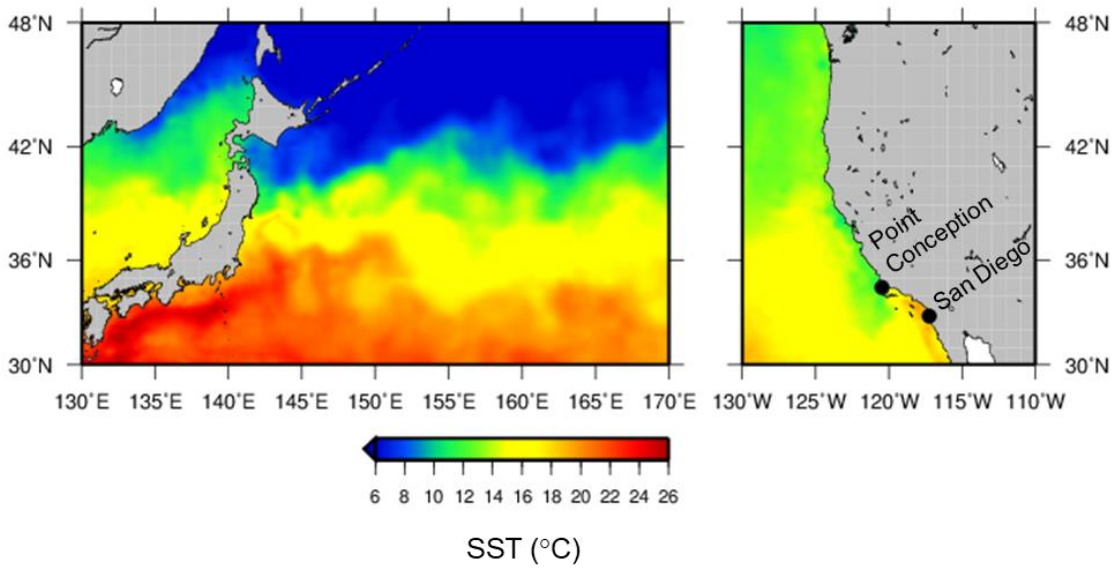

Figure 1. Typical distribution of sea surface temperature in early-summer.
Satellite based SST product for 1th June 2006 from GHRSST Level 4 OSTIA Global Foundation Sea Surface Temperature Analysis (GDS version 2) is shown for Kuroshio-Oyashio system and Californian Current system with the same temperature scale. The warm Kuroshio in the south of Japan Island and wind driven coastal upwelling off central and southern California are clearly evident.

Biomass of the sardine populations are known to show intense fluctuations. In the past several decades, the spawning stock biomass of Japanese sardine peaked over 13 million tons in 1988, then rapidly collapsed into 1/100 in the following 15 years (Yukami et al., 2017). Recently, the abundance is in increasing trend again due to the high recruitment success in 2005, 2008, 2010 and 2015 (Fig. 2). The biomass of the Pacific sardine had increased during 1980s and 1990s (Fig. 2) but started to severely decrease from the mid-2000s, resulting in a ban of sardine fisheries in the United State in recent years (Hill et al., 2017). Scale deposition rates in coastal areas off Japan (Kuwae et al., 2018) and California coasts (e.g. Baumgartner et al., 1992) showed that such intense fluctuations of sardine biomass seem to have existed even before the large-scale commercial fishing began in the 20th century, which suggests natural factors, such as

environmental variability, are the main driver of the fluctuation.

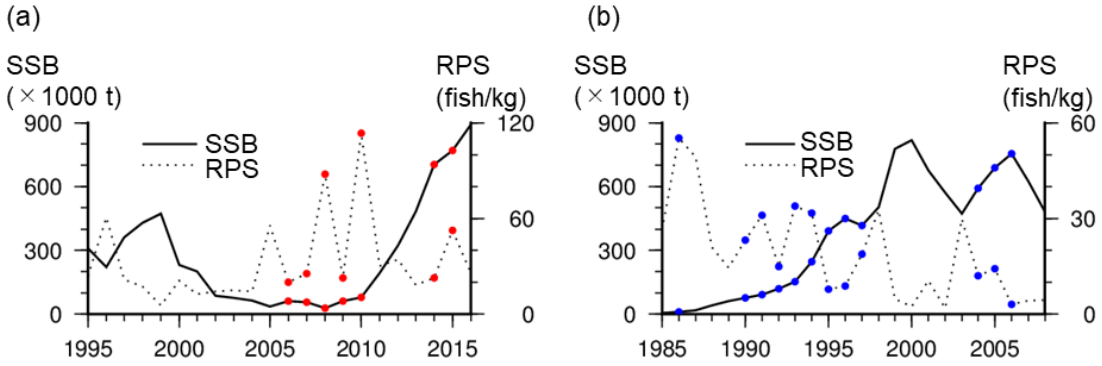

Figure 2. Times series of spawning stock biomass and recruitment per spawner for (a) the Pacific stock of Japanese sardine and (b) the Northern stock of Californian sardine. The colored circles represent the year classes we analyzed in this study. Data from Yukami et al. (2017) and Hill et al. (2008) are used.

A number of studies have concluded through various analytical methods that the Japanese sardine biomass increase in relatively cooler period, while the Pacific sardine increase in warmer period (e.g. Noto and Yasuda, 1999; Yatsu et al., 2005; Nakayama et al., 2018; Jacobson 1995; Sugihara et al., 2012; Lindegren and Checkley, 2012). Many possible mechanisms connecting the temperature change and the increase of sardine biomass have been hypothesised. In the western North Pacific, lower SST in winter induce deepening of mixed layer depth around Kuroshio extension in winter, which may have provided better feeding conditions for the Japanese sardine larvae (Noto and Yasuda, 1999; Nishikawa et al., 2013). In the eastern North Pacific, Rykaczewski and Checkley (2008) showed the production of the Pacific sardine may be responding to variations of intensity of the offshore upwelling driven by wind stress curl, rather than coastal upwellings, through bottom-up effects. On the other hand, Takasuka et al. (2007, 2008) argued that temperature is directly controlling the growth rates of larvae through fish physiology, and thus ultimately driving of the fluctuations. However, there has been no

universally accepted explanation for the opposite responses of biomass to temperature changes, and therefore it is very likely that the mystery holds the essence of how environmental variabilities affect sardine biomass.

Higher growth rates in early life history stages have generally been assumed to enhance fish survival and subsequent recruitment success, by gaining the indirect advantages of larger body size (the bigger-is-better hypothesis; Miller et al., 1988) and shortening high-mortality larval stage (the stage duration hypothesis; Houde 1989), or becoming less vulnerable to predation (Takasuka et al., 2003, 2004). Takahashi et al. (2008) found significant correlations between interannual variations of recruitment and growth rates during the early juvenile stages for the Japanese sardine. Similarly, Takahashi and Checkley (2008) showed for the Pacific sardine that early juveniles with faster growth rate during summer and autumn had a higher probability of survival to the adult stock, both suggesting that growth-survival process may be important for fluctuations of *Sardinpos* spp. populations.

How are the growth rates of sardines in the early life history stages controlled? Heath (1992) suggested that the early life growth rates of fish generally increase with temperature within a favourable temperature range if the food supply is adequate, although the relative influences of temperature and food availability can cancel each other. From comparisons of temperature at catch and growth rate during few days before catch, temperature-growth relationships for the Japanese sardine have been reported as dome-shapes with a peak growth rate at around 16.2°C in larvae (Takasuka et al., 2007) and ~18 °C in early juveniles (Takahashi et al., 2009), suggesting that higher temperature are not suitable in terms of fish physiology or food availability for the Japanese sardine. Still, this approach has the limitation that it is difficult to prepare sample sets from wide range

of temperature within uniform age or body length, and thus difficult to exclude ontogenetic effects on growth rates. In addition, few studies have focused on the relationship between temperature and early life growth for the Pacific sardine in the field.

Oxygen stable isotope ratio ($\delta^{18}O$) in otolith is a well-known temperature proxy based on the temperature dependence of oxygen isotope fractionation during the formation of calcium carbonates. The temperature dependence has recently been confirmed though rearing experiments for both the Japanese sardine (Sakamoto et al., 2017) and the Pacific sardine (Dorval et al., 2011). Although $\delta^{18}O$ had mainly been analysed for whole otolith for sardine (e.g. Javor and Dorval 2014), the recent development of micro-volume analysing system has allowed the analysis on micro-milled samples, thereby providing otolith $\delta^{18}O$ profiles in a high resolution of several 10 days. Furthermore, I developed a quick and efficient procedure to collect the milled powder, which will allow to use commercially available, automatic analysing systems that works routinely without intensive labour but requires larger amounts of sample. With these technical developments, it is now possible to obtain temperature histories in high resolutions, together with their growth trajectories, for large numbers of individuals.

The aim of this study is to clarify how temperature controls early life growth rates in the field and ultimately affects the recruitment of sardines. For this goal, $\delta^{18}O$ and microstructure of archived otoliths of sardine in the two regions, the Kuroshio-Oyashio and the California Current system, were analysed and compared. In addition to temperature, otolith $\delta^{18}O$ is affected by background seawater $\delta^{18}O$. Regarding seawater $\delta^{18}O$ in the habitat of the Japanese sardine, LeGrande and Schmidt (2006) summarized archived global seawater $\delta^{18}O$ data and proposed a seawater $\delta^{18}O$–salinity relationship for the North Pacific. More regionally, Yamamoto et al. (2001) and Oba and Murayama

(2004) proposed a relationship for the Oyashio and the Kuroshio-Oyashio system, respectively, from near shore seawater sampling, although Japanese sardines are also abundant in offshore regions. Seawater $\delta^{18}O$ off southern California has been poorly studied, only data from less than 10 locations exist in Global Seawater Oxygen-18 Database (Shmidt et al., 1999). Therefore, distributions of seawater $\delta^{18}O$ have also been studied with increased spatial coverage and resolution in both western and eastern North Pacific.

4.2 Materials and Methods

4.2.1 Distribution of seawater $\delta^{18}O$

From the western North Pacific, surface seawater samples for water isotope analysis were collected during seven pelagic fish sampling survey cruises conducted by the National Research Institute of Fisheries Science, Fisheries Research Agency (NRIFS) in May–June 2012, September–October 2012, May–June 2013, September–October 2013, April–May 2015, May–June 2016, and September 2016, and the Shinsei-maru KS-15-11 cruise in September 2015. The sampling range encompassed the 34.00–47.48°E, 138.48–172.38°N region, which roughly covers the whole distribution of larval and juvenile Japanese sardine. In all sampling points, the salinity profile was measured with a SBE 9 Plus CTD unit (Sea-Bird Electronics, Inc.), with precision better than 0.01 in all cruises. Seawater samples for $\delta^{18}O$ analysis were taken from the sea surface using a roped plastic bucket on board, or at 5 m depth using CTD-attached Niskin bottles (General Oceanics, Inc.). Water samples were preserved in sealed glass vials to avoid evaporation. Samples obtained in 2012 and 2013 were measured at the Geo Science laboratory using the LWIA DLT-100 system (Los Gatos Research) with precision ± 0.05 ‰. Samples from other cruises were

analysed at the Atmosphere and Ocean Research Institute (AORI), University of Tokyo, using the Picarro L2120-i system with precision ± 0.07 ‰. Samples analysed in AORI were membrane-filtered (pore size: 0.45 μm, Toyo Roshi Kaisha, Ltd.) before their introduction in the Picarro L2120-i system to reduce suspended particles and avoid blocking the sampling line. The correlation between seawater $\delta^{18}O$ and salinity was analysed by the least squares method using surface water $\delta^{18}O$ and salinity measured at 10 m (or 5 m if available) depth by the CTD.

From the eastern North Pacific, surface and sub-surface seawater samples for the isotope analysis were collected during the 1708SR CalCOFI cruise survey conducted by the California Cooperative Oceanic Fisheries Investigations in August 2017. In every two stations on three line transects extending offshore from Southern California Bight, seawater samples for $\delta^{18}O$ analysis were taken from 10m and 50m depth using CTD-attached Niskin bottles and were preserved in sealed glass vials to avoid evaporation. The sampling range covered from inshore area off Southern California Bight to the offshore California Current region, which was assumed to represent larvae and juvenile habitats off Southern California. After membrane-filtering (pore size: 0.45 μm, Toyo Roshi Kaisha, Ltd.), $\delta^{18}O$ were measured at INCT using the Picarro L2120-i system with precision better than ± 0.05 ‰.

4.2.2 Otolith samples

From the western North Pacific, age-0 Japanese sardines sampled in acoustic and sub-surface trawl surveys in the offshore Oyashio region conducted during 2006–2010 and 2014–2015 were collected (Fig. 3a). The survey has been conducted by National Research Institute of Fisheries Science (NRIFS) every autumn since 2005, which aims to estimate

the abundance of small pelagic species. The abundance of sardine young-of-the-year in the region in the season, approximately 10–15 cm in standard length (SL), is considered as a proxy of the abundance of recruits of the Pacific stock and has been used to tune the cohort analysis in stock assessment (Yukami et al., 2017). As representatives for young-of-the-year population in the region, 2–6 trawl stations each year that had larger catch per unit effort were picked up, and 5–6 individuals were randomly selected from each station for otolith analyses. From the eastern North Pacific, archived otoliths of the Pacific sardine captured in pelagic fishery off Southern California Bight during 1987, 1991–1998 and 2005–2007 were collected (Fig. 3b). The accurate data of positions and dates of capture were unavailable. The fish in the size of 10–16 cm SL were regarded as age-1 individuals born in the previous year following Takahashi and Checkley (2008), based on the fact that S. *sagax* can grow as large as 160 mm approximately 1 year after hatching (Butler et al., 1993, 1996) and 50% of females are mature at ca 160 mm SL (Macewicz et al., 1996). The number of individuals varied between year classes in the range of 5–20.

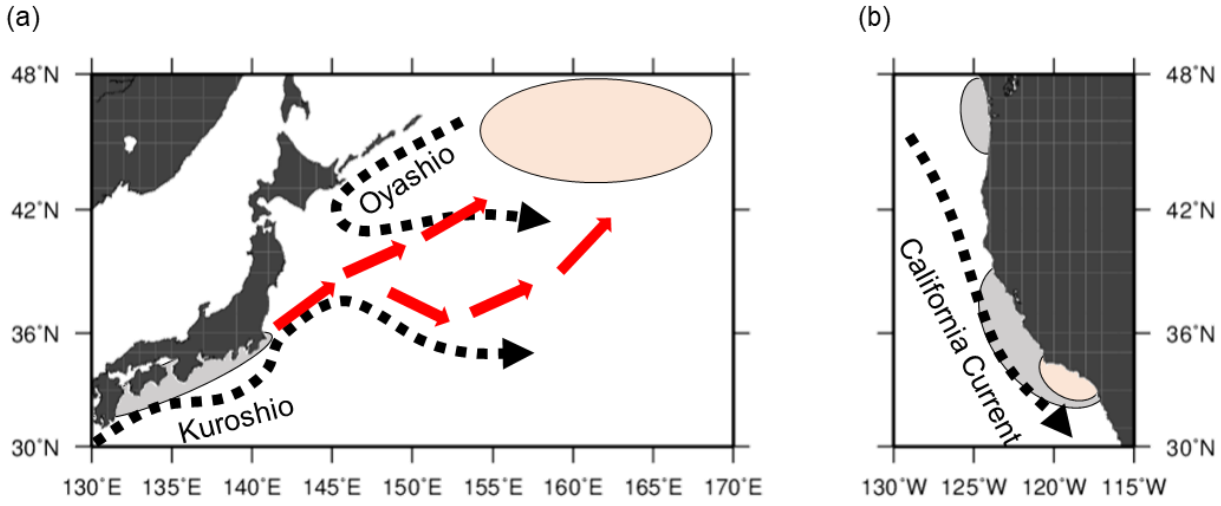

Figure 3. Spawning ground (gray) and sampling location (orange) of (a) Pacific stock of Japanese sardine and (b) Northern stock of Californian sardine. Presumed movements of larval and juvenile Japanese sardine are shown in red arrows.

4.2.3 Otolith processing and micro-structure analysis

Sagittal otoliths were extracted, cleaned, embedded into resin on slide-glass and polished for micro-structure and stable isotope analysis. Using the otolith measurement system RATOC, the number and location of daily increments were examined along the axis in the postrostrum from the core. Although the daily increments were clearly observed until the otolith edge for the Japanese sardine, it was difficult for the Pacific sardine probably because they had experienced winter when otolith growths slow down. Therefore, the rings were counted as far as possible for the Pacific sardine, which typically resulted in more than 150 counts. The first daily rings were assumed to form after 3 days post hatch (dph) for the Japanese sardine, and 8 dph for the Pacific sardine following Takahashi et al. (2008) and Takahashi and Checkley. (2008).

As a proxy of mean daily growth rates for each milling area, mean otolith daily increments width was calculated for 0–30, 31-45, 46–60, 61–75, 76–90, 91–105 and 106–120 dph for the Japanese sardine and 0–30, 31–60, 61–90, 91–120 and 121–150 dph for the Pacific sardine. The standard lengths corresponding to the mean otolith radius at 30, 45, 60, 75, 90, 105 and 120 dph for the Japanese sardine and 30, 60, 90, 120 and 150 dph for the Pacific sardine were calculated through the relationships between otolith radius and standard length for the Japanese sardine larvae (Takasuka et al., 2007) and juveniles (Takahashi et al., 2009). From the standard lengths, developmental stages for each age range were specified based on the definition of Smith et al., (1992).

4.2.4 Micro-milling, powder collection and isotope analysis

The otolith portions deposited during hatch–30, 31–45, 46–60, 61–75, 76–90, 91–105 and 106–120 dph for the Japanese sardine and hatch–30, 31–60, 61–90, 91–120 and 121–150

dph for the Pacific sardine, were milled out sequentially using high-precision micro-milling system Geomill 326. The difference of the temporal resolution came from the slower growth rates of the Pacifc sardine. Milling depth was set to 50 μm for the area nearest to the core, and 100 μm for the rest. After each milling, the otolith was observed under microscope to check the existence of otolith fractions cracked out from other milling area, which were removed using a needle if present. Milled powders were then collected using a needle and a stainless cup, and poured into response vials. After each collection of powder, the otolith was cleaned with an air-duster to avoid cross-contamination between milling paths.

$\delta^{18}O$ of collected otolith powder were determined using micro-volume analysing system MICAL 3c at the National Institute of Technology, Ibaraki College, for the area nearest to the core, and automatic system DELTA V + GAS Bench for the rest at the Atmosphere and Ocean Research Institute, the University of Tokyo, considering the amount of powder because the latter system requires ~20 μg of sample for reliable analyses. Otolith powders were reacted with phosphoric acid at 25 °C and the released CO_2 was purified before being introduced into the mass spectrometer for the MICAL3c system, whereas the response with phosphoric acid was made in 72 °C for DELTA V. The $\delta^{18}O$ values were reported in δ-notation relative to the VPDB (Vienna Pee Dee Belemnite) scale, and given as a ‰ value. Analytical precision was better than ± 0.10 ‰ and ± 0.17 ‰, respectively. The acid fractionation factor of calcite was used to facilitate comparisons with isotopic values reported in previous studies (Amano et al., 2015). Because the difference between acid fractionation factor of calcite and aragonite is temperature dependent (Kim et al., 2007), 0.09 ‰ was added to the $\delta^{18}O$ value determined by DELTA V to adjust for the different response temperature.

4.2.5 Conversion of otolith $\delta^{18}O$ to temperature

Otolith δ^{18}O is affected by both temperature and δ^{18}O of ambient water. In the habitat area of the Pacific sardine, the seawater δ^{18}O in the habitat area did not show large horizontal or vertical variation (see Results). Therefore, seawater δ^{18}O was assumed to be constant at the mean value of -0.32 ‰ to calculate temperature from otolith δ^{18}O of the Pacific sardine. On the contrary, seawater δ^{18}O in the habitat area of the Japanese sardine showed large variation, ranging from -1 ‰ to +0.5 ‰ (see Results), and therefore temperatures were calculated differently for the Japanese sardine.

As seawater δ^{18}O is generally correlated to salinity (Craig and Gordon, 1965), otolith δ^{18}O can be regarded as a function of temperature and salinity. If seawater temperature and salinity are completely independent of each other, it would be impossible to estimate both of them from otolith δ^{18}O but actually they are closely related. Therefore, using the relationship between them, which would vary annually and seasonally, estimating both temperature and salinity from otolith δ^{18}O would become possible, with a certain range of error. To build formulas to calculate temperature from otolith δ^{18}O for each month of each year, surface layer (< 30 dbar in pressure) temperature and salinity observed by Argo floats in the range of 130–150 °E, 30–45 °N but excluding nearshore areas and the Sea of Japan, in February to October 2006–2010 and 2014–2015, were extracted from the Argo float dataset Advanced automatic QC(AQC) Argo Data ver.1.2a distributed by JAMSTEC (Fig. 4a). The number of observations in each month was about 2200 in average, varying from 319 to 5427. For each temperature and salinity pair, corresponding otolith δ^{18}O was calculated using the seawater δ^{18}O-salinity relationship in the Kuroshio-Oyashio system ($\delta^{18}O_{seawater} = 0.56*S - 19.06$: see Results) and the otolith δ^{18}O-temperature and seawater δ^{18}O relationship for the Japanese sardine ($\delta^{18}O_{otolith} =$

$\delta^{18}O_{seawater} - 0.18*T + 2.69$: Sakamoto et al., 2017). Temperature was plotted against the otolith δ^{18}O for each month, which generally showed a curve-shaped relationship (Fig. 4b). A quadratic function was fitted to the plots using the least square method and was used as the formula to estimate temperature from otolith δ^{18}O. The root-mean-square-errors of the formulas, which can be regarded as the proxies of the accuracy of temperature estimation, were 1.0°C in average, varying from 0.3°C to 2.0°C with the tendency to increase in summer months (Fig 4c; Table 1). All otolith δ^{18}O of the Japanese sardine were converted to temperature using the formula made for the month that the median date of each milled area belongs.

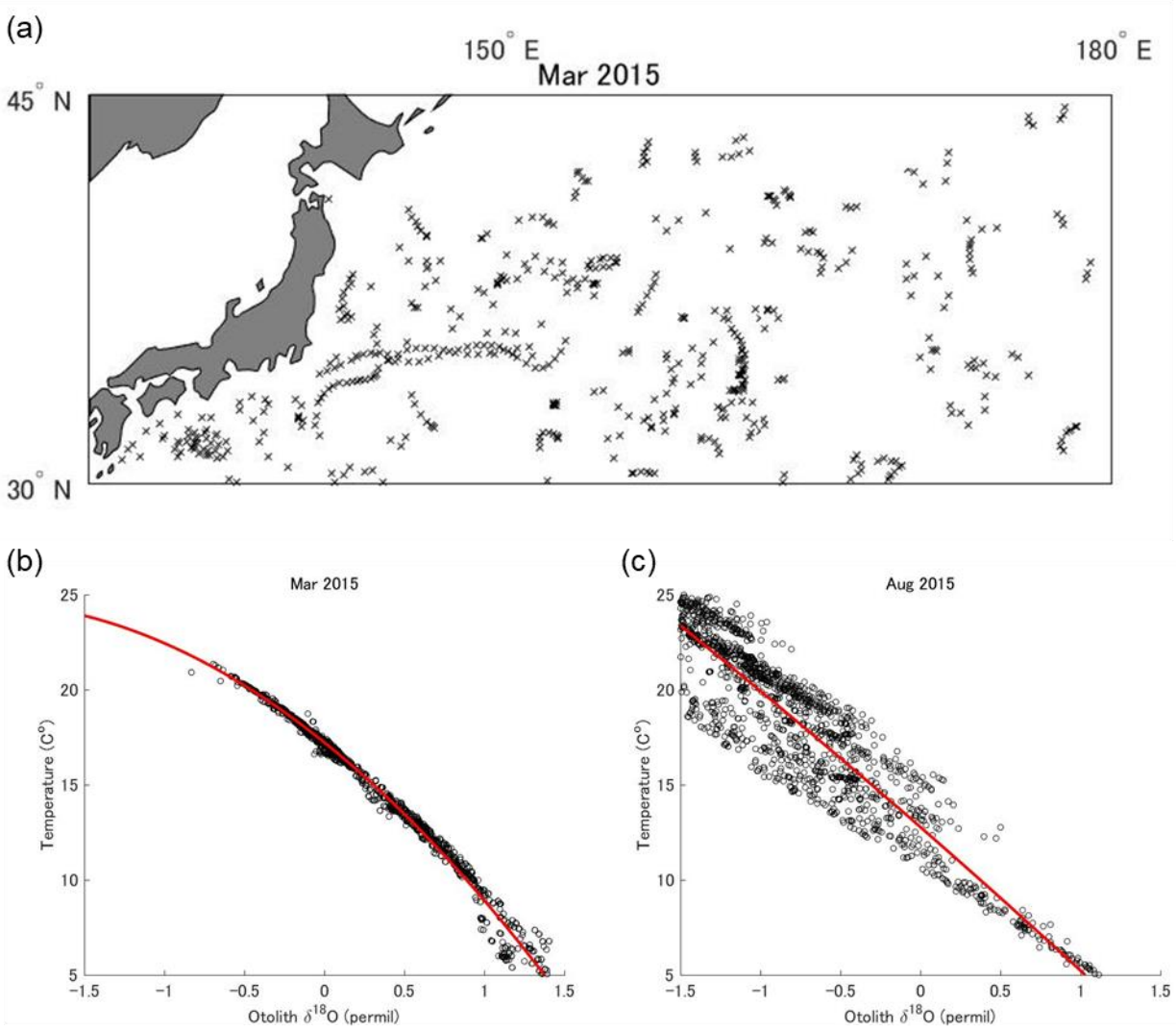

Figure 4. (a) Observation locations of Argo floats in March 2015 and (b) the relationship between temperature and otolith $\delta^{18}O$ predicted from temperature and salinity observations during the month. Quadratic regression line is shown in red. **(c) The relationship between temperature and predicted otolith $\delta^{18}O$ for August 2015, which shows larger variation from the regression line.**

	Feb	Mar	Apr	May	Jun	Jul	Aug	Sep	Oct
2006	0.7	0.4	0.4	0.5	0.6	0.9	1.4	1.8	2.0
2007	0.6	0.4	0.3	0.4	0.8	0.9	1.2	1.5	1.6
2008	0.9	0.7	0.4	0.5	0.7	1.0	1.4	1.9	1.7
2009	0.7	0.6	0.6	0.5	0.7	0.9	1.2	1.5	1.5
2010	0.6	0.4	0.4	0.3	0.7	0.9	1.4	2.0	1.7
2014	0.7	0.5	0.4	0.5	1.2	1.6	1.5	1.7	1.6
2015	0.5	0.5	0.5	0.6	1.0	1.4	1.6	1.8	1.7

Table 1. Root-mean-square-errors of the formulas converting otolith $\delta^{18}O$ to temperature for each month in °C.

4.2.6 Inter-annual variation

Representatives of ambient water temperature for each year class were estimated for comparison with time series of spawning stock biomass, recruits per spawner and environmental indices. For the Pacific sardine, estimated temperatures for each age range were simply averaged within each year class. For the Japanese sardine, to account for the variation of the number of individuals captured in the same station, estimated temperatures for each age range were first averaged within each station, then the station means were averaged within each year, weighted by catch per unit effort.

As environmental indices, monthly Pacific Decadal Oscillation (PDO) index, which is defined as the leading principal component of North Pacific monthly sea surface temperature variability (Zhang et al., 1997; Manuta et al., 1997), was used for both regions. In the Japanese sardine, the inter-annual variations of sardine ambient temperatures in hatch–30 dph, 31–45, 46–60, 61–75, 76–90, 91–105 dph and 106–120 dph were compared to variations of PDO index in April, April, May, May, June, June and July, respectively, based on the mean corresponding months of each milling area. In the Pacific sardine of which hatch dates were not available, variations of the temperature in each age range were compared to variations of PDO of each month from March to September. Additionally, monthly coastal Upwelling Index (Bakun, 1973) which represents the intensity of coastal upwelling, were also compared to sardine ambient temperatures in the California Current region. The mean of UI calculated at 33°N, 119°W and 36°N, 122°W was used.

4.3 Results

4.3.1 Distribution of Seawater $\delta^{18}O$

Surface seawater $\delta^{18}O$ in the Kuroshio-Oyashio system had a clear horizontal variation, showing higher values (> +0.30 ‰) in the Kuroshio region, lower values (< -0.60 ‰) in the Oyashio region, and medium values in the transition zone (Fig. 5a). On the other hand, seawater $\delta^{18}O$ off Southern California Bight did not show large variation both horizontally and vertically, ranging between -0.20 and -0.42 ‰ (Fig. 5b, c).

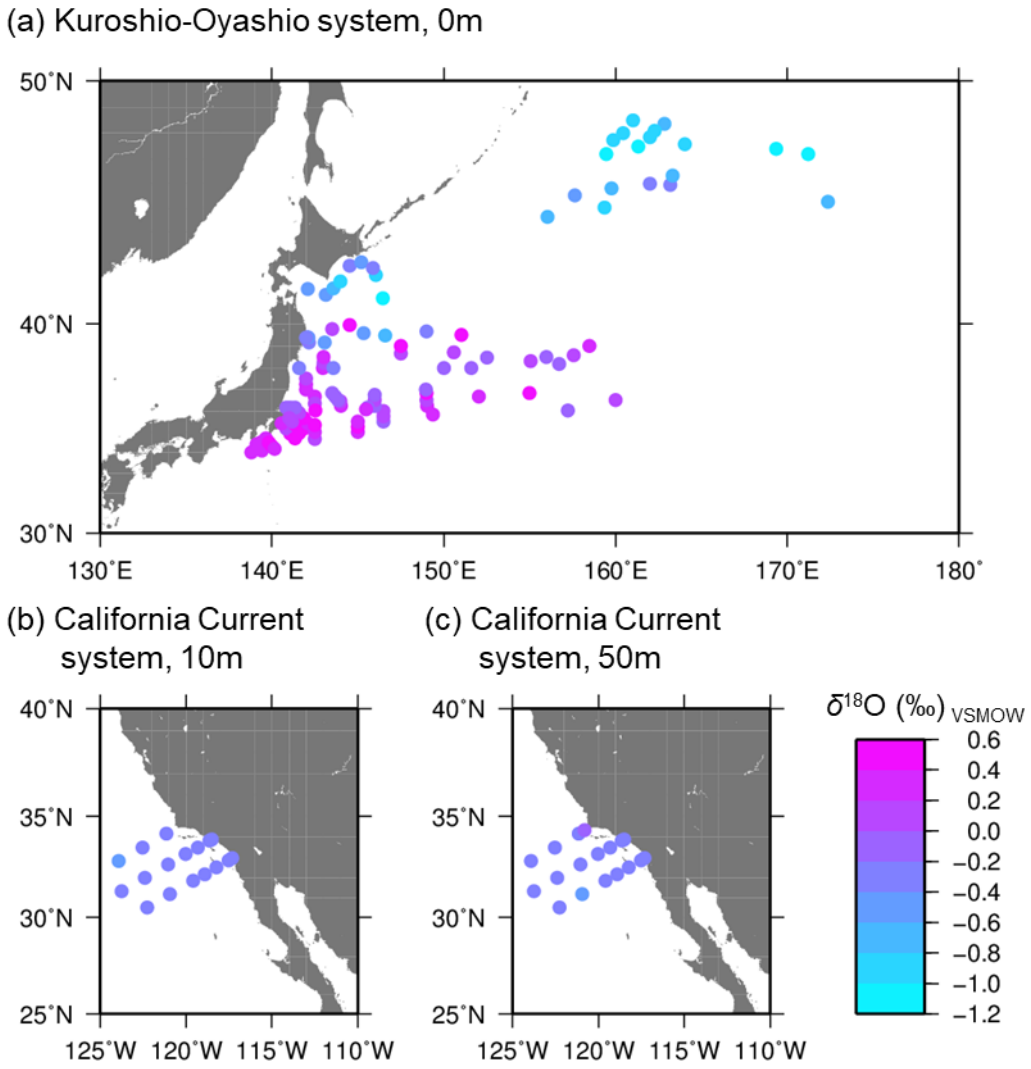

Figure 5. Horizontal distribution of seawater $\delta^{18}O$ in (a) Kuroshio-Oyashio system at surface, (b) California Current system at 10m and (c) 50m.
Note that colour scales are common.

The relationship between seawater $\delta^{18}O$ and salinity in the California Current region was not investigated due to the small variations of them. In the Kuroshio-Oyashio system, a positive correlation was observed between seawater $\delta^{18}O$ and salinity (Fig. 6). Compared to the previously proposed relationships, data obtained north of 40 °N had similar values to the equations for the North Pacific (LeGrand and Schmidt, 2006) or to the near shore Kuroshio-Oyashio system (Oba and Murayama, 2004). However, data obtained south of 36 °N showed higher $\delta^{18}O$, close to that of the line for the Tropical Pacific (LeGrand and Schmidt, 2006), suggesting that the previous equations for the North Pacific (LeGrand and Schmidt, 2006), the Oyashio region (Yamamoto et al., 2001), and the Kuroshio-Oyashio system (Oba and Murayama, 2004) would underestimate seawater $\delta^{18}O$ in the Kuroshio region, probably due to the limited horizontal coverage of their original data. Linear regression analysis by the least squares method resulted in a seawater $\delta^{18}O$–salinity (S) relationship ($r^2 = 0.86$, $p < 0.01$) for the Japanese sardine habitat as follows:

$$\delta^{18}O_{seawater} = 0.56*S - 19.06 \qquad \text{(Eq. 1)}$$

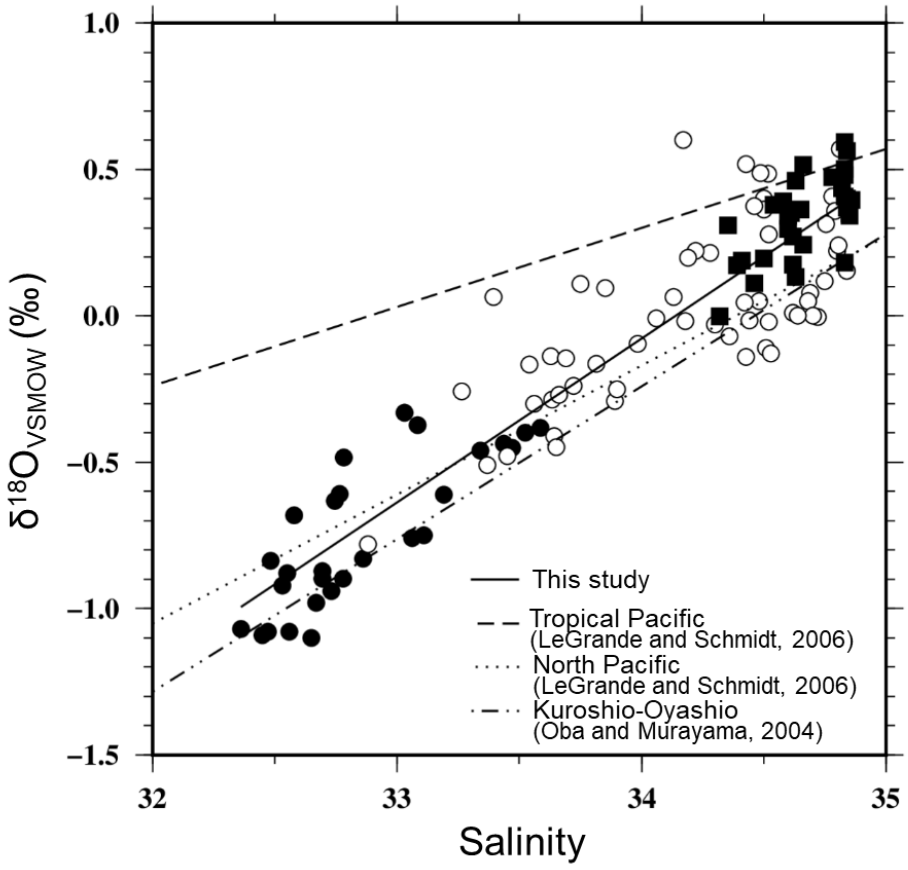

Figure 6. Comparison of seawater δ^{18}O and salinity in the habitat area of Japanese sardine. Closed squares, open circles, and closed circles represent data collected south of 36 ° N, between 36 ° N and 40 ° N, and north of 40 ° N, respectively. The solid line is the linear regression line for all plots.

4.3.2 General characteristics in early-life growth and ambient temperature

The developments of mean ambient water temperatures estimated from otolith δ^{18}O and daily increments width for each region are shown in Fig. 7. Mean ambient water temperatures of the Japanese sardine showed gradual decline from >18°C to <14°C in the first 4 months, whereas those of the Pacific sardine were relatively constant at about 14-16°C in the first 5 months (Fig. 7a). The temperatures in hatch–30 dph were consistent with the observations that weighted mean spawning temperature of the Japanese sardine is 18°C (Checkley, 2009) and Pacific sardine larvae are most abundant at 13°C to 16°C

(Hill et al., 2017), suggesting that the estimated temperatures are reliable. The Japanese sardine showed higher daily increment widths during early life history stages, peaking at about 10 µm at about 60 dph, while the those of the Pacific sardine peaked at about 8 µm at about 80 dph (Fig. 7b). Therefore, basic thermal environments and early life growth rates were apparently different between the regions.

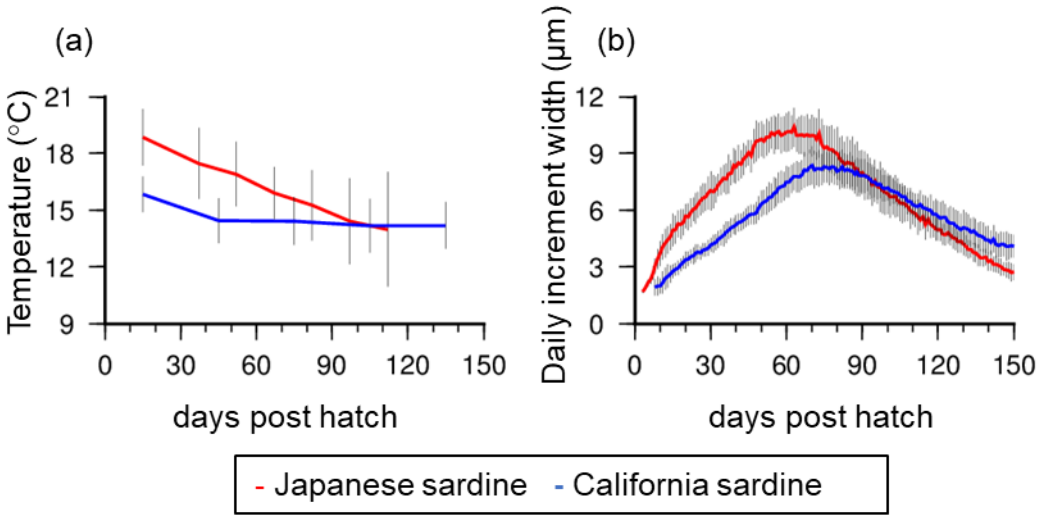

Figure 7. Time series of mean (a)) ambient temperature and (b) daily increment width for Japanese sardine (red) and Californian sardine (blue). Means and standard deviations of within year mean are shown.

The developmental stages determined for each age range are shown in Table 2. In the Japanese sardine, the stages for each age range were early larva, late larva, early juvenile, early juvenile, juvenile I, juvenile II and juvenile II stages (Table 2). In the Pacific sardine, one each from early larval to juvenile II stages were included (Table 2).

Days post hatch	Japanese sardine			Californian sardine		
	Otolith Radius (μm)	Standard Length (mm)	Stage name	Otolith Radius (μm)	Standard Length (mm)	Stage name
hatch						
30	132.9 ± 14.9	*22.7 ± 1.2	Early larva	96.6 ± 10.2	*19.7 ± 0.9	Early larva
45	251.3 ± 24.9	*30.0 ± 1.4	Late larva			Late larva
60	397.4 ± 32.1	48.4 ± 3.7	Early juvenile	283.9 ± 19.3	*31.7 ± 1.0	
75	547.1 ± 32.7	65.8 ± 3.8	Early juvenile			Early juvenile
90	677.7 ± 28.2	80.9 ± 3.3	Juvenile I	525.5 ± 34.8	63.3 ± 4.0	
105	785.9 ± 25.2	93.5 ± 2.9	Juvenile II			Juvenile I
120	872.0 ± 26.8	103.5 ± 3.1	Juvenile II	719.1 ± 32.4	85.7 ± 3.8	
135						Juvenile II
150				855.2 ± 34.0	101.5 ± 3.9	

Table 2. Mean otolith radius at the boundaries of milling areas and the corresponding standard length and the developmental stage.
Standard length was calculated from otolith radius by allometric curve for larvae (*, Takasuka et al., 2007) or linear relationship for juveniles (Takahashi et al., 2008). Stage names are based on the definition in Smith et al., (1992).

4.3.3 Inter-annual variation of ambient temperature

Inter-annual variations of ambient water temperature were apparent in both sardines (Fig. 8) but standard deviations in each age range were basically larger in the Japanese sardine (Japan: 1.3–2.8°C, California: 0.9–1.4°C), suggesting the larger temporal variability in thermal environment of the western North Pacific. Significant correlations between temperature and spawning stock biomass were detected for both sardines, although in opposite ways. In the Japanese sardine, negative correlations were found for all age ranges, except 61–75 dph (Table 3). The correlations were mainly produced by the shift of hatch date, becoming earlier with the growth of biomass, because there were significant correlations between hatch date and temperature in most of the age ranges except 46–60 and 61–75 dph (Table 3). The lack of significant correlation in the early juvenile stages may be due to the large inter-annual variation of environments in the Kuroshio-Oyashio transition area because the temperatures in 46–60, 61–75 and 76–90 dph were significantly correlated with PDO index in the corresponding months (Table 3). In the Pacific sardine, positive correlations between the temperature and biomass were found

for all age ranges, except hatch–30 dph (Table 3). The temperature hatch–30 dph had relatively small inter-annual variation, except for 2006 when the temperature was particularly high, suggesting that spawning off Southern California occur in narrow range of temperature. No correlation was found with PDO index of any month. The coastal upwelling may have an impact on larval thermal environment because the Upwelling Index in April, the month considered to be the main spawning season, were exceptionally low in 2006 and had negative correlation with sardine ambient temperature in 31–60 dph. Multiple regression analysis showed that both the Upwelling Index in April and stock biomass had significant effect on the temperature in the late larval stage ($p < 0.05$). These results indicate that the environment that larvae and juveniles experience are affected by stock biomass in addition to environmental variability.

Japanese sardine

Age range	Stage	SSB	R/S	Hatch date	PDO
hatch-30 dph	Early larva	-0.93*	0.19	0.92*	-0.70
31-45 dph	Late larva	-0.93*	0.25	0.88*	-0.65
46-60 dph	Early juvenile	-0.79*	0.25	0.74	-0.85*
61-75 dph	Early juvenile	-0.57	0.38	0.73	-0.81*
76-90 dph	Juvenile I	-0.86*	0.43	0.88*	-0.77*
91-105 dph	Juvenile I	-0.82*	0.21	0.81*	-0.57
106-120 dph	Juvenile II	-0.82*	0.30	0.86*	-0.65
		(Spearman's rho)			

California sardine

Age range	Stage	SSB	R/S	UI (April)	PDO (April)
hatch-30 dph	Early larva	0.31	-0.17	-0.46	0.04
31-60 dph	Late larva	0.72*	-0.56	-0.72*	0.05
61-90 dph	Early juvenile	0.77*	-0.52	-0.55	0.20
91-120 dph	Juvenile I	0.71*	-0.42	-0.54	0.32
121-150 dph	Juvenile II	0.74*	-0.56	-0.46	0.30

Table 3. r-statistics for the correlations with inter-annual variations of ambient temperature for each age range and other indices.
Pearson correlation coefficients are shown, except vs. spawning stock biomass of Japanese sardine. Significant correlations ($p < 0.05$) are marked with (*).

Between temperature and recruitment per spawner, which is a proxy of survival

rate during larval and juvenile stages, no significant correlation was detected for any age ranges in both the Japanese and the Pacific sardines (Table 3). Even when compared the high and low survival rate years in the similar biomass levels, such as 2006, 2007 vs. 2008, 2009 vs. 2010 and 2014 vs. 2015 in the Japanese sardine, there was no consistent warm or cool events in years of higher survival rate (Fig. 8).

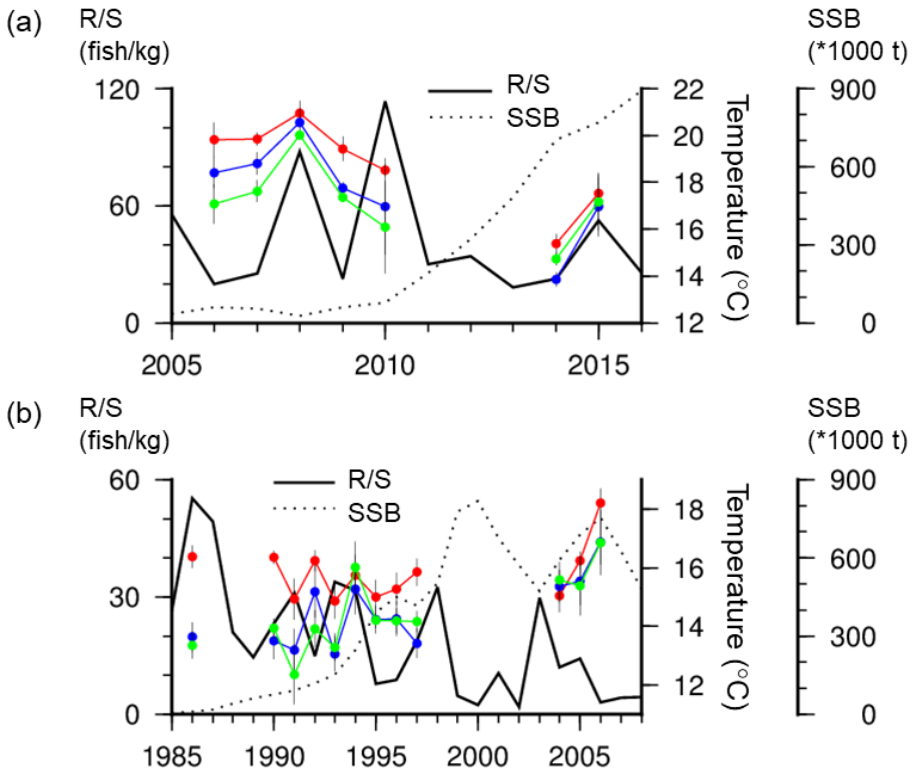

Figure 8. Comparison between time series of recruitment per spawner (R/S, black), spawning stock biomass (SSB, dotted) and ambient water temperature of sardine during early larval (red), late larval (blue) and early juvenile (green) stages for (a) Japanese sardine and (b) Californian sardine. For temperature, in (a) means and standard deviation of station mean, weighted by CPUE, are shown and in (b) Mean and standard error of individual are shown.

4.3.4 Relationships between growth rates and temperature

The comparisons between daily increments and ambient water temperature for each age range and developmental stage are shown in Figure 9. In the early larval stage, strong significant positive correlation was detected for the Japanese sardine ($r^2 = 0.28$, $p < 1.0^{-11}$), while no significant correlation was detected for the Pacific sardine ($p = 0.08$). Similarly, in the late larval stage, significant positive correlations were detected in both the Japanese sardine ($r^2 = 0.14$, $p < 1.0^{-7}$) and the Pacific sardine ($r^2 = 0.07$, $p < 0.01$) but stronger in Japanese sardine, suggesting that growth rates in larval stage respond to warm temperature more positively in the Japanese sardine. In the early juvenile stage, significant positive correlation was detected for 46–60 dph in the Japanese sardine ($r^2 = 0.09$, $p < 0.001$) and not for 61–75 dph ($p = 0.65$), while stronger correlation was detected for the Pacific sardine ($r^2 = 0.21$, $p < 1.0^{-5}$), suggesting that the Pacific sardine benefit more from higher temperature in this stage. During Juvenile I and II stages, no significant correlation was detected for both sardines, except for 76–90 dph in Japanese sardine ($r^2 = 0.05$, $p < 0.01$).

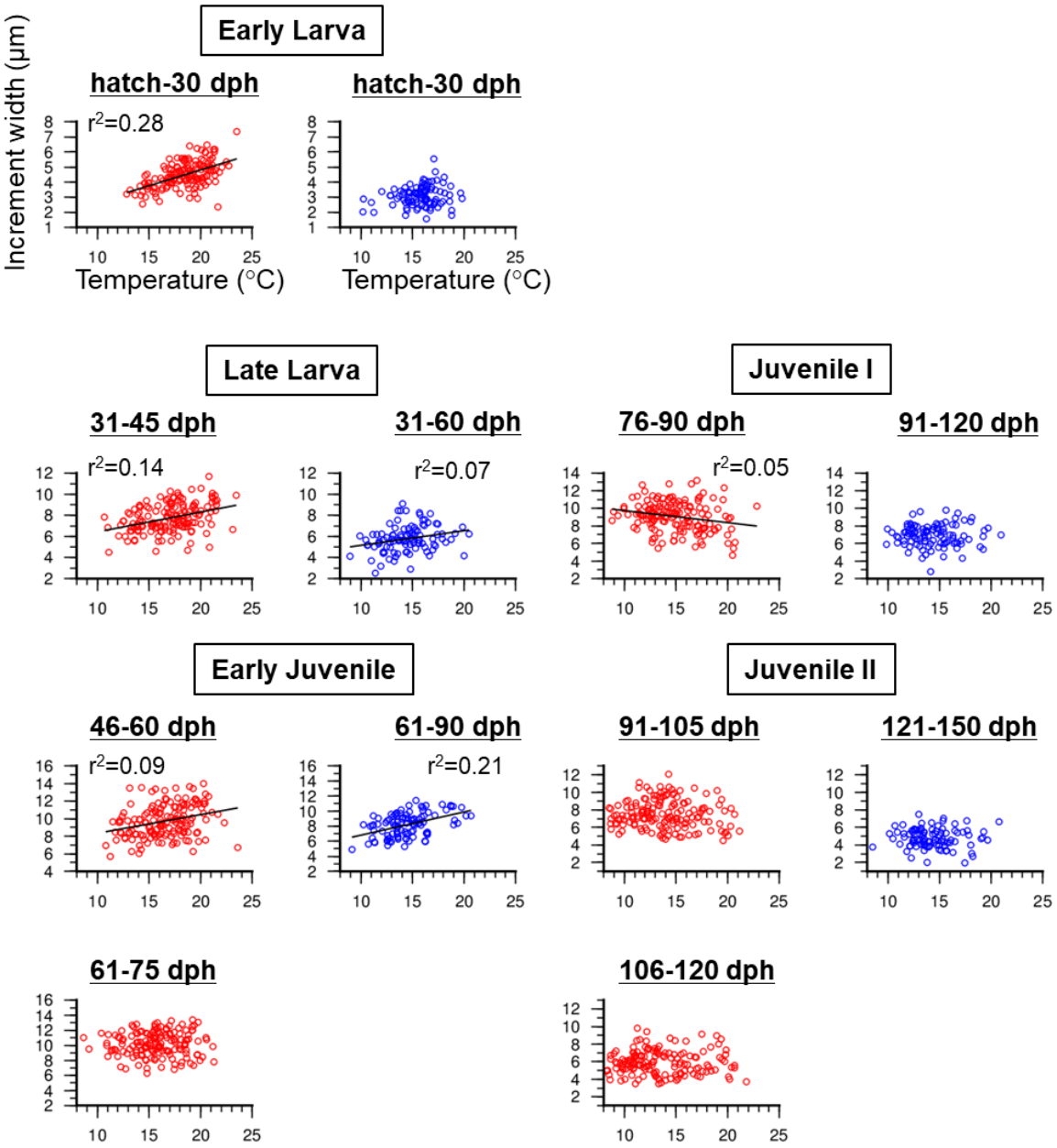

Figure 9. Temperature-growth relationship for Japanese sardine (red) and Californian sardine (blue) for each life history stage. Significant linear correlations are shown in black lines with r^2 value.

4.4 Discussion

A number of studies have suggested that the sardine biomass in the western North Pacific increase during cooler SST period and the biomass in the eastern North Pacific increase during warmer SST period, although the mechanism connecting the environmental change and sardine production are yet to be confirmed. Variability in survival rates during early life history stages has been considered as a key process in the mechanism (e.g. Watanabe et al., 1995). However, describing how environmental variabilities affect the survival rates has been difficult, partially due to the lack of appropriate technique to estimate environments that the sardines experienced in early life history stages. Here, by applying the high resolution oxygen stable isotope analysis on archived otoliths of both the Japanese and the Pacific sardine, ambient water temperature histories during larval and juvenile stages were revealed for over a hundred individuals each from multiple years. This is the first observative study that to provide direct estimates of ambient water history of sardines, and therefore the results have new implications on the mechanism of fluctuation of sardine biomass.

The contrasting thermal environments during larval and juvenile stages of the Japanese and the Pacific sardine suggest different habitat selections in different oceanographic environments. The Japanese sardine showed a clear movement from warm water over 18°C to cool water under 14°C, reflecting the migration from the Kuroshio to the Oyashio region, while the California sardine remained in cool 14–16°C water to complete their life larvae and juvenile stages. The temperature 14–16°C at surface layer in the California Current system corresponds not to the coastal upwelling core but to the frontal area of upwelled waters, suggesting that the Pacific sardine stays in such area throughout larval and juvenile stages. This is a new finding because migration patterns of

Pacific sardine during the stages have not been well documented. The low temperature commonly seen in later juvenile stages indicates that it is better for larger sardines to locate in cooler temperature, probably in terms of energy budget because fish metabolism increases with temperature and body size, and highly productive areas are generally associated with cooler temperature. The reason of the Japanese sardine using warm waters during larval stage is probably the faster growth rates. In addition, Kuroshio and cross-frontal northward currents provide transportation to the northern cool region (Isoguchi et al., 2006), which enables the strategy to switch the habitat from warm to cool waters. Meanwhile, early larval growth rates of the Pacific sardine were not correlated with temperature, suggesting that there is less advantage in spawning in warmer waters in California Current system. In addition, the surface layer advection in this region basically heads south due to the California Current or offshore due to Ekman transport (Weber et al., 2015) and not towards cool and productive coastal area, which may be the reasons that the Pacific sardine stays in cooler waters from larval stages.

Despite the apparent difference of basic thermal environment, ontogenetic developments of the relationship between growth rates and temperature were roughly similar in the two sardines, positively correlated during larval and early juvenile stages and weakly or not correlated in juvenile I and II stages, which suggests the common feature of genus *Sardinops*. Still, there were minor differences in the strength of the correlations that are probably reflecting the region-specific oceanography. It has been generally assumed that growth rates in larval stage increase with temperature in the favourable temperature range when the food supply is sufficient (Heath, 1992; Gaughan et al., 2001). The strong positive correlations between temperature and larval growth rates of the Japanese sardine suggest that the Kuroshio had been stably providing adequate

food for the Japanese sardine larvae in spring. This idea is supported by previous studies that concluded that the Kuroshio waters provide favourable feeding condition for Japanese sardine larvae and juveniles through examinations of copepod production (Nakata et al., 1995), sardine growth and stomach contents (Watanabe and Saito, 1998) and RNA:DNA ratio analysis (Kimura et al., 2000). The weaker correlations for the Pacific sardine larvae suggest that the food availability may not be enough in higher temperature. The sardine basically inhabits frontal areas of coastal upwelling waters but when the upwelling was weak and warmer and less productive waters dominated the habitat area, such as in April 2006, food limitations may have occurred. On the contrary, the positive correlation was stronger for the California sardine than for the Japanese sardine in the early juvenile stage. The weaker correlation in the western North Pacific suggest that food availability is greater in cooler waters, probably due to the high productivity of the Oyashio waters. The stronger correlation in the eastern North Pacific suggest that food supply is sufficient in warmer waters in the season. In summer, the area that offshore upwellings driven by wind-stress curl occur becomes widest in a year (Bakun and Nelson, 1991), which may have contributed to increase the food availability. This idea is consistent with the analysis that annual surplus production of the Pacific sardine is significantly correlated to the intensity of the offshore upwelling (Rykaczewski and Checkley, 2008). The lower growth rates of the Pacific sardine in cooler waters during the early juvenile stage suggest that the feeding condition in coastal upwelling waters are not as suitable as in the Oyashio waters. This can be attributed to the size of prey planktons, because the structure of gill rakers of sardine are more suitable for feeding on small planktons, rather than on large planktons in coastal upwelling waters (van der Lingen et al., 2006).

The relationships between temperature and growth rates suggest that the growth rate during the early juvenile stage, rather than during larval stages, may be the key of biomass fluctuations of *Sardinops* species. The Japanese sardine seems to benefit more from higher temperature than the Pacific sardine in terms of larval growth, which is opposite to the response of biomass to SST variations. Meanwhile, the growth rates during the early juvenile stage were weakly or not significantly correlated with temperature in the Japanese sardine and positively correlated in the Pacific sardine, which is, at least partially, consistent with the response of biomass. The early juvenile growth rates of the Japanese sardine were strongly affected by factors other than temperature, possibly by food availability, which is likely to increase during lower SST period due to the deepening of winter mixed layer (Noto and Yasuda, 1999). On the other hand, the growth rates of the Pacific sardine in the stage would simply increase in warm periods due to active feeding behaviours within sufficient food availability, which is possibly supported by the offshore upwelling. Therefore, it was considered that the link between SST variation and sardine biomass fluctuation is mediated by growth rates in the early juvenile stage, which are enhanced not directly by temperature but through bottom-up effect in western North Pacific, and by direct effects on fish physiology or behaviour in the eastern North Pacific. Because during metamorphosis, extra energy (food) is needed during metamorphosis to remodel larval structures into the juvenile form in addition to the energy that is constantly used for maintenance and growth (Pfeiler and Luna 1984), it can be a critical interval in the early life of marine fishes (Thorisson, 1994). Takahashi et al. (2008) has demonstrated that the inter-annual variation of growth rate after metamorphoses were strongly correlated to recruitment abundance of Japanese sardine in 1996–2003, which further supports our hypothesis.

As fish growth rates are dependent on ages and developmental stages, it is important to compare within similar ages to detect the environmental effect. The positive correlations between temperature and larval growth rates of the Japanese sardine are inconsistent with Takasuka et al. (2007), who compared the temperature at catch and growth rates during few days prior to catch, and reported dome-shaped relationships that shows decrease of growth in higher temperature. Based on the relationship, they suggested the existence of optimal temperature, which was 16.2°C, that physiologically maximizes larval growth rates of the Japanese sardine. In the samples used in Takasuka et al. (2007), there is a tendency that larvae captured in lower temperature are large, some exceeding 30 mm SL, and those captured in higher temperature are small. This bias is reasonable because the Japanese sardine moves from the warmer Kuroshio region to the cooler Kuroshio-Oyashio transition area as it grows (Fig 7b). As suggested in Takahashi et al. (2008), however, growth rates of the sardine are largely affected by body length and sharply increases around 30 mm SL. Therefore, it is likely that the dome shape was created by the product of effects of temperature and body size, which work on opposite directions with the increase of temperature. Itoh et al. (2011), using particle back tracking experiments, showed that larvae found in the offshore Kuroshio that experience higher temperature had faster growth rate than larvae found in the inshore side of the Kuroshio of the temperature. In addition, clear positive correlation was also observed in South African sardines (Chapter 3). I therefore disagree to the existence of the optimal temperature and consider that the growth rates of sardine larvae simply increase with temperature if the food supply is sufficient, as discussed above.

Our results indicate that the stock biomass strongly affects temporal and spatial distribution pattern of larvae and juveniles, which might be one of the mechanisms of

density-dependence of recruitment. With the increase of biomass, ambient water temperature tended to become lower in the Japanese sardine, partially due to the shift of hatch date, and higher in the Pacific sardine, probably due to the offshore shift in distribution. Because the biomass is well correlated with environmental indices that represent thermal environments of ocean, such as PDO or Upwelling Index, the observed correlations between sardine ambient temperature and biomass should not fully attributed to the effect of biomass, although the effect of biomass do seem to exist because the correlations are stronger than those between the temperature and environmental indices. It has been pointed out in many studies that examined the correlation between SST and recruitment of the Pacific sardine, that spawning biomass is more important than SST and other environmental indices in predicting the recruitment (Jacobson 1995; Lindergren and Checkley 2013; Jacobson and McClatchie 2013). Food limitation due to intraspecific competition or cannibalism have been suggested as possible mechanisms for the density effect. The change of temporal and spatial distribution pattern observed in this study may be showing the responses of sardines to relax such intraspecific competitions, although the response can cause disadvantages in other perspectives. In the Japanese sardine, the shift to cooler season would make the duration in vulnerable larval stage longer and in the California sardine, the offshore shift would lower the chance of retention in the coastal area. Therefore, in addition to the intraspecific competitions, the response to avoid them, may be limiting the recruitment rate in high biomass level.

The method to convert otolith $\delta^{18}O$ to temperature using temperature-salinity relationships observed by Argo floats allowed the temperature estimation in the region where seawater $\delta^{18}O$ is highly variable. This is applicable in many regions because Argo floats are distributed in wide range of global oceans, although it has the weakness that the

error originates from variabilities in temperature-salinity relationship becomes as large as 2°C in summer. It is therefore important to analyse large numbers of otoliths to obtain robust results, over a hundred in this study, and to seek for ways for further improvement, such as using the data from more narrow geographical ranges. Because the previous discussions on early-life growth and biomass fluctuation are based on the data in March to June in which the error in temperature conversion is mostly less than 1°C (Table 1), the error caused in this conversion would not largely affect the discussions.

Because individuals that grew faster tend to have smaller otoliths relative to their body length (Takasuka et al., 2008b), the use of daily increment widths as a proxy of growth rates can underestimate fast growth rates and overestimate slow growth rates. Although the biological intercept method (Campana,1990) is often use to adjust for this bias, it was not used in this study because the function type of the relationship between otolith radius and body length is known to change from allometry (Takasuka et al., 2007) to linear (Takahashi et al., 2008) as sardines grow, which makes it difficult to define a single formula as the relationship throughout early life history stages. Because this bias can hide existing correlations between temperature and growth rates but do not create them, however, it will not have significant impacts on the discussions which is mainly based on significant positive correlations.

Overall, our estimations of ambient water temperature based on the otolith δ^{18}O analysis provided new insights how temperature can affect early life growth rates and showed the possibility that growth rates during the early juvenile stage can be the key for the biomass fluctuation. Because the inter-annual variation of ambient water temperature during the early juvenile stage did not show significant correlations with that of recruitment per spawner for both sardines, however, there are apparently other processes

that are affecting sardine biomass, such as top-down controls, which need to be clarified in the future studies. Understanding the true drivers of population fluctuation is a crucial task to forecast how marine resources react to climate change in the future and consider how we can sustainably and efficiently utilize such resources. Although otolith $\delta^{18}O$ can only reveal temperature history, the method that combines otolith $\delta^{18}O$ and numerical simulation (Sakamoto et al., 2018) may allow estimations of other factors, such as food availability, in future. By developing new methods that allows to examine each potential process in detail, we may be able to reveal the whole picture, someday.

Chapter 5

Combining microvolume isotope analysis and numerical simulation to reproduce fish migration history

5.1 Introduction

Marine fish stocks are an important food resource for humans (Crist et al., 2017) and marine predators (Cury et al., 2011), although many have faced severe declines (Pauly et al., 2002). Understanding population structure is a basic and crucial requirement for efficient fisheries management (Cadrin et al., 2014) because, without it, fisheries can exert an unexpectedly high pressure on certain regional populations, leading to overfishing of some stock components (Felix-Uraga et al., 2005; Hüssy et al., 2016). Therefore, revealing seasonal or annual changes in fish distribution at both individual and

population levels has been a key topic in fisheries science (Tsukamoto and Nakai, 1998; Block et al., 2005; Brennan et al., 2015).

Several methods have been developed to track the movements of marine fish in open oceans. Electronic tagging has been valuable for reproducing the migration histories of large fish such as adult Bluefin tuna based on recorded light levels and temperatures (Block et al., 2005). For early life stages in which swimming ability is negligible, numerical particle tracking experiments based on ocean models have allowed a better understanding of how fish disperse from spawning grounds (Allain et al., 2007; Itoh et al., 2011). However, we still lack solid methods for small-sized, but actively swimming, juveniles that cannot be tagged, although survival rate during this stage is crucial for populations fluctuation (Houde, 1987; Anderson, 1988). Recently, numerous individual-based migration models coupled with fish bioenergetics have been developed to estimate migrations of this type of fish (Crowder et al., 1993; Rose et al., 1999; Okunishi et al., 2012), although they still include assumptions that are very difficult to verify empirically, thereby presenting inherent uncertainty.

Otoliths are calcium carbonate crystals formed in the inner ear of fish, and their chemical composition is known to record ambient water chemistry (Campana, 1999; Sturrock et al., 2012). In particular, the oxygen stable isotope ratio ($\delta^{18}O$), which reflects both temperature and $\delta^{18}O$ of surrounding water (Kim et al., 2007), has often been used as a temperature proxy to discuss fish migration (e.g. Carpenter, 2003; Shiao et al., 2009). It has mainly been applied to fish species with large otoliths because conventional isotope ratio mass spectrometry required large sample amounts. Recently, however, the analysing system MICAL3c has been developed. This system requires 1/100 of the sample quantity required for conventional mass spectrometry (Ishimura et al., 2008; Nishida and Ishimura,

2017), thereby allowing an accurate analysis of narrow growth increments in small otoliths (Sakamoto et al., 2017). Despite this drastic technical improvement, interpreting otolith $\delta^{18}O$ values to estimate fish migration history remains difficult. The variability of seawater $\delta^{18}O$, which is primarily related to salinity variation (Craig and Gordon, 1965), often confounds temperature estimation because it is essentially impossible to estimate the two parameters in a single equation. Moreover, because otolith $\delta^{18}O$ can only distinguish water masses of different temperature or salinity, estimations of fish location become impractically rough when uniform water masses are distributed broadly (Torniainen et al., 2017), which is often the case in open oceans.

Here, a new methodology to estimate the migration history of individual small fish is described and demonstrated, by using an interdisciplinary combination of isotopic analysis and numerical simulation. The Japanese sardine was selected as the model for this demonstration because of its dynamic migration from the temperate Kuroshio region to the subarctic Oyashio region within six months after hatching (Kuroda, 1991), and economic and ecological importance in the western North Pacific (Ishida et al., 2009). To our knowledge, this is the first otolith microchemistry study to use numerical migration models to interpret the isotope profile. First, using micro-milling and micro-volume isotope analysis, accurate otolith $\delta^{18}O$ profiles were obtained with high resolution. Furthermore, instead of estimating temperature histories from the otolith $\delta^{18}O$ profiles, migration routes that should be followed to reproduce the $\delta^{18}O$ profile were searched for, using an individual-based model in which a randomly swimming migration scheme was applied to a data-assimilated ocean model.

5.2 Materials and Methods

5.2.1 Fish sampling and otolith micro-milling and $\delta^{18}O$ analyses.

Six young-of-the-year Japanese sardine individuals were used. These were obtained from samples taken offshore Oyashio region in a subsurface trawl survey conducted by the NRIFS; three were sampled in October 2010 and three in September 2014. Individuals [standard length (SL): 107.7–133.7 mm] were immediately frozen after capture and defrosted just before otolith analyses. Sagittal otoliths were extracted, cleaned using a needle and a thin paintbrush under 10–20× magnification, rinsed with Milli-Q water, and air-dried for a few hours. After these procedures, otoliths were embedded in Petropoxy 154 (Burnham Petrographics LLC) resin and kept at 80 °C for 12 h to cure the resin. Embedded otoliths were ground with sandpaper (no. 2000) and polished with an alumina suspension (BAIKOWSKI International Corporation) in sagittal plane to reveal the daily rings from the core to the edge.

The position and number of daily rings in otoliths were examined along the axis of the postrostrum using an otolith measurement system (RATOC System Engineering Co. Ltd.). The daily age at capture was calculated by adding two to the total number of otolith daily rings (Takahashi et al., 2008), because the first daily ring is formed 2–3 days after hatching in Japanese sardine (Hayashi et al., 1989). At every 10 or 15 daily rings, a ring was tracked as far as possible from the axis and used as the boundary of the micro-milling area. Date ranges corresponding to each milling area were back calculated from the capture date by subtracting the number of daily increments from the edge of the otolith. Marked pictures were input to the high-precision micro-milling system GEOMILL 326 that comprises a micro-mill, a CMOS camera, a video monitor, and an image analyser controlled by a computer. This system allows accurate sampling at 1/1000 mm scales

(Sakai, 2009), and it has been used to accurately extract the edge of sardine otoliths (Oda et al., 2016; Sakamoto et al., 2017). Each area between marked daily rings was then sequentially extracted, and the resulting powders (0.3–11.4 μg) were collected into stainless micro-cups (YUKO-PARTS). After each milling, the otolith was cleaned with an air-duster to avoid cross-contamination between milling paths. The micro-milling depth was set at 50 μm for the two areas nearest the core and 50–120 μm for the remaining areas.

Otolith $\delta^{18}O$ was measured using a continuous-flow isotope ratio mass spectrometry system (MICAL3c with IsoPrime 100) at the National Institute of Technology, Ibaraki College. This system allows analysis of $\delta^{18}O$ from sub-microgram carbonate samples (> 0.2 μg) with high precision and accuracy (Ishimura et al., 2004, 2008; Kitagawa et al., 2013; Oda et al., 2016, Nishida and Ishimura, 2017, Sakamoto et al., 2017). Otolith powders reacted with phosphoric acid at 25 °C, and the released CO_2 was purified and then introduced into the mass spectrometer. The $\delta^{18}O$ values were reported in δ-notation relative to the VPDB (Vienna Pee Dee Belemnite) scale, and given as a ‰ value. Analytical precision was better than ± 0.10 ‰ throughout the entire analysis. The acid fractionation factor of calcite was used to facilitate comparisons with isotopic values reported in previous studies (Amano et al., 2015). Although evidence of any errors in the purifying and analysing processes could not been found, a sharp increase was observed in the $\delta^{18}O$ profile (* marked in Fig. 1); this value was excluded from the modelling analysis and considered as a failure of isotope analysis because no migration route that reproduced such a fluctuation were found.

5.2.2 Estimation of migration history.

An individual-based model (IBM) with a random-swimming scheme was applied to an ocean environment reproduced by the data-assimilated ocean model FRA-ROMS. FRA-ROMS is an ocean forecast and reanalysing system developed to realistically simulate mesoscale variations over the Kuroshio-Oyashio region (Kuroda et al., 2016). A random swimming scheme was chosen to find many, ideally all, possible routes that the fish can take to reach capture location, simply based on the distance that can be covered by advection and swimming. It would be interesting to add assumptions, such the fish preference to head the direction where they can yield higher growth rate, to further narrow route prediction. However, I avoided introducing such an assumption because the mechanism by which fish decide their heading direction is currently unknown and I wished to free our model from assumptions that are not empirically confirmed. For each of the six individual fish analysed, approximately 10^9 simulated individuals were released on the hatching date in the survey-based spawning grounds, and advected and diffused by a surface current field reproduced using FRA-ROMS. Individuals were set to swim at a speed of 3*SL/s after metamorphosis, randomly changing their swimming direction once a day. Otolith $\delta^{18}O$ histories were calculated for the individuals that reached the capture point, based on ambient temperature and salinity histories. The possibility of each migration route was calculated as a product of egg abundance in the grid of origin and agreement between calculated otolith $\delta^{18}O$ history and analysed profiles. Possibility-weighted mean position and temperature and water current velocity were calculated daily and considered representatives of estimated routes.

5.2.2.1 FRA-ROMS configuration.

The FRA-ROMS ocean forecast system was developed by the Japan Fisheries Research and Education Agency (FRA), and combines an ocean circulation model based on the Regional Ocean Modeling System (ROMS) with three-dimensional variational (3D-Var) analysis schemes. It is primarily composed of 1/2- and 1/10-degree models connected by one-way nesting, in which volume transport across the lateral boundaries is adjusted. The former parent model covers almost the entire North Pacific and has been designed to simulate basin-scale variations associated with El Nino-Southern Oscillation and the Pacific Decadal Oscillation. These are imposed as external forcing at the lateral boundaries of the child model, whose domain is limited to the western North Pacific to simulate mesoscale variations over the Kuroshio-Oyashio region. The vertical structure of this system comprises 48 layers defined by the specific S-coordinate function in both models. Model specifications and a detailed methodology of numerical simulation can be found in Kuroda et al. (2013, 2016). In situ temperature-salinity profiles and satellite sea surface height and temperature are assimilated into the models by the 3D-Var method using a weekly time window.

Comparison with several oceanographic datasets indicates that FRA-ROMS is able to reproduce representative features of mesoscale variations such as the position of the Kuroshio path and the variability of the Kuroshio Extension (Kuroda et al., 2016), which might have crucial effects on the migration route of Japanese sardine. It should be emphasized that position errors are acceptable between ocean drifters and particles passively transported by currents estimated by FRA-ROMS (Kuroda et al., 2016). The accuracy of reanalysed daily sea surface temperature (SST) was evaluated by comparing it with a daily gridded SST dataset (AVHRR_OI) with a horizontal resolution of 0.25°

(National Climatic Data Center, 2007) for the Kuroshio-Oyashio transition area, and the root-mean-square differences (RMSDs) estimated at monthly intervals were in the range 0.63–1.10 (Kuroda et al., 2016), corresponding to 0.11–0.20 ‰ in otolith δ^{18}O. The accuracy of reanalysed salinity was evaluated by comparing it with a monthly mean dataset of global oceanic salinity derived from Argo float observations with a horizontal resolution of 2.5° × 5° (Hosoda et al., 2008), for the area from 30°N to 50°N and 130°E to 180°E. The RMSDs estimated for monthly means from 2010 to 2014 at 10 m depth were below 0.20, corresponding to 0.12 ‰ in seawater δ^{18}O in areas where the Japanese sardine is distributed (Fig. 1).

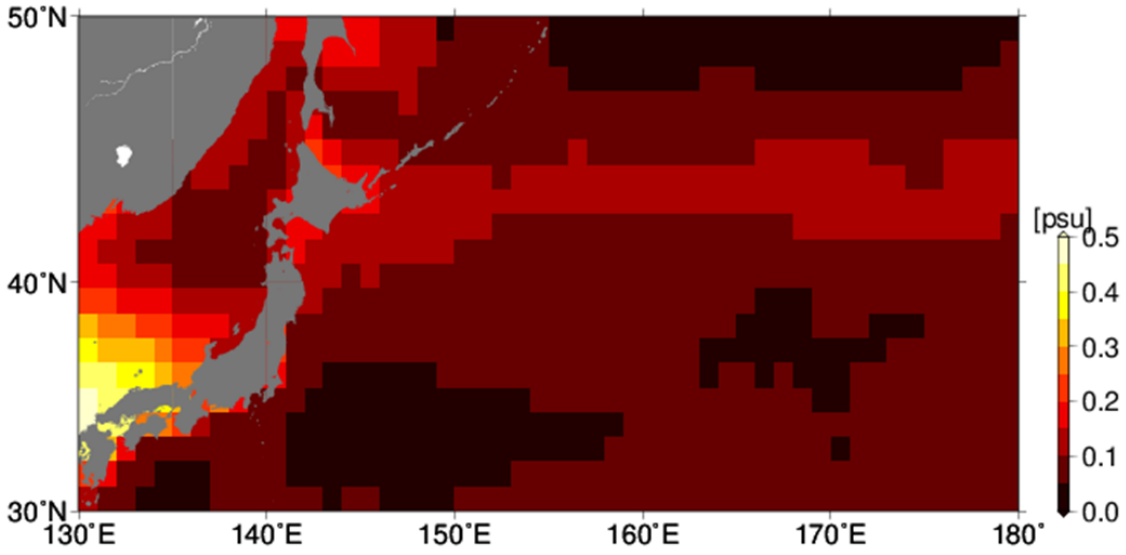

Figure 1 Root-mean-square differences in salinity at 10 m depth between FRA-ROMS and Argo-float based datasets estimated as monthly means from 2010 to 2014.

5.2.2.2 IBM simulation design and route selection.

The survey-based monthly egg abundance data (Oozaki et al., 2007), 1/4° grid scale for individuals from 2010 and 1/2° for individuals from 2014, were used to set the starting points of particle tracking. In the grid cells in which egg abundance was positive in the

month that targeted individuals hatched, 120 × 120 particles were laid at regular intervals on the hatch date. The number of egg-positive grid cells in the southern coast of Japan was 37 and 33 for 2010 and 2014, respectively. The horizontal movement of particles was regulated with advection, diffusion, and active swimming terms using the Euler scheme:

$(x_{n+1}, y_{n+1}) = (x_n, y_n) + (u_n, v_n)\Delta t + (l^x_n, l^y_n) + (mig^x_n, mig^y_n)\Delta t,$

where (x_n, y_n) is the position of a particle at time step n, (u_n, v_n) is the surface current velocity at (x_n, y_n) interpolated linearly from the surface velocity reanalysed by FRA-ROMS, and (l^x_n, l^y_n) is the random walk steps representing horizontal diffusion parameterized by the scheme of Smagorinsky (1963). The term (mig^x_n, mig^y_n) corresponds to the active swimming velocity at time step n, which was updated daily as

$(mig^x_n, mig^y_n) = C \times BSL \times (\cos(2\pi\theta), \sin(2\pi\theta))$,

where C is a constant coefficient to estimate cruising speed from body length, BSL is a back calculated SL on that day, and θ is a random number between 0 and 1. Back calculated SL was based on the linear relationship between SL and otolith radius using a biological intercept method (Campana 1990; Takahashi et al., 2008). Particles were tracked until the capture day and their position, ambient temperature, and salinity were output daily. This trial was repeated 2000 times with different random number sequences. Hara (1987) reported that the cruising speed of the adult Japanese sardine is 1.2–4.1 body length (BL)/s. Although low swimming ability of sardine larvae would be negligible (Silva et al., 2014), metamorphosed juveniles, compared to adults, were assumed to swim equally or slightly faster in proportion to their body size because smaller sized fish have generally higher tail beat frequency (e.g. Bainbridge, 1958; Hunter and Zweifel, 1971). Therefore, C was set to 0 when BSL is under 30 mm, and changed to 3 when BSL exceeded 30 mm. Additional experiments were conducted with C for BSL > 30 mm equal

to 2 or 4, aiming to test the sensitivity of the results to the value of C, using 1000 replicates. As the scheme is essentially a random walk, the scale of dispersal is larger for smaller frequencies of direction changes. To check the sensitivity of the results to the frequency of direction change, further experiments with C equal to 3 were conducted with frequency equal to 2 and 0.5 times/day, using 1000 replicates.

The possibility of each route was calculated as follows. First, the particles with horizontal position out of the ± 0.5° range from the captured location on the capture date were regarded as unrelated and excluded from further analysis. For particles that reached the capture location, egg abundance at the grid of origin was set as the initial weight. Calculation of the δ^{18}O profile was conducted using averaged ambient temperature and salinity of the particle during the date corresponding to each milled otolith area. Salinity was converted into seawater δ^{18}O using a regression between seawater δ^{18}O and salinity in the habitat of the Japanese sardine (Sakamoto et al., 2018; $\delta^{18}O_{seawater} = 0.56*S - 19.06$). Otolith δ^{18}O was then calculated by substituting seawater δ^{18}O and temperature into the equation for the relationship among otolith δ^{18}O, temperature, and seawater δ^{18}O recently proposed for the Japanese sardine (Sakamoto et al., 2017; $\delta_{otolith} - \delta_{seawater} = -0.18*T + 2.69$). The agreement of the calculated δ^{18}O for the required period was computed by substituting the calculated otolith δ^{18}O value into a probability density function of normal distribution $N(\delta^{18}O_{analysed,\ 0.18})$. The overall possibility for each route was calculated as the product of initial weight and agreement for each date range. Routes with possibilities higher than 1/100 of the highest possibility were considered possible routes. For these possible routes, possibility-weighted mean positions, ambient water temperature and water current velocity were calculated daily to discuss the details of selected routes.

5.3 Results

5.3.1 Otolith$\delta^{18}O$ profiles.

Figure 2 shows the otolith $\delta^{18}O$ profiles analysed for the six individuals examined. The temporal resolutions of the otolith $\delta^{18}O$ profiles were 20–30 days for the sample nearest to the core and 10–15 days for all other samples. Unfortunately, some samples nearest to the core or at the edge of the otolith could not be analysed precisely due to their small amount or handling failure. None of the profiles, except one from 2014, showed a remarkable trend, fluctuating between -1 ‰ and +0.2 ‰ throughout the fish life (Fig. 2a-e). A profile from 2014 showed a decreasing trend (Fig. 2f), starting higher than 0 ‰ and ending lower than -0.8 ‰, with a small increase in June to July peaking at about -0.1 ‰.

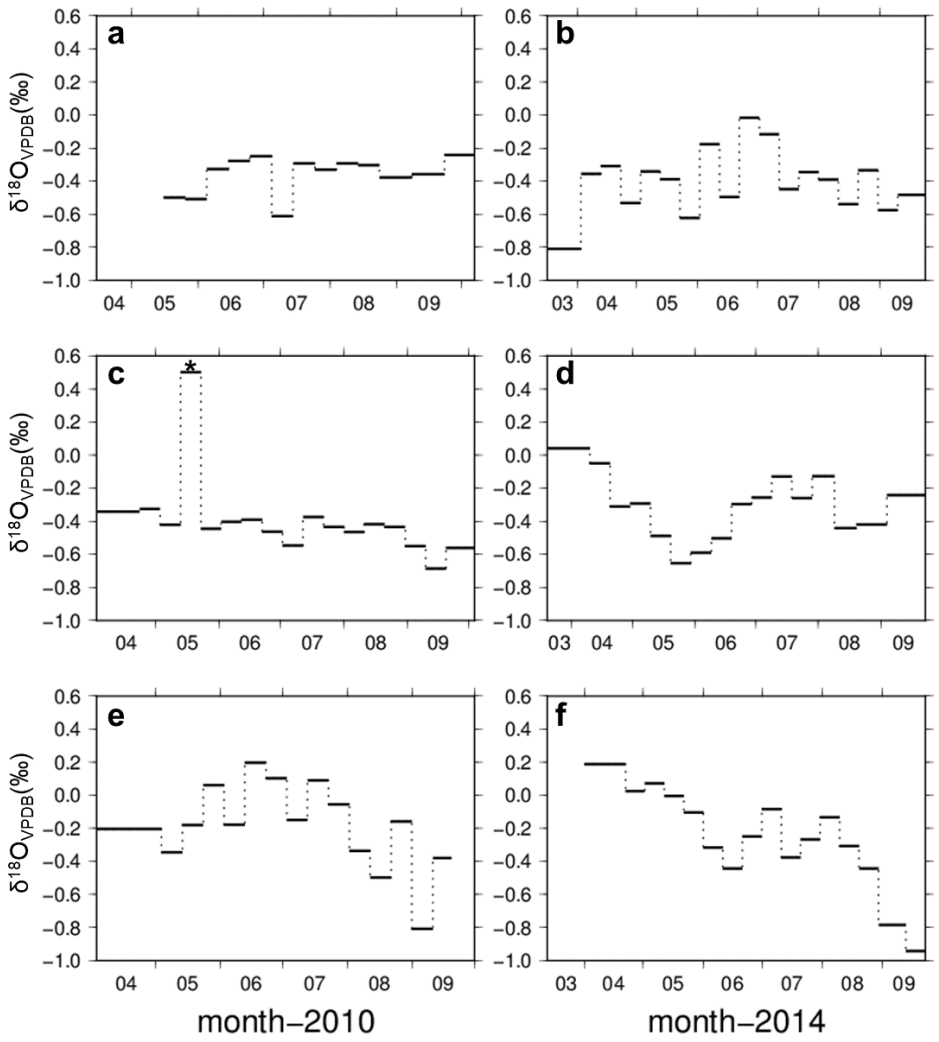

Figure 2 Otolith $\delta^{18}O$ profiles. a, c, e, Profiles for the individuals captured in 2010. **b, d, f,** Profiles for the individuals captured in 2014. The right end of the x-axis is the capture date, and the left end is the hatched date estimated from daily ring counts. Samples taken nearest to the core in (a) and (f), and at the edge in (e) were lost. The * marked value in (c) was considered as an analytical failure and excluded in modelling analysis.

5.3.2 Migration routes estimated using randomly-swimming IBM.

Figure 3 shows the high possibility routes found for each individual using random swimming in the IBM and calculated otolith $\delta^{18}O$ histories for each route. Routes that well reproduced the otolith $\delta^{18}O$ profile were crowded in a certain range, successfully showing the area that the fish should have passed. Although starting points varied between 133 and 140 °E, the overall migration patterns were consistent within a year but different between years. Individuals from 2010 (Fig. 3a, c, e) were transported by the Kuroshio until ~150 °E then started to migrate northeast, while those from 2014 (Fig. 3b, d, f) took more offshore routes, being advected as far as ~165 °E before heading north.

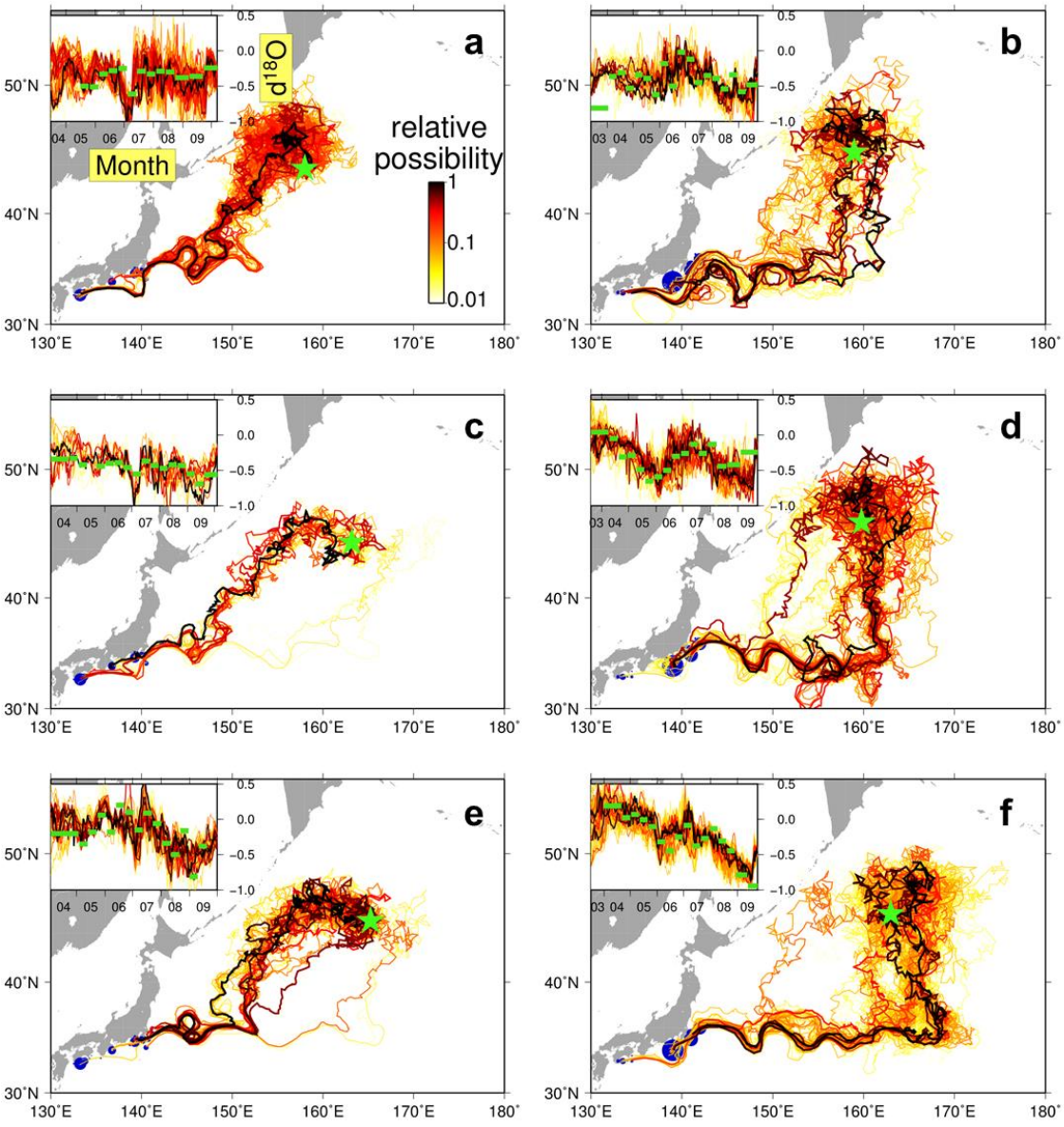

Figure 3 High possibility routes for each individual according to random swimming model estimation. The thicker and darker coloured routes are the routes with higher possibilities. The possibility of each route was divided by the highest possibility for each individual. Capture locations are presented as green stars. The left upper panel within each picture shows calculated otolith $\delta^{18}O$ history for each migration route (yellow-black) and the analysed otolith $\delta^{18}O$ (green). The locations of spawning ground are shown in blue circles in coastal areas, of which size representing the relative abundances of egg.

These routes seemed to be reasonable as, for most individuals analysed, the possibility-weighted mean routes from May to June, corresponding to 40–100 days post hatch, coincided with the area where late-larvae and juvenile sardines were caught during

sampling surveys conducted in the corresponding period (Fig. 4a, b). Mean temperature and water current velocity were also calculated to examine key timings and features of the migration. Sardines were initially transported along the Kuroshio until departing to the north in late May to mid-June (Fig. 4c, d). They entered the Oyashio feeding ground dominated by subarctic water (surface water temperature <15 °C) from the end of June to early July (Fig. 4e, f), and reached the highest latitude (47–48 °N) in late August (Fig. 4c, d). The substantial contribution of the northward water current for sardines reaching the feeding ground was suggested by the positive northward speed of this current in May and June (Fig. 4g, h). Selected routes were similar when swimming speed was changed, but moved slightly inshore with C = 2 (Fig. 5). Similarly, selected routes were robust to changes in the frequency of swimming direction, but shifted inshore with high frequency of these changes (Fig. 6).

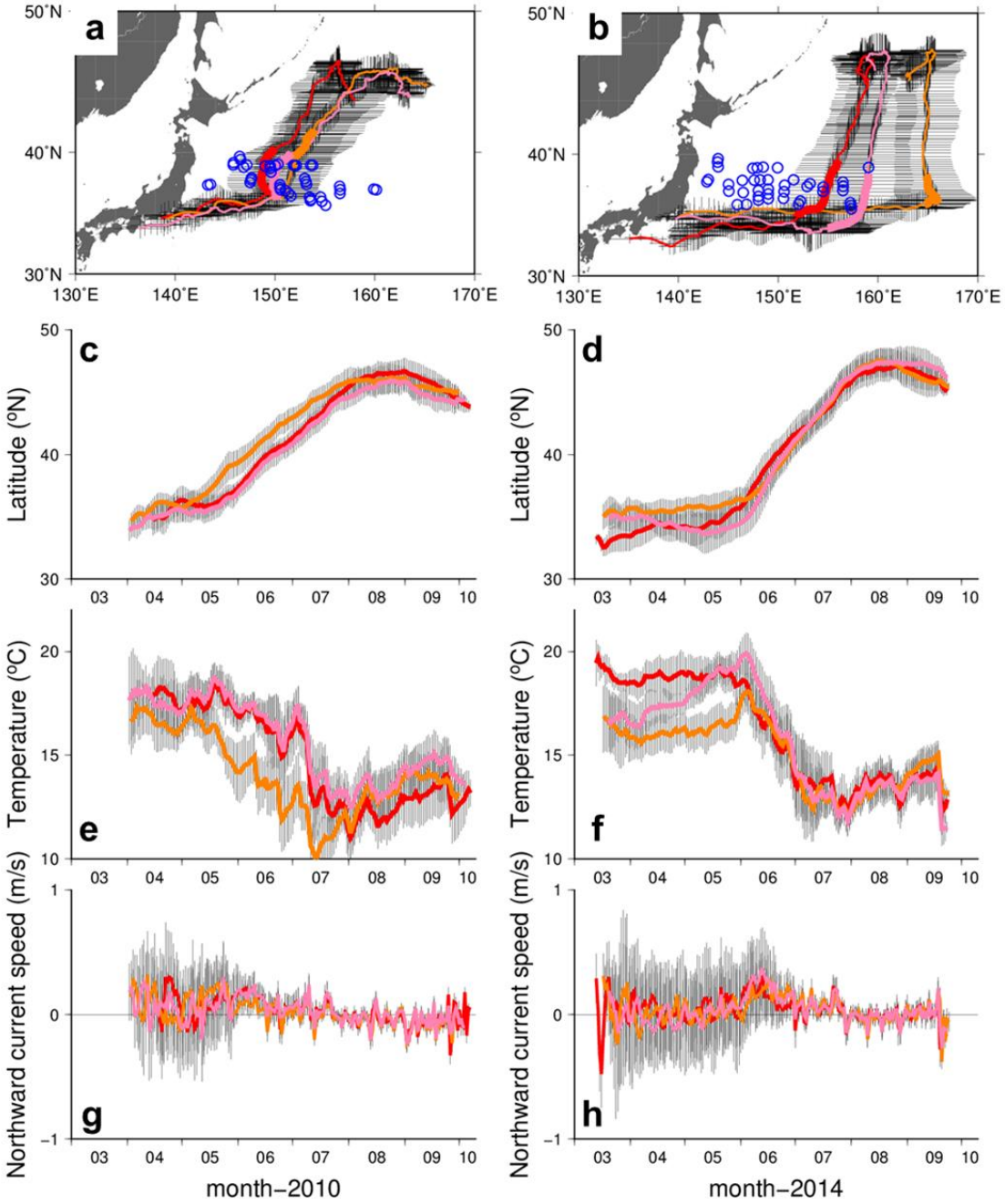

Figure 4 Possibility-weighted mean data obtained from the individual-based migration model. **a, b,** Possibility-weighted means and standard deviations obtained for individual positions and their comparison to the results of the sampling surveys conducted in (a) 26 May- 20 June, 2010 and (b) 24th May-18th June, 2014 . Points at which larvae or juvenile sardines were captured are indicated by blue circles. Mean estimated positions in the date range corresponding to the survey period are shown as thick lines. **c-h,** Timeseries of and likelihood-weighted means and standard deviations of (c),(d) latitude, (e),(f) temperature and (g),(h) northward water current speed. The same colour in the same year indicates the same individual.

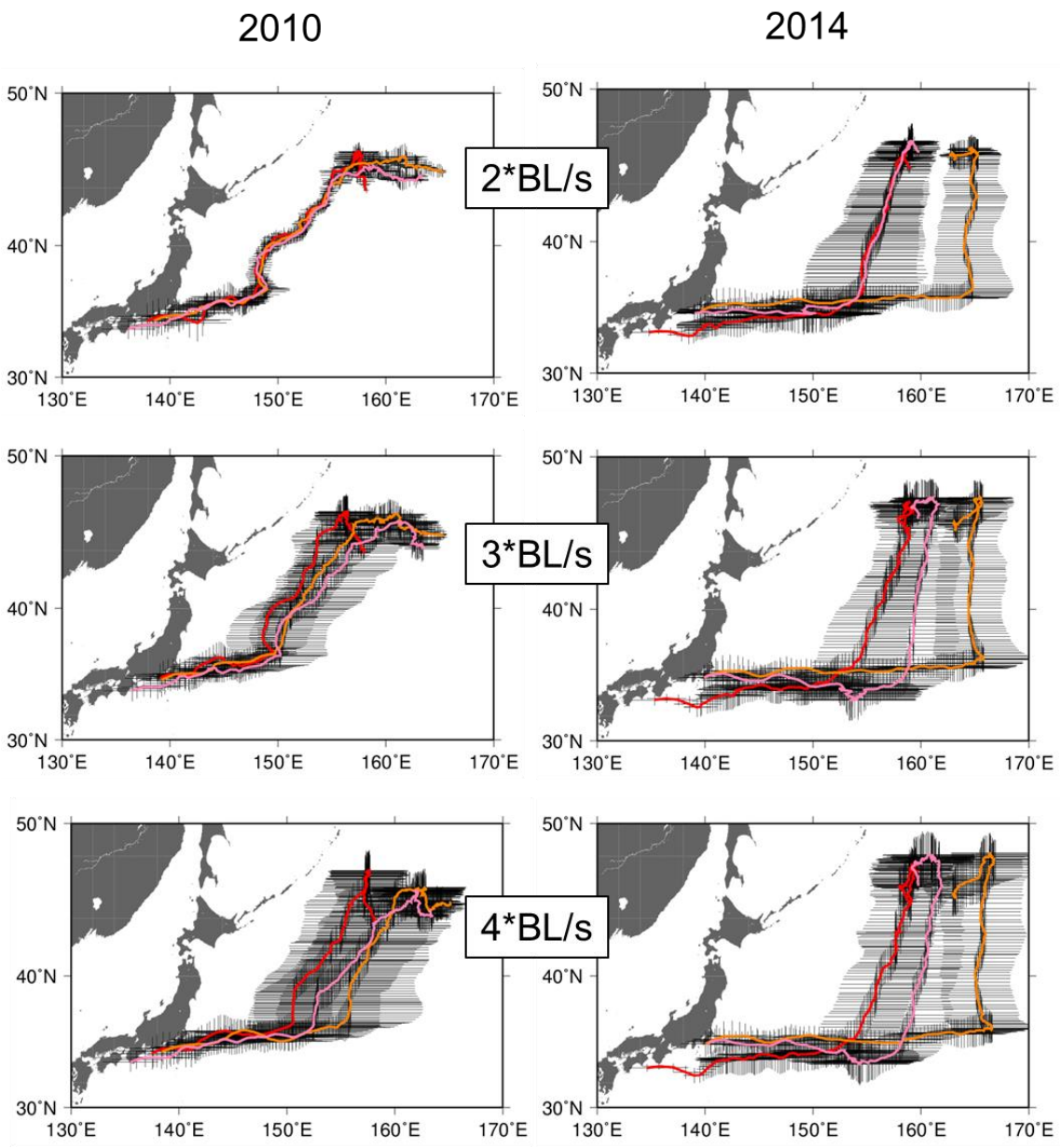

Figure 5. Possibility mean positions for each individual calculated at three different swimming speeds: 2, 3 or 4*BL/s.

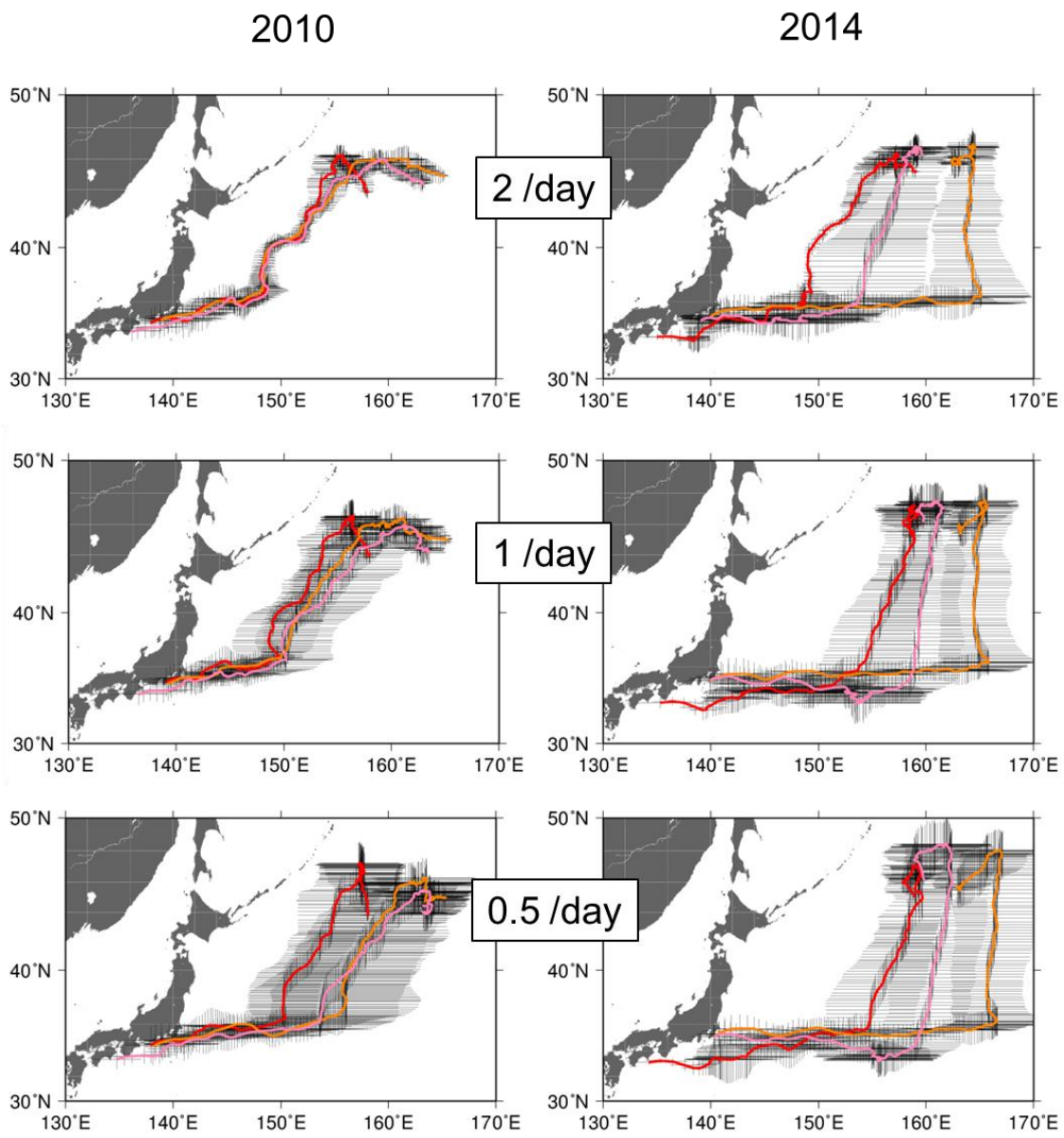

Figure 6. Possibility mean positions for each individual calculated at different frequencies of changes in swimming direction: 2, 1, and 0.5 times/day. Swimming speed was set to 3*BL/s.

5.4 Discussion

Here, the migration history of the small pelagic Japanese sardine was reproduced using the combination of high-resolution otolith $\delta^{18}O$ analysis and numerical migration simulation without any ad hoc assumptions. Accurate micro-milling and micro-volume

isotope analysis showed the remarkable capability of providing otolith δ^{18}O profiles in a resolution of several 10-day periods, even for small otolith species such as sardine. Although otolith δ^{18}O profiles did not show apparent sign of migration, this analysis combined with randomly-swimming IBM simulations showed clear northward migration heading for the capture point in the feeding ground, revealing the true utility of otolith δ^{18}O profiles.

The neutral or decreasing trends of otolith δ^{18}O profiles contradicted the hypothesis that an increasing trend would appear due to migration from the warm Kuroshio to the cold Oyashio water, and the negative correlation between otolith δ^{18}O and temperature. In fact, the signals resulting from decreasing temperature seem to be less important than those resulting from the variation in seawater δ^{18}O, which is approximately 0.8 ‰ lower in the Oyashio than in the Kuroshio region (Fig. 1). Under such strong compensation by seawater δ^{18}O, it is difficult to estimate temperature history and migration route from otolith δ^{18}O profiles alone, and salinity data are also required for a comprehensive analysis.

As so, a simple individual-based migration model was employed to find possible migration routes between the spawning ground and the capture location, which showed the capability of providing detailed movements. Route selection in this estimation can be explained by several processes. Otolith δ^{18}O variations can directly reflect the corresponding latitudinal movements, because temperature and salinity are generally uniform along zonal directions but differ meridionally in open oceans. On the contrary, longitudinal positions cannot be estimated from otolith δ^{18}O and horizontal distributions of temperature and salinity. However, for the Japanese sardine spawning around the Kuroshio, the time at which the northward movement is initiated controls the period of

larvae advection by the Kuroshio, thereby determining the transported distance. Furthermore, when fish have low swimming ability but need to move north, they require strong northward cross-jet currents. In the Kuroshio Extension (KE), a cross-frontal northward current is frequently observed between the trough and the crest of the meander (Sainz-Trápaga and Sugimoto, 2000), as is the case of the Gulf Stream (Bower and Rossby, 1989). Warm streamers are also spread intermittently from the KE (Sainz-Trápaga and Sugimoto, 2000) and quasi-stationary jets extend northeastward in the transitional area between the KE and the Oyashio fronts (Isoguchi et al., 2006), probably providing conditions for longitudinal selection. Although these processes seem unique for the KE, similar processes may occur in other regions as many fish larvae depend on regional flows, such as the coastal jets in the Benguela Current (Hutchings et al., 2002) or the eddies in the California Current (Logerwell et al., 2001), to effectively reach food-rich feeding grounds.

The method used here revealed new aspects of feeding migration of the Japanese sardine. Our estimations suggested that it is from the middle to end of May that sardines start to move northward departing from KE, and it is from the end of June to early July that they enter the Oyashio feeding ground north of 42 °N. Although the spawning grounds and transportation during the larval stage have been well documented through a number of surveys (e.g. Kuroda, 1991), these key timings in the feeding migration are the first to be clarified because this type of information can only be obtained by continuously tracking fish movement. The estimation provided here also showed that sardines utilise the northward current during their northward migration, supporting the hypothesis of Isoguchi et al. (2006), who pointed out that warm tongues and meanders from KE might be the direct routes for the northward migration of pelagic fishes based on their analyses

of surface flow field. Considering all individuals analysed in this study are the survivors that reached the feeding ground, riding the northward current near KE might be an important condition for the sardine to recruit and thus the strength of such currents can significantly affect the recruitment rate. Between the two years analysed, the selected routes in 2014 were more offshore than those in 2010. This shift may be related to the seven-times larger population size in 2014 (Yukami et al., 2017), as sardines tend to expand their habitat area offshore when biomass is increased (Barange et al., 2009). All these detailed descriptions of migration patterns would be useful for narrowing down the season and areas that are important for recruitment variability, studying how fish decide their swimming direction, and testing and improving migration models, which will be the scopes of future studies.

It should be noted that the accuracy of route estimation using such processes largely relies on the reproducibility of the ocean model. The model used in this study was developed to realistically simulate the environment by assimilating numerous satellite and in situ observation data, although the number of observations is still limited, especially for salinity, as this is not measured by satellites. Further accurate estimation requires both expansion of the monitoring network and improvement of simulation models. It is also noteworthy that model schemes require some assumptions on the swimming depth. Because age-0 Japanese sardine vertically migrate mainly within the surface mixed layer (e.g. Takahashi et al., 2008), it was assumed that they experience an environment similar to that on the water surface. When applying this methodology to species distributed in wider depth range, some adjustments, such as averaging the temperature and salinity within the water column, or introducing vertical migrations into IBM, may be needed. In addition, due to spatially and temporally dense observations of

Japanese sardine spawning, these data were used as starting points for IBM estimation, but this is not always the case. In the absence of such survey datasets, modelled spawning grounds can be used (e.g., Zwonlinski et al., 2011).

Overall, the method presented here would be a great alternative to electronic tags understanding movements of fish during early life history or for fish that are otherwise too small to accommodate electronic tags. It would also be useful not only to reveal population structure but also to validate and improve movement models that have been lacking detailed reference data to discuss their accuracy. Moreover, this method has the unique and strong advantage of examining the environmental history of successfully recruited individuals. This is crucial information to understand the environmental conditions necessary for fish to survive, providing clues on how environmental variabilities are driving fish population fluctuations. Because otolith $\delta^{18}O$ is generally recognized as temperature dependent (Høie et al., 2004; Kim et al., 2007; Storm-Suke et al., 2007; Kitagawa et al., 2013; Sakamoto et al., 2013), the method presented here will notably improve the knowledge on the survival and migration ecology of early life stages of numerous fish species.

Chapter 6

General Discussion

In this study, high-resolution otolith $\delta^{18}O$ analysis was introduced into the study of sardines for the first time in the world. The temperature dependence of otolith $\delta^{18}O$ was first calibrated through rearing experiments in different temperatures. The dependence was different from that of inorganic aragonite, which suggested that sardine-specific relationship should be used for interpretations of sardine otolith $\delta^{18}O$. The technique was then applied to the South African sardine to understand its population structure. The sardine is found off entire coast of South Africa and has recently been hypothesised to be comprised of two or three discrete subpopulations. The nursery environment during the first two months from hatch were different between west coast fish and south coast fish,

though the extent varied between seasons. The nursey temperatures are probably reflecting the different oceanographic conditions of cool upwelling in the west and warm Agulhas Current in the south-east, which supports the existence of discrete subpopulations. Next, the technique was applied to two sardines in the western North Pacific, the Japanese and the Pacific sardine to clarify the effect of temperature on early life growth and ultimately biomass fluctuations. The temperature histories and growth trajectories showed that the Japanese sardine inhabits warmer waters than the Pacific sardine does and grows faster during larval and juvenile stages. In both sides of the North Pacific, larval growths were enhanced in relatively warmer waters while juvenile growths showed no or weak negative correlation with temperature, suggesting the general feature of *Sardinops* species. The positive correlations were stronger in the Japanese sardine during larval stages and were stronger in the Pacific sardine during the early juvenile stage, suggesting that the response in the early juvenile stages can be responsible for the response of biomass to the temperature variations. Finally, a method to estimate migration history from otolith $\delta^{18}O$ profile was developed by combining numerical simulations. Reasonable migration histories were reproduced by searching the routes consistent with the otolith $\delta^{18}O$ profile, using an individual-based model with random swimming behaviour. This method allows more detailed descriptions of early life migrations and can be valuable for studying the mechanism of biomass fluctuations in future because it can be used to examine the environmental history of successfully recruited individuals. These results proved that high resolution otolith $\delta^{18}O$ is a powerful tool to study early life ecology of small pelagic fish and provided the materials to discuss general differences of sardines in western boundary current systems and coastal upwelling regions.

The difference of the growth rates during early life history stages between the

Japanese and the Pacific sardine was analogous to that between sardines off the south and the west coasts of South Africa. The growth rates were faster in western boundary current regions during the first 100 days from hatch in both the North Pacific and South Africa coasts (Fig. 1a, b) and ambient temperature during larval stages were 2–3°C higher in the warm current regions. These suggest the general differences in nursery habitat between western boundary current regions and upwelling regions, which would have different advantages and disadvantages. In the western boundary current system, shorter duration of vulnerable larval stage would be beneficial to increase early life survival rate. Because energy consumption due to metabolism is larger in warmer waters, however, transportation or migration success into cooler or high food concentration area may be crucial for survival and reproduction in later stages. On the contrary, in the upwelling system, larval stage duration would be longer, but if they retained in upwelling waters, shortage of energy intake is less likely to occur due to low metabolism and sufficient food supplies. As a result, sardines living in western boundary current systems and upwelling systems would be subject to different risks, which may be the basic explanation for the biomass fluctuations of the Japanese and Pacific sardine that react oppositely to temperature variations. Analysing the responses of South African sardine stocks to environmental variations would be meaningful to test this hypothesis. Because the multiple stock hypothesis was proposed recently, these are yet to be analysed, especially for the southern stock. Recently, de Moor et al. (2017) provided estimation of biomass variation in the past 30 years based on the assumption that multiple subpopulations exist with some extent of mixing, which will allow the analyses in near future.

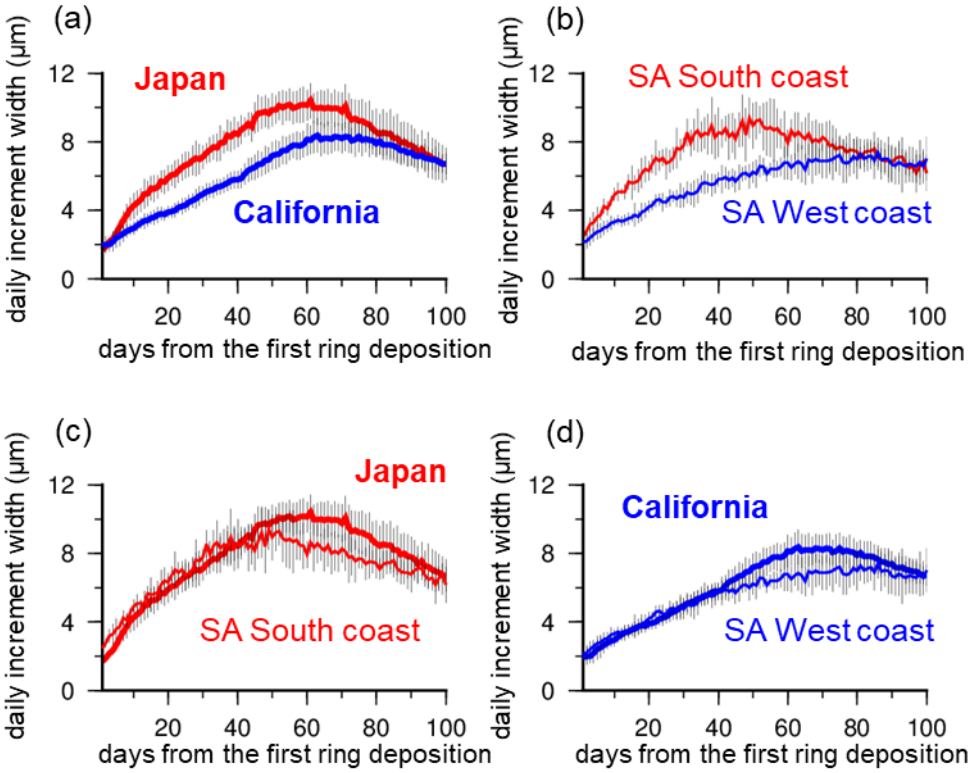

Figure 1. Comparisons of mean daily increment widths of Japanese sardine (thick red), Californian sardine (thick blue) and South African sardine in the south coast (thin red) and west coast (thin blue). The comparisons between stocks in (a) Pacific, (b) South Africa, (c) western boundary current system and (d) eastern boundary current system are shown.

Still, there are differences in growth rates within western and eastern current systems. The South Africa south coast sardine has similar or slightly higher growth rate compared to the Japanese sardine during the first 40 days, but in the following 2 months the Japanese sardine grows remarkably faster (Fig. 1c). If I extrapolate the discussion within the Japanese sardine that growth rates during juvenile stages are not strongly correlated to temperature, the difference may be due to the higher productivity of the Kuroshio-Oyashio transition area, compared to the eastern Agulhas Bank where relatively small scale upwellings occur. Similarly, the Pacific sardine and the South Africa west coast sardine have similar growth rates during the first 40 days, but then the Pacific

sardine growth rate becomes faster (Fig. 1d), which may be suggesting warmer ambient temperature during early-juvenile stages. Therefore, uses of habitats and resources are roughly similar in larval stages but different during juvenile stages between the sardines in South African waters and in the North Pacific. It is also interesting to see how this different affect the relationship between environmental variability and biomass fluctuation. If the early juvenile stage is actually the important stage for recruitment variability as suggested in Chapter 4, the different habitat use in juvenile stages may result in different mechanisms of biomass fluctuation. Analysing the responses of South African sardine stocks to environmental variations can therefore be also utilised as a test to clarify the critical stage.

One large limitation in the discussions of sardine growth rates and biomass fluctuations in this thesis is the complete absence of information of food availability, which is apparently an important factor for fish growth and survival. Recently, methods to analyse nitrogen isotope ratio in otolith has been developed, which may allow estimation of trophic levels of prey (Shiao et al., 2018). Similarly, carbon isotope ratio in otolith, which is a sub-product of oxygen isotope ratio, may reflect the product of fish metabolic rate and trophic level of prey (Kalish, 1991). However, there are no elements that can be used to estimate abundances of prey or amounts of energy intake. This is exactly why the method to estimate the migration route with the combination of otolith $\delta^{18}O$ and numerical simulation was developed in Chapter 5. By comparing of the estimated routes and satellite chlorophyll distributions, or simulated plankton distribution using lower trophic level models such as NEMURO, the North Pacific Ecosystem Model for Understanding Regional Oceanography (Kishi et al., 2007), estimation of food availability may become possible. Further analyses combining numerical models on $\delta^{18}O$

data of archived otoliths of the Japanese and the Pacific sardine may help to understand how bottom up effects influence their biomass.

Animals largely define the selective pressures to which it is subject by its genetically determined use of habitats and resources (Lewontin, 1983; Mullon et al., 2002). Describing detailed behaviours and basic habitat uses of sardines would therefore be helpful to understand the mechanism connecting environmental variabilities and sardine stock biomass. The application of the otolith $\delta^{18}O$ analysis to sardines living in more extreme environments, such as Namibian coast where strong coastal upwellings and the tropical warm Angola Current create highly variable thermal environments, or Canadian coast which is probably the coolest area among world sardine habitats, or south Australia coast characterized by low productivity, would enable drawing more general features and highlighting region-specific characteristics of sardine ecology. Moreover, the otolith $\delta^{18}O$ analysis can be applied to various fish species as the temperature dependence of otolith $\delta^{18}O$ is a general feature of Teleostei (e.g. Kim et al., 2007). The application to anchovies that often dominantly play critical roles in energy transfer from low to high trophic levels together with sardines (Cury et al, 2000) and tend to show out of phase synchronization of biomass with sardines (Schwartzlose et al., 1999), would be of particular importance to predict how marine ecosystems react to the ongoing global climate change.

As a conclusion, our pioneer works of introducing high-resolution otolith $\delta^{18}O$ analysis to small pelagic fish studies have successfully provided new aspects of early life ecology of sardines in western and eastern boundary current systems. Although they were not enough to solve the long-lasting debates of biomass fluctuations, future applications for other sardine stocks, together with numerical simulations, may contribute to finish off

the problem. As the temperature dependence of otolith $\delta^{18}O$ is widely recognised in various species, the technique and the methods described here will be valuable for studying ecology of numerous fishes, which would lead to better relationships between human and marine living resources in the future world.

References

Chapter 1

M. Barange, J. Coetzee, A. Takasuka, K. Hill, M. Gutierrez, Y. Oozeki, C. van der Lingen, V. Agostini, Habitat expansion and contraction in anchovy and sardine populations. *Prog. Oceanogr.* **83**, 251-260 (2009).

B. Bowen, W. S. Grant, Phylogeography of the sardines (Sardinops spp.): assessing biogeographic models and population histories in temperate upwelling zones. *Evolution.* **51**, 1601-1610 (1997).

S. E. Campana, Chemistry and composition of fish otoliths: pathways, mechanisms and applications. *Mar. Ecol. Prog. Ser.*, 263-297 (1999).

S. J. Carpenter, J. M. Erickson, F. Holland Jr, Migration of a Late Cretaceous fish. *Nature.* **423**, 70 (2003).

D. Checkley, P. Ayon, T. R. Baumgartner, M. Bernal, J. C. Coetzee, R. Emmett, R. Guevara-Carrasco, L. Hutchings, L. Ibaibarriaga, H. Nakata, Y. Oozeki, B. Planque, J. Schweigert, Y. Stratoudakis, C. van der Lingen, Habitats. in *Climate change and small pelagic fish* (Cambridge University Press, Cambridge, 2009), p. 12-44.

J. C. Coetzee, Van der Lingen, Carl D, L. Hutchings, T. P. Fairweather, Has the fishery contributed to a major shift in the distribution of South African sardine? *ICES J. Mar. Sci.* **65**, 1676-1688 (2008).

P. Cury, A. Bakun, R. J. Crawford, A. Jarre, R. A. Quinones, L. J. Shannon, H. M. Verheye, Small pelagics in upwelling systems: patterns of interaction and structural changes

in “wasp-waist” ecosystems. *ICES J. Mar. Sci.* **57**, 603-618 (2000).

W. Grant, B. W. Bowen, Shallow population histories in deep evolutionary lineages of marine fishes: insights from sardines and anchovies and lessons for conservation. *J. Hered.* **89**, 415-426 (1998).

T. Ishimura, U. Tsunogai, T. Gamo, Stable carbon and oxygen isotopic determination of sub-microgram quantities of CaCO3 to analyse individual foraminiferal shells. *Rapid Communications in Mass Spectrometry.* **18**, 2883-2888 (2004).

T. Ishimura, U. Tsunogai, F. Nakagawa, Grain-scale heterogeneities in the stable carbon and oxygen isotopic compositions of the international standard calcite materials (NBS 19, NBS 18, IAEA-CO-1, and IAEA-CO-8). *Rapid Communications in Mass Spectrometry.* **22**, 1925-1932 (2008).

S. Kim, J. R. O’Neil, C. Hillaire-Marcel, A. Mucci, Oxygen isotope fractionation between synthetic aragonite and water: influence of temperature and Mg2 concentration. *Geochim. Cosmochim. Acta.* **71**, 4704-4715 (2007).

G. Merino, M. Barange, J. L. Blanchard, J. Harle, R. Holmes, I. Allen, E. H. Allison, M. C. Badjeck, N. K. Dulvy, J. Holt, S. Jennings, C. Mullon, L. D. Rodwell, Can marine fisheries and aquaculture meet fish demand from a growing human population in a changing climate? *Global Environmental Change.* **22**, 795-806 (2012).

G. Merino, M. Barange, C. Mullon, Role of Anchovies and Sardines as Reduction Fisheries in the World Fish Meal. in *Biology and ecology of sardines and anchovies* (CRC Press, Boca Raton, 2014), p. 285-307.

K. Nishida, T. Ishimura, Grain-scale stable carbon and oxygen isotopic variations of the international reference calcite, IAEA-603. *Rapid Communications in Mass*

Spectrometry. **31**, 1875-1880 (2017).

T. Okazaki, T. Kobayashi, Y. Uozumi, Genetic relationships of pilchards (genus: Sardinops) with anti-tropical distributions. *Mar. Biol.* **126**, 585-590 (1996).

R. Parrish, R. Serra, W. Grant, The monotypic sardines, Sardina and Sardinops: their taxonomy, distribution, stock structure, and zoogeography. *Can. J. Fish. Aquat. Sci.* **46**, 2019-2036 (1989).

K. A. Rose, J. Fiechter, E. N. Curchitser, K. Hedstrom, M. Bernal, S. Creekmore, A. Haynie, S. Ito, S. Lluch-Cota, B. A. Megrey, Demonstration of a fully-coupled end-to-end model for small pelagic fish using sardine and anchovy in the California Current. *Prog. Oceanogr.* **138**, 348-380 (2015).

S. Sakai, Micromilling and sample recovering techniques using high-precision micromill GEOMILL326. *JAMSTEC-Rep.Res.Develop*. **10**, 4–5 (2009).

R. A. Schwartzlose, J. Alheit, A. Bakun, T. R. Baumgartner, R. Cloete, R. J. M. Crawford, W. J. Fletcher, Y. Green-Ruiz, E. Hagen, T. Kawasaki, D. Lluch-Belda, S. E. Lluch-Cota, A. D. MacCall, Y. Matsuura, M. O. Nevárez-Martínez, R. H. Parrish, C. Roy, R. Serra, K. V. Shust, M. N. Ward, J. Z. Zuzunaga, Worldwide large-scale fluctuations of sardine and anchovy populations. *South African Journal of Marine Science.* **21**, 289-347 (1999).

J. Shiao, T. Yui, H. Høie, U. Ninnemann, S. Chang, Otolith O and C stable isotope compositions of southern bluefin tuna *Thunnus maccoyii* (Pisces: *Scombridae*) as possible environmental and physiological indicators. *Zool. Stud.* **48**, 71-82 (2009).

C. Van der Lingen, L. Hutchings, J. Field, Comparative trophodynamics of anchovy *Engraulis encrasicolus* and sardine *Sardinops sagax* in the southern Benguela: are species alternations between small pelagic fish trophodynamically mediated?

African Journal of Marine Science. **28**, 465-477 (2006).

Chapter 2

B. A. Block, S. L. Teo, A. Walli, A. Boustany, M. J. Stokesbury, C. J. Farwell, K. C. Weng, H. Dewar, T. D. Williams, Electronic tagging and population structure of Atlantic bluefin tuna. *Nature.* **434**, 1121 (2005).

S. E. Campana, Chemistry and composition of fish otoliths: pathways, mechanisms and applications. *Mar. Ecol. Prog. Ser.*, 263-297 (1999).

E. Dorval, K. Piner, L. Robertson, C. S. Reiss, B. Javor, R. Vetter, Temperature record in the oxygen stable isotopes of Pacific sardine otoliths: experimental vs. wild stocks from the Southern California Bight. *J. Exp. Mar. Biol. Ecol.* **397**, 136-143 (2011).

A. J. Geffen, Otolith oxygen and carbon stable isotopes in wild and laboratory-reared plaice (*Pleuronectes platessa*). *Environ. Biol. Fishes.* **95**, 419-430 (2012).

J. A. Godiksen, M. Svenning, J. B. Dempson, M. Marttila, A. Storm-Suke, M. Power, Development of a species-specific fractionation equation for Arctic charr (*Salvelinus alpinus* (L.)): an experimental approach. *Hydrobiologia.* **650**, 67-77 (2010).

H. Høie, E. Otterlei, A. Folkvord, Temperature-dependent fractionation of stable oxygen isotopes in otoliths of juvenile cod (Gadus morhua L.). *ICES J. Mar. Sci.* **61**, 243-251 (2004).

R. Humston, J. S. Ault, M. Lutcavage, D. B. Olson, Schooling and migration of large pelagic fishes relative to environmental cues. *Fish. Oceanogr.* **9**, 136-146 (2000).

T. Ishimura, U. Tsunogai, T. Gamo, Stable carbon and oxygen isotopic determination of sub-microgram quantities of CaCO3 to analyse individual foraminiferal shells.

Rapid Communications in Mass Spectrometry. **18**, 2883-2888 (2004).

T. Ishimura, U. Tsunogai, F. Nakagawa, Grain-scale heterogeneities in the stable carbon and oxygen isotopic compositions of the international standard calcite materials (NBS 19, NBS 18, IAEA-CO-1, and IAEA-CO-8). *Rapid Communications in Mass Spectrometry.* **22**, 1925-1932 (2008).

J. Kalish, Oxygen and carbon stable isotopes in the otoliths of wild and laboratory-reared Australian salmon (*Arripis trutta*). *Mar. Biol.* **110**, 37-47 (1991).

S. Kim, J. R. O'Neil, C. Hillaire-Marcel, A. Mucci, Oxygen isotope fractionation between synthetic aragonite and water: influence of temperature and Mg2 concentration. *Geochim. Cosmochim. Acta.* **71**, 4704-4715 (2007).

S. Kim, J. R. O'Neil, Equilibrium and nonequilibrium oxygen isotope effects in synthetic carbonates. *Geochim. Cosmochim. Acta.* **61**, 3461-3475 (1997).

T. Kitagawa, T. Ishimura, R. Uozato, K. Shirai, Y. Amano, A. Shinoda, T. Otake, U. Tsunogai, S. Kimura, Otolith δ18O of Pacific bluefin tuna *Thunnus orientalis* as an indicator of ambient water temperature. *Mar. Ecol. Prog. Ser.* **481**, 199-209 (2013).

H. Nishikawa, I. Yasuda, K. Komatsu, H. Sasaki, Y. Sasai, T. Setou, M. Shimizu, Winter mixed layer depth and spring bloom along the Kuroshio front: implications for the Japanese sardine stock. *Mar. Ecol. Prog. Ser.* **487**, 217-229 (2013).

M. Noto, I. Yasuda, Population decline of the Japanese sardine, *Sardinops melanostictus*, in relation to sea surface temperature in the Kuroshio Extension. *Can. J. Fish. Aquat. Sci.* **56**, 973-983 (1999).

M. Oda, T. Tetsu, S. Sakai, T. Ishimura, Discrimination of the migration pattern for Japanese sardine in Pacific stock using microscale stable isotopic analytical

technique. *Bull. Jpn. Soc. Fish. Oceanogr.* **80**, 48–55 (2016) (in Japanese with English abstract).

T. Okunishi, S. ITO, D. Ambe, A. Takasuka, T. Kameda, K. Tadokoro, T. Setou, K. Komatsu, A. Kawabata, H. Kubota, A modeling approach to evaluate growth and movement for recruitment success of Japanese sardine (*Sardinops melanostictus*) in the western Pacific. *Fish. Oceanogr.* **21**, 44-57 (2012).

T. Okunishi, Y. Yamanaka, S. Ito, A simulation model for Japanese sardine (*Sardinops melanostictus*) migrations in the western North Pacific. *Ecol. Model.* **220**, 462-479 (2009).

R. Radtke, P. Lenz, W. Showers, E. Moksness, Environmental information stored in otoliths: insights from stable isotopes. *Mar. Biol.* **127**, 161-170 (1996).

S. Sakai, Micromilling and sample recovering techniques using high-precision micromill GEOMILL326. *JAMSTEC-Rep.Res.Develop*. **10**, 4–5 (2009).

T. Sharma, R. N. Clayton, Measurement of $O^{18}O^{16}$ ratios of total oxygen of carbonates. *Geochimica Et Cosmochimica Acta.* **29**, 1347-1353 (1965).

A. Storm-Suke, J. B. Dempson, J. D. Reist, M. Power, A field-derived oxygen isotope fractionation equation for Salvelinus species. *Rapid Commun. Mass Spectrom.* **21**, 4109-4116 (2007).

M. Takahashi, H. Nishida, A. Yatsu, Y. Watanabe, Year-class strength and growth rates after metamorphosis of Japanese sardine (*Sardinops melanostictus*) in the western North Pacific Ocean during 1996–2003. *Can. J. Fish. Aquat. Sci.* **65**, 1425-1434 (2008).

M. Takahashi, Y. Watanabe, A. Yatsu, H. Nishida, Contrasting responses in larval and juvenile growth to a climate–ocean regime shift between anchovy and sardine.

Can. J. Fish. Aquat. Sci. **66**, 972-982 (2009).

A. Takasuka, Y. Oozeki, I. Aoki, Optimal growth temperature hypothesis: Why do anchovy flourish and sardine collapse or vice versa under the same ocean regime? *Can. J. Fish. Aquat. Sci.* **64**, 768-776 (2007).

A. Takasuka, Y. Oozeki, H. Kubota, S. E. Lluch-Cota, Contrasting spawning temperature optima: why are anchovy and sardine regime shifts synchronous across the North Pacific? *Prog. Oceanogr.* **77**, 225-232 (2008).

S. R. Thorrold, S. E. Campana, C. M. Jones, P. K. Swart, Factors determining δ13C and δ18O fractionation in aragonitic otoliths of marine fish. *Geochim. Cosmochim. Acta.* **61**, 2909-2919 (1997).

Y. Watanabe, Recruitment variability of small pelagic fish populations in the Kuroshio-Oyashio transition region of the Western North Pacific. *J.Northw.Atl.Fish.Sci.* **41**, 197-204 (2009).

Y. Watanabe, H. Zenitani, R. Kimura, Population decline off the Japanese sardine *Sardinops melanostictus* owing to recruitment failures. *Can. J. Fish. Aquat. Sci.* **52**, 1609-1616 (1995).

I. Yasuda, H. Sugisaki, Y. Watanabe, S. MINOBE, Y. Oozeki, Interdecadal variations in Japanese sardine and ocean/climate. *Fish. Oceanogr.* **8**, 18-24 (1999).

A. Yatsu, T. Watanabe, M. Ishida, H. Sugisaki, L. D. Jacobson, Environmental effects on recruitment and productivity of Japanese sardine *Sardinops melanostictus* and chub mackerel *Scomber japonicus* with recommendations for management. *Fish. Oceanogr.* **14**, 263-278 (2005).

Chapter 3

V. N. Agostini, A. Bakun, Ocean triads' in the Mediterranean Sea: physical mechanisms potentially structuring reproductive habitat suitability (with example application to European anchovy, Engraulis encrasicolus). *Fish. Oceanogr.* **11**, 129-142 (2002).

R. E. Baldwin, M. A. Banks, K. C. Jacobson, Integrating fish and parasite data as a holistic solution for identifying the elusive stock structure of Pacific sardines (Sardinops sagax). *Rev. Fish Biol. Fish.* **22**, 137-156 (2012).

S. E. Campana, Chemistry and composition of fish otoliths: pathways, mechanisms and applications. *Mar. Ecol. Prog. Ser.*, 263-297 (1999).

S. E. Campana, How reliable are growth back-calculations based on otoliths? *Can. J. Fish. Aquat. Sci.* **47**, 2219-2227 (1990).

J. C. Coetzee, C. D. Van der Lingen, L. Hutchings, T. P. Fairweather, Has the fishery contributed to a major shift in the distribution of South African sardine? *ICES J. Mar. Sci.* **65**, 1676-1688 (2008).

A. Connell, A 21-year ichthyoplankton collection confirms sardine spawning in KwaZulu-Natal waters. *African Journal of Marine Science.* **32**, 331-336 (2010).

C. L. de Moor, D. S. Butterworth, C. D. van der Lingen, The quantitative use of parasite data in multistock modelling of South African sardine (*Sardinops sagax*). *Can. J. Fish. Aquat. Sci.* **74**, 1895-1903 (2017).

S. Garrido, A. Cristóvão, C. Caldeira, R. Ben-Hamadou, N. Baylina, H. Batista, E. Saiz, M. Peck, P. Ré, A. Santos, Effect of temperature on the growth, survival, development and foraging behaviour of *Sardina pilchardus* larvae. *Mar. Ecol. Prog. Ser.* **559**, 131-145 (2016).

D. J. Gaughan, W. J. Fletcher, J. P. McKinlay, Functionally distinct adult assemblages

within a single breeding stock of the sardine, Sardinops sagax: management units within a management unit. *Fisheries Research.* **59**, 217-231 (2002).

A. Hayashi, Y. Yamashita, H. Kawaguchi, T. Ishii, Rearing method and daily otolith ring of Japanese sardine larvae, *Sardinops melanostictus*. *Nippon Suisan Gakkaishi* **55**, 997-1000 (1989).

H. Høie, E. Otterlei, A. Folkvord, Temperature-dependent fractionation of stable oxygen isotopes in otoliths of juvenile cod *(Gadus morhua* L.). *ICES J. Mar. Sci.* **61**, 243-251 (2004).

L. Hutchings, C. Van der Lingen, L. Shannon, R. Crawford, H. Verheye, C. Bartholomae, A. Van der Plas, D. Louw, A. Kreiner, M. Ostrowski, The Benguela Current: An ecosystem of four components. *Prog. Oceanogr.* **83**, 15-32 (2009).

T. Ishimura, U. Tsunogai, T. Gamo, Stable carbon and oxygen isotopic determination of sub-microgram quantities of CaCO3 to analyse individual foraminiferal shells. *Rapid Communications in Mass Spectrometry.* **18**, 2883-2888 (2004).

T. Ishimura, U. Tsunogai, F. Nakagawa, Grain-scale heterogeneities in the stable carbon and oxygen isotopic compositions of the international standard calcite materials (NBS 19, NBS 18, IAEA-CO-1, and IAEA-CO-8). *Rapid Communications in Mass Spectrometry.* **22**, 1925-1932 (2008).

T. Kodama, T. Wagawa, S. Ohshimo, H. Morimoto, N. Iguchi, K. Fukudome, T. Goto, M. Takahashi, T. Yasuda, Improvement in recruitment of Japanese sardine with delays of the spring phytoplankton bloom in the Sea of Japan. *Fish. Oceanogr.* **27**, 289-301 (2018).

T. Lamont, M. García-Reyes, S. Bograd, C. van der Lingen, W. Sydeman, Upwelling indices for comparative ecosystem studies: Variability in the Benguela Upwelling

System. *J. Mar. Syst.* **188**, 3-16 (2018).

J. Lutjeharms, J. Cooper, M. Roberts, Upwelling at the inshore edge of the Agulhas Current. *Cont. Shelf Res.* **20**, 737-761 (2000).

D. C. Miller, C. L. Moloney, van der Lingen, Carl D, C. Lett, C. Mullon, J. G. Field, Modelling the effects of physical–biological interactions and spatial variability in spawning and nursery areas on transport and retention of sardine *Sardinops sagax* eggs and larvae in the southern Benguela ecosystem. *J. Mar. Syst.* **61**, 212-229 (2006).

H. Nishikawa, I. Yasuda, Japanese sardine (*Sardinops melanostictus*) mortality in relation to the winter mixed layer depth in the Kuroshio Extension region. *Fish. Oceanogr.* **17**, 411-420 (2008).

T. Sakamoto, K. Komatsu, M. Yoneda, T. Ishimura, T. Higuchi, K. Shirai, Y. Kamimura, C. Watanabe, A. Kawabata, Temperature dependence of $\delta^{18}O$ in otolith of juvenile Japanese sardine: Laboratory rearing experiment with micro-scale analysis. *Fisheries Research.* **194**, 55-59 (2017).

V. Swart, J. Largier, Thermal structure of Agulhas Bank water. *South African Journal of Marine Science.* **5**, 243-252 (1987).

M. Takahashi, H. Nishida, A. Yatsu, Y. Watanabe, Year-class strength and growth rates after metamorphosis of Japanese sardine (Sardinops melanostictus) in the western North Pacific Ocean during 1996–2003. *Can. J. Fish. Aquat. Sci.* **65**, 1425-1434 (2008).

P. R. Teske, T. R. Golla, J. Sandoval-Castillo, A. Emami-Khoyi, van der Lingen, Carl D, S. von der Heyden, B. Chiazzari, B. J. van Vuuren, L. B. Beheregaray, Mitochondrial DNA is unsuitable to test for isolation by distance. *Scientific*

Reports. **8**, 8448 (2018).

R. Thomas, Growth of larval pelagic fish in the South-East Atlantic from daily otolith rings in 1982/83 and 1983/84. *South African Journal of Marine Science.* **4**, 61-77 (1986).

C. D. Van Der Lingen, A. McGrath, Incorporating seasonality in sardine spawning into estimations of the transport success of eggs spawned on the South Coast to the West Coast nursery area. FISHERIES/FEB/2017/SWG-PEL/08, (2017)

C. D. Van Der Lingen, L. F. Weston, N. N. Ssempa, C. C. Reed, Incorporating parasite data in population structure studies of South African sardine Sardinops sagax. *Parasitology.* **142**, 156-167 (2015).

C. D. Van Der Lingen, J. Coetzee, L. Hutchings, Overview of the KwaZulu-Natal sardine run. *African Journal of Marine Science.* **32**, 271-277 (2010).

L. F. Weston, C. C. Reed, M. Hendricks, H. Winker, van der Lingen, Carl D, Stock discrimination of South African sardine (Sardinops sagax) using a digenean parasite biological tag. *Fisheries Research.* **164**, 120-129 (2015).

Chapter 4

Y. Amano, J. Shiao, T. Ishimura, K. Yokouchi, K. Shirai, Otolith geochemical analysis for stock discrimination and migratory ecology of tunas. *By T.Kitagawa and S.Kimura.CRC Press, Boca Raton, USA.*, 225-257 (2015).

A. Bakun, Coastal upwelling indices, west coast of North America, 1946-71. *US Dept.Commerce NOAA Tech.Rep.NMFS-SSRF.* **671**, 1-103 (1973).

T. R. Baumgartner, A. Soutar, V. Ferreira-Bartrina, Reconstruction of the history of Pacific sardine and Northern Pacific anchovy populations over the past two millennia from sediments of the Santa Barbara basin, *CalCOFI Rep*. **33,** 24-40

(1992).

J. L. Butler, P. E. Smith, N. C. Lo, The effect of natural variability of life-history parameters on anchovy and sardine population growth. *CalCOFI Rep.* **34**, 104-111 (1993).

D. Checkley, R. C. Dotson, D. A. Griffith, Continuous, underway sampling of eggs of Pacific sardine (Sardinops sagax) and northern anchovy (Engraulis mordax) in spring 1996 and 1997 off southern and central California. *Deep Sea Research Part II: Topical Studies in Oceanography.* **47**, 1139-1155 (2000).

D. Checkley, P. Ayon, T. R. Baumgartner, M. Bernal, J. C. Coetzee, R. Emmett, R. Guevara-Carrasco, L. Hutchings, L. Ibaibarriaga, H. Nakata, Y. Oozeki, B. Planque, J. Schweigert, Y. Stratoudakis, C. van der Lingen, Habitats. in *Climate change and small pelagic fish* (Cambridge University Press, Cambridge, 2009), p. 12-44.

E. Dorval, K. Piner, L. Robertson, C. S. Reiss, B. Javor, R. Vetter, Temperature record in the oxygen stable isotopes of Pacific sardine otoliths: experimental vs. wild stocks from the Southern California Bight. *J. Exp. Mar. Biol. Ecol.* **397**, 136-143 (2011).

D. Gaughan, W. Fletcher, K. White, Growth rate of larval Sardinops sagax from ecosystems with different levels of productivity. *Mar. Biol.* **139**, 831-837 (2001).

W. Grant, B. W. Bowen, Shallow population histories in deep evolutionary lineages of marine fishes: insights from sardines and anchovies and lessons for conservation. *J. Hered.* **89**, 415-426 (1998).

M. R. Heath, Field Investigations of the Early Life Stages of Marine Fish. *Advances in Marine Biology.* **28**, 1-174 (1992).

K. T. Hill, L. Jacobson, N. Lo, M. Yaremko, M. Dege, Stock assessment of Pacific sardine

for 1998 with management recommendations for 1999. *Marine Region Administrative Report 99-4* (1999).

K. T. Hill, P. R. Crone, J. P. Zwolinski, Assessment of the Pacific sardine resource in 2017 for U.S. management in 2017-18. *Pacific Fishery Management Council, April 2017 Briefing Book* (2017).

E. Houde, Subtleties and episodes in the early life of fishes. *J. Fish Biol.* **35**, 29-38 (1989).

E. Houde, Fish early life dynamics and recruitment variability. *Am. Fish. Soc. Symp.* **2**, 17-29 (1987).

T. Ishimura, U. Tsunogai, T. Gamo, Stable carbon and oxygen isotopic determination of sub-microgram quantities of CaCO3 to analyse individual foraminiferal shells. *Rapid Communications in Mass Spectrometry.* **18**, 2883-2888 (2004).

T. Ishimura, U. Tsunogai, F. Nakagawa, Grain-scale heterogeneities in the stable carbon and oxygen isotopic compositions of the international standard calcite materials (NBS 19, NBS 18, IAEA-CO-1, and IAEA-CO-8). *Rapid Communications in Mass Spectrometry.* **22**, 1925-1932 (2008).

O. Isoguchi, H. Kawamura, E. Oka, Quasi-stationary jets transporting surface warm waters across the transition zone between the subtropical and the subarctic gyres in the North Pacific. *Journal of Geophysical Research: Oceans.* **111**(2006).

S. Itoh, T. Saruwatari, H. Nishikawa, I. Yasuda, K. Komatsu, A. Tsuda, T. Setou, M. Shimizu, Environmental variability and growth histories of larval Japanese sardine (Sardinops melanostictus) and Japanese anchovy (Engraulis japonicus) near the frontal area of the Kuroshio. *Fish. Oceanogr.* **20**, 114-124 (2011).

L. D. Jacobson, S. J. Bograd, R. H. Parrish, R. Mendelssohn, F. B. Schwing, An ecosystem-based hypothesis for climatic effects on surplus production in

California sardine (Sardinops sagax) and environmentally dependent surplus production models. *Can. J. Fish. Aquat. Sci.* **62**, 1782-1796 (2005).

L. D. Jacobson, A. D. MacCall, Stock-recruitment models for Pacific sardine (Sardinops sagax). *Can. J. Fish. Aquat. Sci.* **52**, 566-577 (1995).

L. D. Jacobson, S. McClatchie, Comment on temperature-dependent stock–recruit modeling for Pacific sardine (Sardinops sagax) in Jacobson and MacCall (1995), McClatchie et al.(2010), and Lindegren and Checkley (2013). *Can. J. Fish. Aquat. Sci.* **70**, 1566-1569 (2013).

B. Javor, E. Dorval, Geography and ontogeny influence the stable oxygen and carbon isotopes of otoliths of Pacific sardine in the California Current. *Fisheries Research.* **154**, 1-10 (2014).

S. Kim, J. R. O'Neil, C. Hillaire-Marcel, A. Mucci, Oxygen isotope fractionation between synthetic aragonite and water: influence of temperature and Mg2 concentration. *Geochim. Cosmochim. Acta.* **71**, 4704-4715 (2007).

R. Kimura, Y. Watanabe, H. Zenitani, Nutritional condition of first-feeding larvae of Japanese sardine in the coastal and oceanic waters along the Kuroshio Current. *ICES J. Mar. Sci.* **57**, 240-248 (2000).

K. Kuroda, Studies on the recruitment process focusing on the early life history of the Japanese sardine, *Sardinops melanostictus* (Schelegen). *Bull. Natl .Res. Inst. Fish. Sci.*, **3**, 25-278 (1991) (in Japanese with English abstract).

M. Kuwae, M. Yamamoto, T. Sagawa, K. Ikehara, T. Irino, K. Takemura, H. Takeoka, T. Sugimoto, Multidecadal, centennial, and millennial variability in sardine and anchovy abundances in the western North Pacific and climate–fish linkages during the late Holocene. *Progress in Oceanography.* **159**, 86-98 (2017).

A. N. LeGrande, G. A. Schmidt, Global gridded data set of the oxygen isotopic composition in seawater. *Geophys. Res. Lett.* **33**(2006).

M. Lindegren, D. M. Checkley Jr, Temperature dependence of Pacific sardine (Sardinops sagax) recruitment in the California Current Ecosystem revisited and revised. *Can. J. Fish. Aquat. Sci.* **70**, 245-252 (2012).

R. J. Lynn, Variability in the spawning habitat of Pacific sardine (Sardinops sagax) off southern and central California. *Fish. Oceanogr.* **12**, 541-553 (2003).

B. J. Macewicz, J. J. Castko-Gonzalez, J. Hunter, Adult reproductive parameters of Pacific sardine (Sardwops sagax) during 1994. *California Cooperative Oceanic Fisheries Investigations Reports.* **37**, 140-151 (1996).

N. J. Mantua, S. R. Hare, Y. Zhang, J. M. Wallace, R. C. Francis, A Pacific interdecadal climate oscillation with impacts on salmon production. *Bull. Am. Meteorol. Soc.* **78**, 1069-1080 (1997).

T. J. Miller, L. B. Crowder, J. A. Rice, E. A. Marschall, Larval size and recruitment mechanisms in fishes: toward a conceptual framework. *Can. J. Fish. Aquat. Sci.* **45**, 1657-1670 (1988).

K. Nakata, H. Zenitani, D. Inagake, Differences in food availability for Japanese sardine larvae between the frontal region and the waters on the offshore side of Kuroshio. *Fish. Oceanogr.* **4**, 68-79 (1995).

S. Nakayama, A. Takasuka, M. Ichinokawa, H. Okamura, Climate change and interspecific interactions drive species alternations between anchovy and sardine in the western North Pacific: Detection of causality by convergent cross mapping. *Fish. Oceanogr.* **27**, 312-322 (2018).

K. Nishida, T. Ishimura, Grain-scale stable carbon and oxygen isotopic variations of the

international reference calcite, IAEA-603. *Rapid Communications in Mass Spectrometry.* **31**, 1875-1880 (2017).

H. Nishikawa, I. Yasuda, K. Komatsu, H. Sasaki, Y. Sasai, T. Setou, M. Shimizu, Winter mixed layer depth and spring bloom along the Kuroshio front: implications for the Japanese sardine stock. *Mar. Ecol. Prog. Ser.* **487**, 217-229 (2013).

M. Noto, I. Yasuda, Population decline of the Japanese sardine, Sardinops melanostictus, in relation to sea surface temperature in the Kuroshio Extension. *Can. J. Fish. Aquat. Sci.* **56**, 973-983 (1999).

T. Oba, M. Murayama, Sea-surface temperature and salinity changes in the northwest Pacific since the Last Glacial Maximum. *Journal of Quaternary Science.* **19**, 335-346 (2004).

Y. Oozeki, A. Takasuka, H. Kubota, M. Barange, Characterizing Spawning Habitats of Japanese Sardine, Sardinops Melanostictus, Japanese Anchovy, Engraulis Japonicus, and Pacific Round Herring, Etrumeus Teres, in the Northwestern Pacific. *California Cooperative Oceanic Fisheries Investigations Report.* **48**, 191 (2007).

E. Pfeiler, A. Luna, Changes in biochemical composition and energy utilization during metamorphosis of leptocephalous larvae of the bonefish (Albula). *Environ. Biol. Fishes.* **10**, 243-251 (1984).

C. S. Reiss, D. M. Checkley Jr, S. J. Bograd, Remotely sensed spawning habitat of Pacific sardine (Sardinops sagax) and Northern anchovy (Engraulis mordax) within the California Current. *Fish. Oceanogr.* **17**, 126-136 (2008).

R. R. Rykaczewski, D. M. Checkley Jr, Influence of ocean winds on the pelagic ecosystem in upwelling regions. *Proc. Natl. Acad. Sci. U. S. A.* **105**, 1965-1970 (2008).

G. A. Schmidt, G. R. Bigg, E. J. Rohling. Global Seawater Oxygen-18 Database - v1.22, (1999) https://data.giss.nasa.gov/o18data/

T. Sakamoto, K. Komatsu, K. Shirai, T. Higuchi, T. Ishimura, T. Setou, Y. Kamimura, C. Watanabe, A. Kawabata, Combining microvolume isotope analysis and numerical simulation to reproduce fish migration history. *Methods in Ecology and Evolution.*(2018).

T. Sakamoto, K. Komatsu, M. Yoneda, T. Ishimura, T. Higuchi, K. Shirai, Y. Kamimura, C. Watanabe, A. Kawabata, Temperature dependence of δ18O in otolith of juvenile Japanese sardine: Laboratory rearing experiment with micro-scale analysis. *Fisheries Research.* **194**, 55-59 (2017).

P. E. Smith, Life-stage duration and survival parameters as related to interdecadal population variability in Pacific sardine. *CalCOFI Rep.* **33**, 41-47 (1992).

G. Sugihara, R. May, H. Ye, C. H. Hsieh, E. Deyle, M. Fogarty, S. Munch, Detecting causality in complex ecosystems. *Science.* **338**, 496-500 (2012).

M. Takahashi, D. M. Checkley Jr, Growth and survival of Pacific sardine (Sardinops sagax) in the California Current region. *J. Northwest Atl. Fish. Sci.* **41**, 129-136 (2008).

M. Takahashi, H. Nishida, A. Yatsu, Y. Watanabe, Year-class strength and growth rates after metamorphosis of Japanese sardine (Sardinops melanostictus) in the western North Pacific Ocean during 1996–2003. *Can. J. Fish. Aquat. Sci.* **65**, 1425-1434 (2008).

M. Takahashi, Y. Watanabe, A. Yatsu, H. Nishida, Contrasting responses in larval and juvenile growth to a climate–ocean regime shift between anchovy and sardine. *Can. J. Fish. Aquat. Sci.* **66**, 972-982 (2009).

A. Takasuka, I. Aoki, I. Mitani, Three synergistic growth-related mechanisms in the short-term survival of larval Japanese anchovy Engraulis japonicus in Sagami Bay. *Mar. Ecol. Prog. Ser.* **270**, 217-228 (2004).

A. Takasuka, I. Aoki, I. Mitani, Evidence of growth-selective predation on larval Japanese anchovy Engraulis japonicus in Sagami Bay. *Mar. Ecol. Prog. Ser.* **252**, 223-238 (2003).

A. Takasuka, Y. Oozeki, I. Aoki, Optimal growth temperature hypothesis: Why do anchovy flourish and sardine collapse or vice versa under the same ocean regime? *Can. J. Fish. Aquat. Sci.* **64**, 768-776 (2007).

A. Takasuka, Y. Oozeki, H. Kubota, S. E. Lluch-Cota, Contrasting spawning temperature optima: why are anchovy and sardine regime shifts synchronous across the North Pacific? *Prog. Oceanogr.* **77**, 225-232 (2008).

A. Takasuka, Y. Oozeki, I. Aoki, R. Kimura, H. Kubota, H. Sugisaki, T. Akamine, Growth effect on the otolith and somatic size relationship in Japanese anchovy and sardine larvae. *Fisheries Science.* **74**, 308-313 (2008).

J. L. Uutleii, Barnes, M. L. Granados, G. J. Thomas, M. Yakemko, B. J. Macewicz, Age composition, growth, and maturation of the Pacific sardine (Sardinops sagax) during 1994. (1996).

C. Van der Lingen, L. Hutchings, J. Field, Comparative trophodynamics of anchovy Engraulis encrasicolus and sardine Sardinops sagax in the southern Benguela: are species alternations between small pelagic fish trophodynamically mediated? *African Journal of Marine Science.* **28**, 465-477 (2006).

Y. Watanabe, H. Saito, Feeding and growth of early juvenile Japanese sardines in the Pacific waters off central Japan. *J. Fish Biol.* **52**, 519-533 (1998).

Y. Watanabe, H. Zenitani, R. Kimura, Population decline off the Japanese sardine *Sardinops melanostictus* owing to recruitment failures. *Can. J. Fish. Aquat. Sci.* **52**, 1609-1616 (1995).

E. D. Weber, Y. Chao, F. Chai, S. McClatchie, Transport patterns of Pacific sardine Sardinops sagax eggs and larvae in the California Current System. *Deep Sea Research Part I: Oceanographic Research Papers.* **100**, 127-139 (2015).

M. Yamamoto, N. Tanaka, S. Tsunogai, Okhotsk Sea intermediate water formation deduced from oxygen isotope systematics. *Journal of Geophysical Research: Oceans.* **106**, 31075-31084 (2001).

A. Yatsu, T. Watanabe, M. Ishida, H. Sugisaki, L. D. Jacobson, Environmental effects on recruitment and productivity of Japanese sardine Sardinops melanostictus and chub mackerel Scomber japonicus with recommendations for management. *Fish. Oceanogr.* **14**, 263-278 (2005).

R. Yukami, C. Wanatabe, Y. Kamimura, S. Furuichi, T. Akamine, T. Kishida, Stock assessment and evaluation for the Pacific stock of Japanese sardine (fiscal year 2016). in *Marine fisheries stock assessment and evaluation for Japanese waters (fiscal year 2016/2017)*. (Fisheries Agency and Fisheries Research and Education Agency of Japan, Yokohama, 2017) pp. 15-52 (in Japanese).

Y. Zhang, J. M. Wallace, D. S. Battisti, ENSO-like interdecadal variability: 1900–93. *J. Clim.* **10**, 1004-1020 (1997).

Chapter 5

G. Allain, P. Petitgas, P. Lazure, P. Grellier, Biophysical modelling of larval drift, growth and survival for the prediction of anchovy (Engraulis encrasicolus) recruitment in

the Bay of Biscay (NE Atlantic). *Fish. Oceanogr.* **16**, 489-505 (2007).

Y. Amano, J. Shiao, T. Ishimura, K. Yokouchi, K. Shirai, Otolith geochemical analysis for stock discrimination and migratory ecology of tunas. *By T.Kitagawa and S.Kimura.CRC Press, Boca Raton, USA.*, 225-257 (2015).

J. T. Anderson, A review of size dependent survival during pre-recruit stages of fishes in relation to recruitment. *Journal of Northwest Atlantic Fishery Science.* **8**, 55-66 (1988).

R. Bainbridge, The speed of swimming of fish as related to size and to the frequency and amplitude of the tail beat. *J. Exp. Biol.* **35**, 109-133 (1958).

M. Barange, J. Coetzee, A. Takasuka, K. Hill, M. Gutierrez, Y. Oozeki, C. van der Lingen, V. Agostini, Habitat expansion and contraction in anchovy and sardine populations. *Prog. Oceanogr.* **83**, 251-260 (2009).

B. A. Block, S. L. Teo, A. Walli, A. Boustany, M. J. Stokesbury, C. J. Farwell, K. C. Weng, H. Dewar, T. D. Williams, Electronic tagging and population structure of Atlantic bluefin tuna. *Nature.* **434**, 1121 (2005).

A. Bower, T. Rossby, Evidence of cross-frontal exchange processes in the Gulf Stream based on isopycnal RAFOS float data. *J. Phys. Oceanogr.* **19**, 1177-1190 (1989).

S. R. Brennan, C. E. Zimmerman, D. P. Fernandez, T. E. Cerling, M. V. McPhee, M. J. Wooller, Strontium isotopes delineate fine-scale natal origins and migration histories of Pacific salmon. *Science Advances.* **1**, e1400124 (2015).

S. E. Campana, Chemistry and composition of fish otoliths: pathways, mechanisms and applications. *Mar. Ecol. Prog. Ser.*, 263-297 (1999).

S. E. Campana, How reliable are growth back-calculations based on otoliths? *Can. J. Fish. Aquat. Sci.* **47**, 2219-2227 (1990).

S. J. Carpenter, J. M. Erickson, F. Holland Jr, Migration of a Late Cretaceous fish. *Nature.* **423**, 70 (2003).

F. P. Chavez, J. Ryan, S. E. Lluch-Cota, C. M. Niquen, From anchovies to sardines and back: multidecadal change in the Pacific Ocean. *Science.* **299**, 217-221 (2003).

H. Craig, L. I. Gordon, Deuterium and oxygen 18 variations in the ocean and the marine atmosphere. (1965).

R. Crawford, P. Sabarros, T. Fairweather, L. Underhill, A. Wolfaardt, Implications for seabirds off South Africa of a long-term change in the distribution of sardine. *African Journal of Marine Science.* **30**, 177-184 (2008).

E. Crist, C. Mora, R. Engelman, The interaction of human population, food production, and biodiversity protection. *Science.* **356**, 260-264 (2017).

P. Cury, A. Bakun, R. J. Crawford, A. Jarre, R. A. Quinones, L. J. Shannon, H. M. Verheye, Global seabird response to forage fish depletion--one-third for the birds. *Science.* **334**, 1703-1706 (2011).

R. Felix-Uraga, V. M. Gomez-Munoz, C. Quinonez-Velazquez, F. N. Melo-Barrera, K. T. Hill, W. García-Franco, Pacific sardine (Sardinops sagax) stock discrimination off the west coast of baja california and southern california using otolith mophometry. *California Cooperative Oceanic Fisheries Investigations Report.* **46**, 113 (2005).

I. Hara, Swimming speed of sardine school on the basis of aerial survey. *Nippon Suisan Gakkaishi* **53**, 223–227 (1987) (in Japanese with English abstract).

H. Høie, E. Otterlei, A. Folkvord, Temperature-dependent fractionation of stable oxygen isotopes in otoliths of juvenile cod (Gadus morhua L.). *ICES J. Mar. Sci.* **61**, 243-251 (2004).

S. Hosoda, T. Ohira, T. Nakamura, A monthly mean dataset of global oceanic temperature

and salinity derived from Argo float observations. *JAMSTEC Report of Research and Development.* **8**, 47-59 (2008).

E. Houde, Fish early life dynamics and recruitment variability. *Am. Fish. Soc. Symp.* **2**, 17-29 (1987).

J. Hunter, Swimming speed, tail beat frequency, tail beat amplitude and size in jack mackerel, Trachurus symmetricus, and other fishes. *Fish. Bull.* **69**, 253-266 (1971).

K. Hüssy, H. Mosegaard, C. M. Albertsen, E. E. Nielsen, J. Hemmer-Hansen, M. Eero, Evaluation of otolith shape as a tool for stock discrimination in marine fishes using Baltic Sea cod as a case study. *Fisheries Research.* **174**, 210-218 (2016).

L. Hutchings, L. Beckley, M. Griffiths, M. Roberts, S. Sundby, C. Van der Lingen, Spawning on the edge: spawning grounds and nursery areas around the southern African coastline. *Marine and Freshwater Research.* **53**, 307-318 (2002).

Y. Ishida, T. Funamoto, S. Honda, K. Yabuki, H. Nishida, C. Watanabe, Management of declining Japanese sardine, chub mackerel and walleye pollock fisheries in Japan. *Fisheries Research.* **100**, 68-77 (2009).

T. Ishimura, U. Tsunogai, T. Gamo, Stable carbon and oxygen isotopic determination of sub-microgram quantities of CaCO3 to analyze individual foraminiferal shells. *Rapid Communications in Mass Spectrometry.* **18**, 2883-2888 (2004).

T. Ishimura, U. Tsunogai, F. Nakagawa, Grain-scale heterogeneities in the stable carbon and oxygen isotopic compositions of the international standard calcite materials (NBS 19, NBS 18, IAEA-CO-1, and IAEA-CO-8). *Rapid Communications in Mass Spectrometry.* **22**, 1925-1932 (2008).

O. Isoguchi, H. Kawamura, E. Oka, Quasi-stationary jets transporting surface warm waters across the transition zone between the subtropical and the subarctic gyres

in the North Pacific. *Journal of Geophysical Research: Oceans.* **111**(2006).

S. Itoh, T. Saruwatari, H. Nishikawa, I. Yasuda, K. Komatsu, A. Tsuda, T. Setou, M. Shimizu, Environmental variability and growth histories of larval Japanese sardine (Sardinops melanostictus) and Japanese anchovy (Engraulis japonicus) near the frontal area of the Kuroshio. *Fish. Oceanogr.* **20**, 114-124 (2011).

S. Kim, J. R. O'Neil, C. Hillaire-Marcel, A. Mucci, Oxygen isotope fractionation between synthetic aragonite and water: influence of temperature and Mg2 concentration. *Geochim. Cosmochim. Acta.* **71**, 4704-4715 (2007).

T. Kitagawa, T. Ishimura, R. Uozato, K. Shirai, Y. Amano, A. Shinoda, T. Otake, U. Tsunogai, S. Kimura, Otolith δ18O of Pacific bluefin tuna Thunnus orientalis as an indicator of ambient water temperature. *Mar. Ecol. Prog. Ser.* **481**, 199-209 (2013).

H. Kuroda, T. Setou, S. Kakehi, S. Ito, T. Taneda, T. Azumaya, D. Inagake, Y. Hiroe, K. Morinaga, M. Okazaki, Recent Advances in Japanese Fisheries Science in the Kuroshio-Oyashio Region through Development of the FRA-ROMS Ocean Forecast System: Overview of the Reproducibility of Reanalysis Products. *Open Journal of Marine Science.* **7**, 62 (2016).

H. Kuroda, T. Setou, K. Aoki, D. Takahashi, M. Shimizu, T. Watanabe, A numerical study of the Kuroshio-induced circulation in Tosa Bay, off the southern coast of Japan. *Continental Shelf Research.* **53**, 50-62 (2013).

K. Kuroda, Studies on the recruitment process focusing on the early life history of the Japanese sardine, *Sardinops melanostictus* (Schelegen). *Bull. Natl .Res. Inst. Fish. Sci.*, **3**, 25-278 (1991) (in Japanese with English abstract).

K. Nishida, T. Ishimura, Grain-scale stable carbon and oxygen isotopic variations of the

international reference calcite, IAEA-603. *Rapid Communications in Mass Spectrometry.* **31**, 1875-1880 (2017).

Okunishi, S. Ito, D. Ambe, A. Takasuka, T. Kameda, K. Tadokoro, T. Setou, K. Komatsu, A. Kawabata, H. Kubota, A modeling approach to evaluate growth and movement for recruitment success of Japanese sardine (Sardinops melanostictus) in the western Pacific. *Fish. Oceanogr.* **21**, 44-57 (2012).

D. Pauly, V. Christensen, S. Guénette, T. J. Pitcher, U. R. Sumaila, C. J. Walters, R. Watson, D. Zeller, Towards sustainability in world fisheries. *Nature.* **418**, 689 (2002).

J. A. Rice, T. J. Miller, K. A. Rose, L. B. Crowder, E. A. Marschall, A. S. Trebitz, D. L. DeAngelis, Growth rate variation and larval survival: inferences from an individual-based size-dependent predation model. *Can. J. Fish. Aquat. Sci.* **50**, 133-142 (1993).

K. A. Rose, E. S. Rutherford, D. S. McDermot, J. L. Forney, E. L. Mills, Individual-Based Model Of Yellow Perch And Walleye Populations In Oneida Lake. *Ecol. Monogr.* **69**, 127-154 (1999).

S. Sainz-Trápaga, T. Sugimoto, Three-dimensional velocity field and cross-frontal water exchange in the Kuroshio Extension. *J. Oceanogr.* **56**, 79-92 (2000).

S. Sakai, Micromilling and sample recovering techniques using high-precision micromill GEOMILL326. *JAMSTEC-Rep.Res.Develop.*, **10**, 4–5 (2009).

T. Sakamoto, K. Komatsu, K. Shirai, T. Higuchi, T. Ishimura, T. Setou, Y. Kamimura, C. Watanabe, A. Kawabata, Combining microvolume isotope analysis and numerical simulation to reproduce fish migration history. *Methods in Ecology and Evolution.*(2018).

T. Sakamoto, K. Komatsu, M. Yoneda, T. Ishimura, T. Higuchi, K. Shirai, Y. Kamimura, C. Watanabe, A. Kawabata, Temperature dependence of δ18O in otolith of juvenile Japanese sardine: Laboratory rearing experiment with micro-scale analysis. *Fisheries Research.* **194**, 55-59 (2017).

J. Shiao, T. Yui, H. Høie, U. Ninnemann, S. Chang, Otolith O and C stable isotope compositions of southern bluefin tuna Thunnus maccoyii (Pisces: Scombridae) as possible environmental and physiological indicators. *Zool. Stud.* **48**, 71-82 (2009).

L. Silva, A. Faria, M. A. Teodósio, S. Garrido, Ontogeny of swimming behaviour in sardine Sardina pilchardus larvae and effect of larval nutritional condition on critical speed. *Mar. Ecol. Prog. Ser.* **504**, 287-300 (2014).

J. Smagorinsky, General circulation experiments with the primitive equations: I. The basic experiment. *Mon. Weather Rev.* **91**, 99-164 (1963).

A. Storm-Suke, J. B. Dempson, J. D. Reist, M. Power, A field-derived oxygen isotope fractionation equation for Salvelinus species. *Rapid Commun. Mass Spectrom.* **21**, 4109-4116 (2007).

A. Sturrock, C. Trueman, A. Darnaude, E. Hunter, Can otolith elemental chemistry retrospectively track migrations in fully marine fishes? *J. Fish Biol.* **81**, 766-795 (2012).

M. Takahashi, H. Nishida, A. Yatsu, Y. Watanabe, Year-class strength and growth rates after metamorphosis of Japanese sardine (Sardinops melanostictus) in the western North Pacific Ocean during 1996–2003. *Can. J. Fish. Aquat. Sci.* **65**, 1425-1434 (2008).

J. Torniainen, A. Lensu, P. J. Vuorinen, E. Sonninen, M. Keinänen, R. I. Jones, W. P. Patterson, M. Kiljunen, Oxygen and carbon isoscapes for the Baltic Sea: Testing

their applicability in fish migration studies. *Ecology and Evolution.* **7**, 2255-2267 (2017).

K. Tsukamoto, I. Nakai, Do all freshwater eels migrate? *Nature.* **396**, 635 (1998).

R. Yukami, C. Wanatabe, Y. Kamimura, S. Furuichi, T. Akamine, T. Kishida, Stock assessment and evaluation for the Pacific stock of Japanese sardine (fiscal year 2016). in *Marine fisheries stock assessment and evaluation for Japanese waters (fiscal year 2016/2017)*. (Fisheries Agency and Fisheries Research and Education Agency of Japan, Yokohama, 2017) pp. 15-52 (in Japanese).

J. P. Zwolinski, R. L. Emmett, D. A. Demer, Predicting habitat to optimize sampling of Pacific sardine (Sardinops sagax). *ICES J. Mar. Sci.* **68**, 867-879 (2011).

Chapter 6

P. Cury, A. Bakun, R. J. Crawford, A. Jarre, R. A. Quinones, L. J. Shannon, H. M. Verheye, Small pelagics in upwelling systems: patterns of interaction and structural changes in “wasp-waist” ecosystems. *ICES J. Mar. Sci.* **57**, 603-618 (2000).

C. L. de Moor, D. S. Butterworth, van der Lingen, Carl D, The quantitative use of parasite data in multistock modelling of South African sardine (Sardinops sagax). *Can. J. Fish. Aquat. Sci.* **74**, 1895-1903 (2017).

J. Kalish, Oxygen and carbon stable isotopes in the otoliths of wild and laboratory-reared Australian salmon (Arripis trutta). *Mar. Biol.* **110**, 37-47 (1991).

S. Kim, J. R. O’Neil, C. Hillaire-Marcel, A. Mucci, Oxygen isotope fractionation between synthetic aragonite and water: influence of temperature and Mg2 concentration. *Geochim. Cosmochim. Acta.* **71**, 4704-4715 (2007).

M. J. Kishi, M. Kashiwai, D. M. Ware, B. A. Megrey, D. L. Eslinger, F. E. Werner, M.

Noguchi-Aita, T. Azumaya, M. Fujii, S. Hashimoto, NEMURO—a lower trophic level model for the North Pacific marine ecosystem. *Ecol. Model.* **202**, 12-25 (2007).

R. C. Lewontin, The organism as the subject and object of evolution. (1983).

C. Mullon, P. Cury, P. Penven, Evolutionary individual-based model for the recruitment of anchovy (Engraulis capensis) in the southern Benguela. *Can. J. Fish. Aquat. Sci.* **59**, 910-922 (2002).

R. A. Schwartzlose, J. Alheit, A. Bakun, T. R. Baumgartner, R. Cloete, R. J. M. Crawford, W. J. Fletcher, Y. Green-Ruiz, E. Hagen, T. Kawasaki, D. Lluch-Belda, S. E. Lluch-Cota, A. D. MacCall, Y. Matsuura, M. O. Nevárez-Martínez, R. H. Parrish, C. Roy, R. Serra, K. V. Shust, M. N. Ward, J. Z. Zuzunaga, Worldwide large-scale fluctuations of sardine and anchovy populations. *South African Journal of Marine Science.* **21**, 289-347 (1999).

J. Shiao, K. Shirai, K. Tanaka, N. Takahata, Y. Sano, S. Hsiao, D. Lee, Y. Tseng, Assimilation of nitrogen and carbon isotopes from fish diets to otoliths as measured by nanoscale secondary ion mass spectrometry. *Rapid Communications in Mass Spectrometry.*(2018).